Brigham Young University

BYU ScholarsArchive

2007-11-30

Analysis and Implementation of High-Order Compact Finite Difference Schemes

Jonathan G. Tyler
Brigham Young University - Provo

ANALYSIS AND IMPLEMENTATION OF HIGH-ORDER

COMPACT FINITE DIFFERENCE SCHEMES

by

Jonathan Tyler

A thesis submitted to the faculty of

Brigham Young University

in partial fulfillment of the requirements for the degree of

Master of Science

Department of Mathematics

Brigham Young University

December 2007

BRIGHAM YOUNG UNIVERSITY

GRADUATE COMMITTEE APPROVAL

of a thesis submitted by

Jonathan Tyler

This thesis has been read by each member of the following graduate committee and by majority vote has been found to be satisfactory.

_____   _____
Date   Vianey Villamizar, Chair

_____   _____
Date   Shue-Sum Chow

_____   _____
Date   Kening Lu

BRIGHAM YOUNG UNIVERSITY

As chair of the candidate's graduate committee, I have read the thesis of Jonathan Tyler in its final form and have found that (1) its format, citations, and bibliographical style are consistent and acceptable and fulfill university and department style requirements; (2) its illustrative materials including figures, tables, and charts are in place; and (3) the final manuscript is satisfactory to the graduate committee and is ready for submission to the university library.

_____
Date

_____
Vianey Villamizar
Chair, Graduate Committee

Accepted for the Department

_____
William E. Lang
Graduate Coordinator

Accepted for the College

_____
Thomas Sederberg, Associate Dean
College of Physical and Mathematical Sciences

ABSTRACT

ANALYSIS AND IMPLEMENTATION OF HIGH-ORDER
COMPACT FINITE DIFFERENCE SCHEMES

Jonathan Tyler

Department of Mathematics

Master of Science

The derivation of centered compact schemes at interior and boundary grid points is performed and an analysis of stability and computational efficiency is given. Compact schemes are high order implicit methods for numerical solutions of initial and/or boundary value problems modeled by differential equations. These schemes generally require smaller stencils than the traditional explicit finite difference counterparts. To avoid numerical instabilities at and near boundaries and in regions of mesh non-uniformity, a numerical filtering technique is employed. Experiments for non-stationary linear problems (convection, heat conduction) and also for nonlinear problems (Burgers' and KdV equations) were performed. The compact solvers were combined with Euler and fourth-order Runge-Kutta time differencing. In most cases, the order of convergence of the numerical solution to the exact solution was the same as the formal order of accuracy of the compact schemes employed.

ACKNOWLEDGMENTS

Contents

List of Tables

List of Figures

xii

1 Introduction

Efficient and accurate numerical methods for generating numerical approximations of initial and/or boundary value problems (IVBP) modeled by differential equations appearing in the sciences and engineering has been a goal of mathematicians, engineers, physicists, and other scientists for decades. In the last fifty years, three approaches have dominated the numerical approximations: finite difference, finite element, and integral equation methods. From the 1950s to the 1980s, finite difference methods were widely popular and saw much theoretical development and application. In more recent years, the finite element methods have gained considerable popularity. However, the finite difference approach still remains as a fundamental technique in many commercial computer-aided engineering (CAE) software in diverse physical fields such as geophysics, electro-magnetics, and fluid mechanics.

Numerical schemes based of first and second order explicit or implicit finite difference schemes are commonly used because their implementation is relatively simple. For example, a typical explicit finite difference scheme to approximate the first derivative is the centered scheme given by $\phi_i' \approx \dfrac{\phi_{i+1} - \phi_{i-1}}{2h}$, $i = 0, \pm 1, \pm 2, \ldots$, where h is the step size of a uniform partition of the domain of ϕ. The local truncation error, or the measure by which the differencing formula approximates the first derivative, is $\tau_i = -\dfrac{1}{6} h^2 \phi_{i+\xi}'''$, where $\xi \in (i, i+1)$. Assuming that ϕ''' is bounded, the local truncation error approaches zero at the same rate that h^2 approaches zero, when $h \to 0$. It is simply said that the local truncation error is of order h^2, which is denoted by the symbols $\mathcal{O}(h^2)$.

Implicit methods increase the complexity of the algorithm since they require matrix inversion but are still relatively uncomplicated. Better approximations can be obtained by increasing the order of the truncation error of the finite difference scheme. This is commonly accomplished by including more points in the stencil of the numerical schemes. As an example, consider an explicit centered finite difference formula

1

with a five point stencil approximating the first derivative,

$$\phi'_i \approx \frac{\phi_{i-2} - 8\phi_{i-1} + 8\phi_{i+1} - \phi_{i+2}}{12h}, \tag{1.1}$$

which has a local truncation error of $\mathcal{O}(h^4)$ given by

$$\tau_i = -\frac{1}{30}h^4\phi^{(5)}_{i+\xi}. \tag{1.2}$$

The smaller truncation error is more advantageous, but it requires a larger stencil as shown in Figure 1.
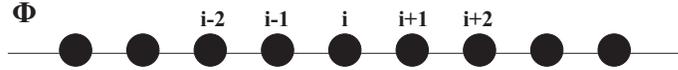
Figure 1: Stencil for (1.1)

A disadvantage of this approach is the need to include more equations for grid points near and at the boundaries. Also, for higher order implicit schemes, the inversion of the matrices with the increased number of non-zero diagonals may be too costly.

An alternative is to not enlarge the stencil, but involve values of the derivative at some nodes where the function is already evaluated. For instance, consider the finite difference approximation of the first derivative proposed in 1966 by Collatz [6], pp. 538, which approximates the derivative values at three grid points with known function values over the same three grid points:

$$\frac{1}{4}\phi'_{i-1} + \phi'_i + \frac{1}{4}\phi'_{i+1} \approx \frac{3}{4h}\left(\phi_{i+1} - \phi_{i-1}\right). \tag{1.3}$$

The stencil for this scheme is shown in Figure 2.

As it will be proven later, this new scheme has a local truncation error of $\mathcal{O}(h^4)$,

2
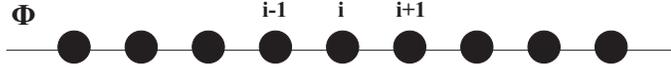
Figure 2: Stencil for (1.3)

similar to (1.1). However, if (1.1) is used over a discretized domain, four additional formulas are needed at the two points on both ends where the stencil protrudes the domain. On the contrary, scheme (1.3) only requires additional formulas at each of the endpoints. Assuming that at least one boundary condition is known, only one additional formula may be needed. Thus the proposed implicit scheme (1.3) gives a distinct advantage over the explicit equation (1.1).

The development and application of the above implicit finite difference formula (1.3) to solve IVBP modeled by partial differential equations is of more recent appearance. In [6], they are called Hermitian finite difference schemes. This name is due to the analogy with Hermite's interpolation formula which, in addition to the values of the function, also uses the value of the derivatives at several points. In view of their smaller stencils, the Hermitian finite difference equations are mainly known as compact finite difference schemes.

Compact finite differencing expressions have been known for almost fifty years. As mentioned above, some particular formulas are reported by Collatz, [6] pp. 538. However, their implementation as difference schemes approximating partial differential equations began in the early 1970s for some fluid mechanics problems [2, 11, 22]. Since that time, several distinct classes of compact schemes have been developed. The two most common are the upwind and the centered schemes. In 1992, Lele [15] published a seminal paper with an in-depth analysis of centered compact schemes. In recent years, due to the appearance of faster and more powerful computing possibilities as well as the development of algorithms for fast matrix inversion, compact schemes are proving more advantageous. The current emphasis of these higher-order

3

methods has been to the field of fluid mechanics as well as other areas of aero-acoustics and electro-magnetics.

In the last ten years, much work has been done with compact schemes by many authors. For instance, Visbal [9, 26, 27, 28] and Sherer [19, 20] have used compact schemes on several problems dealing with wall-bounded flows described by the Navier-Stokes equations, in large-eddy simulation of supersonic boundary-layer flow, and also in the scattering of electromagnetic waves.

This work discusses the formulation of two different approaches for compact finite difference schemes, the order-optimized or Padé scheme and the spectral scheme. Fourier analysis is used to characterize the errors of the difference approximations based on compact finite differencing. For this, the procedure follows as described in [24]. The resolving efficiency introduced by [15] is also studied. Compact schemes of various orders are compared and analyzed. These compact schemes are then applied to the one-dimensional wave equation which is perhaps the most basic means for examining the qualities of a numerical scheme. They are also applied to the nonlinear Burgers' equation and the standard Korteweg-de Vries equation which serve to test how the numerical method manages nonlinearities. Finally, the compact schemes are analyzed with the heat equation and a two-dimensional initial value problem consisting of a sharp Gaussian pulse convected in a circular pattern around the origin as performed in [7]. The proposed schemes may also be applied to many other important physical problems such as the acoustic scattering problem studied in [25].

1.1   Consistency, Stability, and Convergence

The discussion to this point has been centered on increasing the order of the truncation error by which a finite difference formula approximates the first derivative or by which a finite difference scheme approximates a continuous partial differential equation. Since the ultimate goal of using finite difference schemes is the accurate

approximation of the analytic solution of a given boundary value problem (BVP) or initial value boundary value problem, it is expedient to discuss the relationship between the finite difference numerical schemes with higher order truncation errors (higher order schemes) and high accurate approximations of the exact solution.

Finite difference schemes approximating partial differential equations are analyzed according to three important properties: consistency, stability, and convergence. To introduce these important concepts, consider the following initial value problem for the one-dimensional wave equation,

$$u_t - u_x = \varphi(x, t), \qquad -\infty < x < \infty, \quad 0 \le t \le T, \qquad (1.4)$$

$$u(x, 0) = \psi(x), \qquad -\infty < x < \infty. \qquad (1.5)$$

It is supposed that φ and ψ are continuous and bounded in their respective domains.

The remainder of this section follows the discussion of Godunov [10]. Let the differential operator $\mathcal{L}$ and the vector function $\boldsymbol{f}$ be such that the initial value problem (IVP) (1.4) - (1.5) can be written as $\mathcal{L}u = \boldsymbol{f}$, where

$$\mathcal{L}u = \begin{cases} u_t - u_x, & -\infty < x < \infty, \quad 0 \le t \le T, \\ u(x, 0), & -\infty < x < \infty, \end{cases} \qquad (1.6)$$

$$\boldsymbol{f} = \begin{cases} \varphi(x, t), & -\infty < x < \infty, \quad 0 \le t \le T, \\ \psi(x), & -\infty < x < \infty. \end{cases} \qquad (1.7)$$

To obtain a numerical approximation of this IVP, a grid formed by points in the domain of the function u must be defined. By selecting h and τ as uniform step sizes along the x-axis and t-axis respectively, the grid points

$$x = ih, \quad i = 0, \pm 1, \pm 2, \ldots, \quad \text{and} \quad t = n\tau, \quad n = 0, 1, \ldots, N \qquad (1.8)$$

5

are defined where $N = \dfrac{T}{\tau}$. It is also assumed that $\tau = rh$ for a constant r. Hence, the parameter h is enough to define the set of grid points (1.8). This set of points will be denoted by $\mathcal{D}_h$. The values of the function u at grid points $(ih, n\tau)$ will be represented by u_i^n. Likewise, φ_i^n and ψ_i are used for values of φ and ψ at each grid point respectively. Employing forward difference approximations for u_t and u_x on the grid points, equation (1.4) is approximated by a finite difference equation. As a consequence, the continuous IVP (1.4) - (1.5) is replaced by a new discrete problem given by

$$\frac{U_i^{n+1} - U_i^n}{\tau} - \frac{U_{i+1}^n - U_i^n}{h} = \varphi_i^n \tag{1.9}$$

$$U_i^0 = \psi_i, \tag{1.10}$$

for $i = 0, \pm 1, \pm 2, \ldots$, and $n = 0, 1, \ldots, N - 1$. This discrete problem is also called a finite difference scheme corresponding to the continuous IVP (1.4) - (1.5). The goal is to find a discrete solution U_i^n for the problem (1.9) - (1.10) that approximates in some sense the solution u of the continuous problem (1.4) - (1.5).

To arrive to a precise mathematical definition of approximation between U_i^n and u, two linear normed spaces are defined. The first, $\mathcal{U}_h$, is formed by all bounded discrete functions $U_h = U_i^n$ defined on the grid points in $\mathcal{D}_h$ with norm $\|U_h\| = \max_n \sup_i |U_i^n|$. The other is the normed linear space $\mathcal{F}_h$ consisting of all pairs of bounded discrete functions $\boldsymbol{f}_h = (\varphi_i^n, \psi_i)^T$ with norm $\|\boldsymbol{f}_h\| = \max_n \sup_i |\varphi_i^n| + \sup_i |\psi_i|$. The discrete problem (1.9) - (1.10) can also be written using a discrete differential operator $\mathcal{L}_h$ acting on the discrete functions $U_h \in \mathcal{U}_h$ as $\mathcal{L}_h U_h = \boldsymbol{f}_h$, where $\boldsymbol{f}_h \in \mathcal{F}_h$. In fact,

$$\mathcal{L}_h U_h = \begin{cases} \dfrac{U_i^{n+1} - U_i^n}{\tau} - \dfrac{U_{i+1}^n - U_i^n}{h} \\[2mm] u_i^0 \end{cases} \tag{1.11}$$

6

with

$$\boldsymbol{f}_h = \begin{cases} \varphi_i^n, \\ \\ \psi_i \end{cases} \tag{1.12}$$

for $i = 0, \pm 1, \pm 2, \ldots$, and $n = 0, 1, \ldots, N - 1$.

The above formulation (in terms of the continuous and discrete operators $\mathcal{L}$ and $\mathcal{L}_h$ respectively) can be extended to any initial and/or boundary value problem governed by a partial differential equation. Thus in what follows, $\mathcal{L}u = \boldsymbol{f}$ will represent any continuous problem and $\mathcal{L}_h U_h = \boldsymbol{f}_h$ will denote the corresponding discrete problem.

The effectiveness of a finite difference scheme is measured on how well the discrete solution approximates the exact solution of the corresponding continuous problem. Establishing this fact requires definitions of basic concepts such as consistency, stability, and convergence of a discrete solution to the exact or continuous solution.

If the exact solution u is evaluated at the grid points in $\mathcal{D}_h$, a discrete function $u_h \in \mathcal{U}_h$ is obtained. The concept of convergence from [10] is now presented.

Definition 1. *The solution U_h of the difference scheme*

$$\mathcal{L}_h U_h = \boldsymbol{f}_h \tag{1.13}$$

converges (as the grid $\mathcal{D}_h$ is refined or h is made smaller) to the solution u of the continuous problem

$$\mathcal{L}u = \boldsymbol{f} \tag{1.14}$$

if

$$\|u_h - U_h\| \to 0 \tag{1.15}$$

as $h \to 0$. Moreover, if there exists a constant $k > 0$ and a constant $C_0 > 0$ that does not depend on k such that

$$\|u_h - U_h\| \le C_0 h^k, \tag{1.16}$$

then it is said that the convergence is of order h^k and the difference scheme has k-th order accuracy.

In general, the restriction u_h of the exact solution u to the grid $\mathcal{D}_h$ does not satisfy the discrete problem (1.13). Therefore, by substituting u_h into (1.11) - (1.12), a residual term $\delta\boldsymbol{f}_h$ results. In fact, u_h satisfies

$$\mathcal{L}_h u_h = \boldsymbol{f}_h + \delta\boldsymbol{f}_h. \tag{1.17}$$

Definition 2. *The residual $\delta\boldsymbol{f}_h$ is a vector in $\mathcal{F}_h$ obtained when the discrete differential operator $\mathcal{L}_h$ acts on the restriction of the exact solution u to the grid $\mathcal{D}_h$ of the continuous problem (1.9) - (1.10).*

The consistency of a finite difference scheme roughly means that the difference scheme is a good approximation of the continuous problem modeled by the corresponding partial differential equation. The following definition is similarly attributed to Godunov [10].

Definition 3. *The difference scheme (1.13) is consistent with the continuous problem (1.14) if the residual term in (1.17) is such that $\|\delta\boldsymbol{f}_h\| \to 0$ when $h \to 0$. Moreover, if the inequality*

$$\|\delta\boldsymbol{f}_h\| \le C_1 h^k \tag{1.18}$$

is satisfied for positive constants C_1 and k, then it is said that the difference scheme (1.13) is of order h^k consistent with the continuous problem (1.14).

It is important to note that the residual vector's first component is the local truncation error defined in the previous section. Another important property for difference schemes is their sensitivity to small perturbations in the forcing terms, boundary conditions, and/or initial conditions. This property known as stability is now defined.

8

Definition 4. *The difference scheme (1.13) is stable if there exists $h_0 > 0$ and $\delta > 0$ such that for any $h < h_0$ and any $\epsilon_h \in \mathcal{F}_h$ satisfying $\|\epsilon_h\| < \delta$, the perturbed difference problem $\mathcal{L}_h w_h = \mathbf{f}_h + \delta \epsilon_h$ has one and only one solution, w_h, satisfying*

$$\|w_h - U_h\| \leq C \|\epsilon_h\| \tag{1.19}$$

where U_h is the solution of the unperturbed difference problem (1.13) and $C > 0$ does not depend on h.

The following theorem of Godunov [10] expresses a very important relationship between the three properties: consistency, stability, and convergence defined above.

Theorem 1. *If the difference scheme (1.13) is stable and is also consistent (with order h^k) with the continuous problem (1.14), then, the discrete solution U_h of (1.13) converges to the solution u of (1.14) and satisfies*

$$\|u_h - U_h\| \leq CC_1 h^k, \tag{1.20}$$

where C and C_1 are the positive constants used in the inequalities (1.19) and (1.18) respectively. In other words, the order of accuracy of the difference scheme coincides with the order by which the difference scheme approximates the continuous problem.

Proof. Since the difference scheme is consistent, it is verified that $\|\delta \mathbf{f}_h\| \leq C_1 h^k \to 0$ as $h \to 0$. Therefore, it is possible to have a grid $\mathcal{D}_h$ such that

$$h < h_0, \tag{1.21}$$

$$\delta \mathbf{f}_h < \delta \tag{1.22}$$

$$\tag{1.23}$$

9

as in Definition 4, and

$$\mathcal{L}_h u_h = \boldsymbol{f}_h + \delta \mathbf{f}_h. \tag{1.24}$$

Therefore, u_h satisfies the conditions for stability. As a consequence,

$$\|u_h - U_h\| \leq C\|\delta \boldsymbol{f}_h\| \leq C(C_1 h^k). \tag{1.25}$$

Hence, the discrete solution U_h of (1.13) converges to the continuous solution u of (1.14) with order h^k. $\qquad \square$

It shall therefore be an important consideration for this work to determine the consistency and stability of the compact schemes considered. High-order accuracy of the numerical scheme is sought in general to obtain improved approximate solutions and to obtain those solutions at less computational expense.

2 The Compact Scheme

In view of the previous section, a stable and consistent numerical scheme of order $\mathcal{O}(h^k)$ will have a discrete solution that converges to the exact continuous solution with the same order of accuracy $\mathcal{O}(h^k)$. This fact motivates the development of consistent schemes of high order, or simply, "higher order schemes." However, verification of the stability condition usually is not easy due to the boundary and initial conditions of the problem. That is why some authors [9, 15] refer to the order of the local truncation error for a discrete equation approximating a continuous one as the "formal order of accuracy." An obvious disadvantage of increasing the order of the schemes too much is the larger stencils which may make them computationally inefficient as explained earlier.

This study of high order schemes begins by considering high order approximations for the first derivative of a function ϕ. Among the class of high order approximations

of the derivatives of a function ϕ are the implicit compact schemes as defined in [6], pp. 538-539. It will be shown below that these schemes have smaller stencils than their explicit centered counterparts with the same formal order of accuracy.

Consider a function ϕ of one variable defined on the real line $\mathbb{R}$. A uniform partition formed by discrete points x_i, $i = 0, \pm 1, \pm 2, \ldots$, is defined in $\mathbb{R}$. An implicit numerical approximation of the first derivative ϕ' at the grid points can be given by

$$\alpha \phi'_{i-1} + \phi'_i + \alpha \phi'_{i+1} \approx a \frac{\phi_{i+1} - \phi_{i-1}}{2h}, \tag{2.1}$$

where α and a are arbitrary constants. In fact, equation (2.1) represents a family of numerical approximations for ϕ'.

Theorem 2. *If ϕ is an $n + 1$ times differentiable function on $\mathbb{R}$ ($n \geq 4$) and x_i, $i = 0, \pm 1, \pm 2, \ldots$, is a uniform partition of $\mathbb{R}$ with step size h, then the implicit finite difference equation (2.1) defines a one parameter family of numerical approximations for ϕ' with second order formal accuracy. Fourth order maximum formal accuracy is obtained for $a = \frac{3}{2}$ and $\alpha = \frac{1}{4}$ with local truncation error*

$$\tau_i = \frac{1}{120} h^4 \phi_{i+\xi}^{(5)}, \qquad -1 < \xi < 1. \tag{2.2}$$

Proof. Grouping all terms of equation (2.1) on the left-hand side, expanding the functions ϕ and its first derivative ϕ' at each node according to their Taylor expansions (as demonstrated in Appendix C), and substituting them into (2.1) leads to

$$
\begin{aligned}
&\alpha \phi'_{i-1} + \phi'_i + \alpha \phi'_{i+1} - a \frac{\phi_{i+1} - \phi_{i-1}}{2h} \\
&= 2\alpha \left(\phi'_i + \frac{h^2}{2!} \phi'''_i + \frac{h^4}{4!} \phi_i^{(5)} + \cdots \right) + \phi'_i \\
&\quad - \frac{a}{2h} \left[\left(\phi_i + h\phi'_i + \frac{h^2}{2!} \phi''_i + \frac{h^3}{3!} \phi'''_i + \frac{h^4}{4!} \phi_i^{(4)} + \frac{h^5}{5!} \phi_i^{(5)} + \cdots \right) \right. \\
&\qquad \left. - \left(\phi_i - h\phi'_i + \frac{h^2}{2!} \phi''_i - \frac{h^3}{3!} \phi'''_i + \frac{h^4}{4!} \phi_i^{(4)} - \frac{h^5}{5!} \phi_i^{(5)} + \cdots \right) \right].
\end{aligned}
$$

11

Combining like terms gives

$$\alpha\phi'_{i-1} + \phi'_i + \alpha\phi'_{i+1} - a\frac{\phi_{i+1} - \phi_{i-1}}{2h} = (2\alpha + 1 - a)\phi'_i + \left(2\frac{\alpha}{2!} - \frac{a}{3!}\right)h^2\phi'''_i$$
$$+ \left(2\frac{\alpha}{4!} - \frac{a}{5!}\right)h^4\phi_i^{(5)} + \dots. \qquad (2.3)$$

By setting $2\alpha + 1 - a = 0$, the first term is eliminated and equation (2.1) becomes a one parameter family of second order schemes, that is, the constant a is uniquely determined by the parameter α as $a = 2\alpha + 1$. The truncation error is given by

$$\tau_i = \left(2\frac{\alpha}{2!} - \frac{a}{3!}\right)h^2\phi'''_{i+\xi} = \frac{4\alpha - 1}{6}h^2\phi'''_{i+\xi}.$$

In addition, if the second coefficient term in (2.3) is forced to zero, that is, $\frac{2\alpha}{2!} - \frac{a}{3!} = 0$, then both constants α and a are uniquely determined. These values are $\alpha = \frac{1}{4}$ and $a = \frac{3}{2}$ which are the constants defining (1.3). The local truncation error is

$$\tau_i = \left(2\frac{\alpha}{4!} - \frac{a}{5!}\right)h^4\phi_{i+\xi}^{(5)} = \frac{1}{120}h^4\phi_{i+\xi}^{(5)}$$

which proves that the implicit compact scheme

$$\frac{1}{4}\phi'_{i-1} + \phi'_i + \frac{1}{4}\phi'_{i+1} \approx \frac{3}{4h}(\phi_{i+1} - \phi_{i-1})$$

has the same formal fourth order of accuracy as the five point explicit centered finite difference scheme (1.1). $\qquad\square$

An important advantage of the scheme (2.1) is that its stencil only consists of three points instead of five as in the explicit centered counterpart. The extra work to obtain the approximations of the derivative values at the nodes x_i is not a major computational load since the matrix to be inverted is tridiagonal.

The formal order of accuracy for the implicit scheme (2.1) can be easily increased

12

by enlarging its stencil, maintaining a tridiagonal matrix for the unknown derivative values. More precisely, consider the scheme

$$\alpha\phi'_{i-1} + \phi'_i + \alpha\phi'_{i+1} \approx a\frac{\phi_{i+1} - \phi_{i-1}}{2h} + b\frac{\phi_{i+2} - \phi_{i-2}}{4h}, \qquad i = 0, \pm 1, \pm 2, \ldots. \quad (2.4)$$

The analog of Theorem 2 for this new scheme can be formulated as follows here.

Theorem 3. *If ϕ is an $n + 1$ times differentiable function on $\mathbb{R}$ ($n \geq 6$) and x_i, $i = 0, \pm 1, \pm 2, \ldots$, is a uniform partition of $\mathbb{R}$ with step size h, then the implicit finite difference equation (2.4) defines a one parameter family of numerical approximations for ϕ' with fourth order formal accuracy. A sixth order maximum formal accuracy is obtained for $a = \frac{14}{9}$, $\alpha = \frac{1}{3}$, and $b = \frac{1}{9}$ with local truncation error*

$$\tau_i = -\frac{1}{1260}h^6\phi^{(7)}_{i+\xi}, \qquad -2 < \xi < 2. \quad (2.5)$$

Proof. Grouping all terms of equation (2.4) on the left-hand side, expanding the functions ϕ and its first derivative ϕ' at each node according to their Taylor expansions, substituting them into (2.4), and combining like terms leads to

$$\alpha\phi'_{i-1} + \phi'_i + \alpha\phi'_{i+1} - a\frac{\phi_{i+1} - \phi_{i-1}}{2h} - b\frac{\phi_{i+2} - \phi_{i-2}}{4h}$$
$$= (2\alpha + 1 - a - b)\phi'_i + \left(2\frac{\alpha}{2!} - \frac{a}{3!} - \frac{2^2 b}{3!}\right)h^2\phi'''_i$$
$$+ \left(2\frac{\alpha}{4!} - \frac{a}{5!} - \frac{2^4 b}{5!}\right)h^4\phi^{(5)}_i + \left(2\frac{\alpha}{6!} - \frac{a}{7!} - \frac{2^6 b}{7!}\right)h^6\phi^{(7)}_i \ldots.$$

By setting $2\alpha + 1 - a - b = 0$, and $2\frac{\alpha}{2!} - \frac{a}{3!} - \frac{2^2 b}{3!} = 0$, the first two terms in the right hand side are eliminated and the equation (2.4) becomes a one parameter family of fourth order schemes. That is, the constants a and b are uniquely determined by the parameter α. The truncation error is given by the $\mathcal{O}(h^4)$ term in the right hand side. If this third term is also forced to zero, then all constants α, a, and b are

13

uniquely determined. These values are $\alpha = \frac{1}{3}$, $a = \frac{14}{9}$, and $b = \frac{1}{9}$. As a consequence, the following sixth order compact scheme approximation for the first derivative is obtained:

$$\frac{1}{3}\phi'_{i-1} + \phi'_i + \frac{1}{3}\phi'_{i+1} \approx \frac{7}{9h}\left(\phi_{i+1} - \phi_{i-1}\right) + \frac{1}{36h}\left(\phi_{i+2} - \phi_{i-2}\right). \tag{2.6}$$

The local truncation error for this particular scheme is

$$\tau_i = -\frac{1}{1260}h^6\phi^{(7)}_{i+\xi}, \quad -2 < \xi < 2.$$

$\square$

Note that the presence of factorial terms yields a coefficient of the truncation error that is very small. This may in fact result in an even higher order of formal accuracy for the given scheme than is suggested by $\mathcal{O}(h^6)$.

In the literature dealing with compact schemes, it is common to use the equality symbol "=" instead of the approximation symbol "≈". It is implicitly understood that there is a truncation error associated with the given differencing formula. For instance, the previous sixth order scheme (2.6) is usually written as

$$\frac{1}{3}\phi'_{i-1} + \phi'_i + \frac{1}{3}\phi'_{i+1} = \frac{7}{9h}\left(\phi_{i+1} - \phi_{i-1}\right) + \frac{1}{36h}\left(\phi_{i+2} - \phi_{i-2}\right). \tag{2.7}$$

The following will also adopt the same convention.

Similar procedures as those used in proving the above theorems can be followed to derive other compact schemes. When dealing with boundary value problems, the complete compact differencing scheme consists of two different types of formulas. The interior formula, which is the heart of the compact scheme, approximates derivative values at all but the boundary and near boundary points. To approximate derivative values at these points, one-sided difference schemes that mimic the implicit nature and the formal order of accuracy of the interior scheme may be used. The number of

14

points excluded by the interior scheme depends on the stencil.

2.1   Interior Scheme

The compact scheme for the first derivative at interior points (2.1) and (2.4) are particular cases of the more general schemes defined by De and Eswaran [7]:

$$\sum_{k=-L}^{L} \beta_k \phi'_{i+k} = \frac{1}{h} \sum_{l=-M}^{M} a_l \phi_{i+l}, \quad \beta_0 = 1, \quad \beta_k = \beta_{-k}. \tag{2.8}$$

By expanding the summations, the schemes are shown as

$$\beta_L \phi'_{i-L} + \cdots + \beta_1 \phi'_{i-1} + \phi'_i + \beta_1 \phi'_{i+1} + \cdots + \beta_L \phi_{i+L}$$
$$= \frac{1}{h} \left(a_{-M} \phi_{i-M} + \cdots + a_{-1} \phi_{i-1} + a_0 \phi_i + a_1 \phi_{i+1} + \cdots + a_M \phi_{i+M} \right).$$

The left-hand side involves $2L + 1$ derivative values and the right-hand side has a $2M + 1$ node stencil. Due to the computational complexity in the use of implicit schemes, the implicit stencil is generally restricted to $L \leq 2$. The derivation of the coefficients of the compact schemes presented here will be mostly limited to the tridiagonal and pentadiagonal cases, although coefficients of septadiagonal schemes will also be given in an attempt to determine any advantages of choosing larger implicit stencils than the explicit right-hand side stencil. The right-hand stencil will be restricted to $M \leq 4$. The maximum attainable formal order of accuracy of any scheme can be increased by increasing either of the values of L or M.

Only centered compact schemes are considered in the present work. (For a discussion on non-centered schemes, see [22].) The right-hand terms of the centered scheme are arranged as second order accurate centered finite differences. Centered schemes generally have smaller stencils in comparison to the upwind schemes.

In particular, for $L = 3$ and $M = 4$, the formula (2.8) for the first derivative

15

reduces to

$$\gamma\phi'_{i-3} + \beta\phi'_{i-2} + \alpha\phi'_{i-1} + \phi'_i + \alpha\phi'_{i+1} + \beta\phi'_{i+2} + \gamma\phi'_{i+3} = a\frac{\phi_{i+1} - \phi_{i-1}}{2h} + b\frac{\phi_{i+2} - \phi_{i-2}}{4h}$$
$$+ c\frac{\phi_{i+3} - \phi_{i-3}}{6h} + d\frac{\phi_{i+4} - \phi_{i-4}}{8h}.$$
$$(2.9)$$

Further study of compact schemes will be reduced to the $L = 2$ case where $\gamma = 0$.

For higher order derivatives, similar compact centered schemes can be defined replacing ϕ'_i by $\phi''_i, \phi'''_i, \ldots$ on the left-hand side and using centered finite difference approximations for the derivative on the right-hand side. While compact schemes for higher derivatives could be made to depend on lower derivatives, the schemes considered here do not. The second derivative scheme is

$$\beta\phi''_{i-2} + \alpha\phi''_{i-1} + \phi''_i + \alpha\phi''_{i+1} + \beta\phi''_{i+2}$$
$$= a\frac{\phi_{i+1} - 2\phi_i + \phi_{i-1}}{h^2} + b\frac{\phi_{i+2} - 2\phi_i + \phi_{i-2}}{4h^2} + c\frac{\phi_{i+3} - 2\phi_i + \phi_{i-3}}{9h^2}.$$
$$(2.10)$$

Similarly, a third derivative centered compact scheme is given by

$$\beta\phi'''_{i-2} + \alpha\phi'''_{i-1} + \phi'''_i + \alpha\phi'''_{i+1} + \beta\phi'''_{i+2} = a\frac{\phi_{i+2} - 2\phi_{i+1} + 2\phi_{i-1} - \phi_{i-2}}{2h^3}$$
$$+ b\frac{\phi_{i+3} - 3\phi_{i+1} + 3\phi_{i-1} - \phi_{i-3}}{8h^3}.$$
$$(2.11)$$

Finally, a fourth derivative centered compact scheme can be written as

$$\beta\phi^{(4)}_{i-2} + \alpha\phi^{(4)}_{i-1} + \phi^{(4)}_i + \alpha\phi^{(4)}_{i+1} + \beta\phi^{(4)}_{i+2} = a\frac{\phi_{i+2} - 4\phi_{i+1} + 6\phi_i - 4\phi_{i-1} + \phi_{i-2}}{h^4}. \quad (2.12)$$

As was demonstrated earlier in Section 2, the formal order of accuracy of the compact schemes can be obtained by expanding each term in the above equations in Taylor series about x_i and then matching the Taylor series coefficients for like terms in the scheme as performed in theorems 2 and 3.

16

Here, the derivation of centered compact differencing formulas is extended in general form to schemes with pentadiagonal implicit matrix and up to 9 grid point stencils. First, consider the Taylor expansions for the left-hand side terms in (2.9) with $\gamma = 0$:

$$\phi'_{i-2} = \phi'_i - 2h\phi''_i + \frac{2^2 h^2}{2!}\phi'''_i - \cdots - \frac{2^9 h^9}{9!}\phi_i^{(10)} + \frac{2^{10} h^{10}}{10!}\phi_i^{(11)} + R_{11}(x)$$

$$\phi'_{i-1} = \phi'_i - h\phi''_i + \frac{h^2}{2!}\phi'''_i - \cdots - \frac{h^9}{9!}\phi_i^{(10)} + \frac{h^{10}}{10!}\phi_i^{(11)} + R_{11}(x)$$

$$\phi'_i = \phi'_i$$

$$\phi'_{i+1} = \phi'_i + h\phi''_i + \frac{h^2}{2!}\phi'''_i + \cdots + \frac{h^9}{9!}\phi_i^{(10)} + \frac{h^{10}}{10!}\phi_i^{(11)} + R_{11}(x)$$

$$\phi'_{i+2} = \phi'_i + 2h\phi''_i + \frac{2^2 h^2}{2!}\phi'''_i + \cdots + \frac{2^9 h^9}{9!}\phi_i^{(10)} + \frac{2^{10} h^{10}}{10!}\phi_i^{(11)} + R_{11}(x).$$

Similarly, Taylor expansions of the right-hand side terms are given by

$$\phi_{i-4} = \phi_i - 4h\phi'_i + \frac{4^2 h^2}{2!}\phi''_i - \cdots - \frac{4^9 h^9}{9!}\phi_i^{(9)} + \frac{4^{10} h^{10}}{10!}\phi_i^{(10)} - R_{11}(x)$$

$$\phi_{i-3} = \phi_i - 3h\phi'_i + \frac{3^2 h^2}{2!}\phi''_i - \cdots - \frac{3^9 h^9}{9!}\phi_i^{(9)} + \frac{3^{10} h^{10}}{10!}\phi_i^{(10)} - R_{11}(x)$$

$$\phi_{i-2} = \phi_i - 2h\phi'_i + \frac{2^2 h^2}{2!}\phi''_i - \cdots - \frac{2^9 h^9}{9!}\phi_i^{(9)} + \frac{2^{10} h^{10}}{10!}\phi_i^{(10)} - R_{11}(x)$$

$$\phi_{i-1} = \phi_i - h\phi'_i + \frac{h^2}{2!}\phi''_i - \cdots - \frac{h^9}{9!}\phi_i^{(9)} + \frac{h^{10}}{10!}\phi_i^{(10)} - R_{11}(x)$$

$$\phi_{i+1} = \phi_i + h\phi'_i + \frac{h^2}{2!}\phi''_i + \cdots + \frac{h^9}{9!}\phi_i^{(9)} + \frac{h^{10}}{10!}\phi_i^{(10)} + R_{11}(x)$$

$$\phi_{i+2} = \phi_i + 2h\phi'_i + \frac{2^2 h^2}{2!}\phi''_i + \cdots + \frac{2^9 h^9}{9!}\phi_i^{(9)} + \frac{2^{10} h^{10}}{10!}\phi_i^{(10)} + R_{11}(x)$$

$$\phi_{i+3} = \phi_i + 3h\phi'_i + \frac{3^2 h^2}{2!}\phi''_i + \cdots + \frac{3^9 h^9}{9!}\phi_i^{(9)} + \frac{3^{10} h^{10}}{10!}\phi_i^{(10)} + R_{11}(x)$$

$$\phi_{i+4} = \phi_i + 4h\phi'_i + \frac{4^2 h^2}{2!}\phi''_i + \cdots + \frac{4^9 h^9}{9!}\phi_i^{(9)} + \frac{4^{10} h^{10}}{10!}\phi_i^{(10)} + R_{11}(x).$$

Following a similar procedure as in theorems 2 and 3, the Taylor series expansions

17

are substituted into (2.9) and like terms are gathered. Ignoring the remainders gives

$$(1 + 2\alpha + 2\beta)\phi_i' + \frac{2}{2!}(\alpha + 2^2\beta)h^2\phi_i''' + \frac{2}{4!}(\alpha + 2^4\beta)h^4\phi_i^{(5)} + \frac{2}{6!}(\alpha + 2^6\beta)h^6\phi_i^{(7)}$$

$$+ \frac{2}{8!}(\alpha + 2^8\beta)h^8\phi_i^{(9)} + \frac{2}{10!}(\alpha + 2^{10}\beta)h^{10}\phi_i^{(11)} + \cdots$$

$$= (a + b + c + d)\phi_i' + \frac{1}{3!}(a + 2^2b + 3^2c + 4^2d)h^2\phi_i''' + \frac{1}{5!}(a + 2^4b + 3^4c + 4^4d)h^4\phi_i^{(5)}$$

$$+ \frac{1}{7!}(a + 2^6b + 3^6c + 4^6d)h^6\phi_i^{(7)} + \frac{1}{9!}(a + 2^8b + 3^8c + 4^8d)h^4\phi_i^{(9)}$$

$$+ \frac{1}{11!}(a + 2^{10}b + 3^{10}c + 4^{10}d)h^{10}\phi_i^{(11)} + \cdots .$$

As a consequence of the second order centered terms on the right-hand side and the symmetry of the left-hand side, the odd-order terms are annihilated leaving only even-order terms. Equating coefficients with the same power of h gives the following system of six equations with six unknowns:

$$a + b + c + d = 2(\alpha + \beta) + 1 \tag{2.13}$$

$$a + 2^2b + 3^2c + 4^2d = 2\frac{3!}{2!}(\alpha + 2^2\beta) \tag{2.14}$$

$$a + 2^4b + 3^4c + 4^4d = 2\frac{5!}{4!}(\alpha + 2^4\beta) \tag{2.15}$$

$$a + 2^6b + 3^6c + 4^6d = 2\frac{7!}{6!}(\alpha + 2^6\beta) \tag{2.16}$$

$$a + 2^8b + 3^8c + 4^8d = 2\frac{9!}{8!}(\alpha + 2^8\beta) \tag{2.17}$$

$$a + 2^{10}b + 3^{10}c + 4^{10}d = 2\frac{11!}{10!}(\alpha + 2^{10}\beta). \tag{2.18}$$

The factorial terms are written together on the same side of the equation to show explicitly how the factorials combine. When using the system of equations to determine the values of the constants, the factorial terms are easily simplified.

Satisfaction of each equation in this system represents two additional orders of formal accuracy that can be obtained for the compact scheme. That is, by requiring only (2.13) to be satisfied by the coefficients a, b, c, d, α, and β, a five parameter

18

family of second order schemes may be produced. By requiring both (2.13) and (2.14) to be satisfied, a four parameter family of fourth order formal accuracy schemes is developed. Similarly (2.13) - (2.15) produce a three parameter family of sixth order formal accuracy schemes. Continuing in the same fashion, satisfying (2.13) - (2.18) will uniquely determine the values of all the coefficients resulting in a scheme with twelfth order formal accuracy.

It should be noted however that this twelfth order scheme involves a large stencil on the right-hand side. Setting the most distant coefficients to zero reduces the size of the stencil but also reduces the maximum order of accuracy attainable by the scheme. Thus setting $d = 0$ reduces the scheme to tenth order maximum degree of formal accuracy. Alternatively, setting $\beta = 0$ reduces the scheme to a family of tridiagonal schemes with a maximum of tenth order formal accuracy.

The schemes obtained by uniquely determining the coefficients for a specific stencil are called order-optimized or Padé schemes. These schemes are so called due to the Padé or rational function approximation of the derivative of ϕ from which they can be derived. This alternative Padé rational approximation derivation is the subject of the next section.

Coefficients of these schemes for various orders of formal accuracy are presented in Table 1. The 'TN' schemes represent the coefficients of the tridiagonal schemes of order 'N'. The 'PN' schemes are pentadiagonal schemes of order 'N'. Two additional schemes are given, S8 and S10, which are septadiagonal schemes for the first derivative of order eight and ten. By increasing the band width of the matrix for the first derivative from five to seven, the minimum order of formal accuracy is increased by two. The parameter γ is the additional term in the left-hand side of the compact scheme when the bandwidth is increased from five to seven.

An analogous procedure can be applied to the second derivative scheme (2.10). In Table 2, values of the coefficients for the various orders of formal accuracy are listed.

Scheme	γ	β	α	a	b	c	d	Order
T4			$\frac{1}{4}$	$\frac{3}{2}$				4
T6			$\frac{1}{3}$	$\frac{14}{9}$	$\frac{1}{9}$			6
T8			$\frac{3}{8}$	$\frac{25}{16}$	$\frac{1}{5}$	$\frac{-1}{80}$		8
T10			$\frac{2}{5}$	$\frac{39}{25}$	$\frac{4}{15}$	$\frac{-1}{35}$	$\frac{1}{525}$	10
P6		$\frac{-1}{114}$	$\frac{17}{57}$	$\frac{30}{19}$				6
P8		$\frac{1}{36}$	$\frac{4}{9}$	$\frac{40}{27}$	$\frac{25}{54}$			8
P10		$\frac{1}{20}$	$\frac{1}{2}$	$\frac{17}{12}$	$\frac{101}{150}$	$\frac{1}{100}$		10
P12		$\frac{1}{15}$	$\frac{8}{15}$	$\frac{308}{225}$	$\frac{182}{225}$	$\frac{4}{175}$	$\frac{-1}{1575}$	12
S8	$\frac{5}{4688}$	$\frac{-9}{586}$	$\frac{487}{1519}$	$\frac{945}{586}$				8
S10	$\frac{-1}{2540}$	$\frac{111}{2540}$	$\frac{249}{508}$	$\frac{182}{127}$	$\frac{161}{254}$			10

Table 1: Coefficients of interior schemes for first derivative

Scheme	β	α	a	b	c	d	Order
T4		$\frac{1}{10}$	$\frac{6}{5}$				4
T6		$\frac{2}{11}$	$\frac{12}{11}$	$\frac{3}{11}$			6
T8		$\frac{9}{38}$	$\frac{147}{152}$	$\frac{51}{95}$	$\frac{-23}{760}$		8
T10		$\frac{8}{29}$	$\frac{1126}{1305}$	$\frac{988}{1305}$	$\frac{-74}{1015}$	$\frac{43}{9135}$	10
P6	$\frac{-1}{194}$	$\frac{12}{97}$	$\frac{120}{97}$				6
P8	$\frac{23}{2358}$	$\frac{344}{1179}$	$\frac{320}{393}$	$\frac{310}{393}$			8
P10	$\frac{43}{1798}$	$\frac{334}{899}$	$\frac{1065}{1798}$	$\frac{1038}{899}$	$\frac{79}{1798}$		10

Table 2: Coefficients of interior schemes for second derivative

Centered compact schemes for higher order derivatives are easily constructed in the same manner. A few coefficients for the third derivative schemes are given in Table 3 as derived by [17] and [15].

Scheme	α	a	b	Order
T4	$\frac{1}{2}$	2		4
T6	$\frac{7}{16}$	2	$-\frac{1}{8}$	6

Table 3: Coefficients of interior schemes for third derivative

2.2 Padé Approximations

As stated earlier, one of the first formulation of compact schemes was given by Kopal [12] in 1961. This formulation was not clear as was the notation of Collatz [6] as Kopal used a distinct operator notation for the differencing scheme. The following presents a detailed derivation of Kopal's result. First, a uniform sequence of real numbers (with step size h) given by $x_0, x_1, \ldots, x_i, \ldots$ defined as $x_i = x_0 + ih$. The differencing operator E is defined as

$$E = e^{h\, d/dx} = I + h\frac{d}{dx} + \frac{h^2}{2!}\frac{d^2}{dx^2} + \frac{h^3}{3!}\frac{d^3}{dx^3} + \cdots . \tag{2.19}$$

This operator is called the forward shift operator due to the fact that

$$E\phi_i = E\phi(x_i) = \phi(x_i) + h\,\phi'(x_i) + \frac{h^2}{2!}\phi''(x_i) + \frac{h^3}{3!}\phi'''(x_i) + \cdots = \phi(x_i + h) = \phi_{i+1}.$$

From (2.19), it is found that the first derivative operator can be written in terms of E as

$$\frac{d}{dx} = \frac{\log(E)}{h}.$$

Other well-known differencing operators are

$$\mu\phi_i = \frac{1}{2}(\phi_{i+1/2} + \phi_{i-1/2}) \quad \text{and} \quad \delta\phi_i = \phi_{i+1/2} - \phi_{i-1/2}.$$

Remark 1. *The operator μ can be written as*

$$\mu = \sqrt{1 + \frac{1}{4}\delta^2} \tag{2.20}$$

First, note that

$$\mu^2\phi_i = \frac{1}{4}\left(\phi_{i+1} + 2\phi_i + \phi_{i-1}\right)$$

and

$$\left(1 + \frac{1}{4}\delta^2\right)(\phi_i) = \phi_i + \frac{1}{4}(\phi_{i+1} - 2\phi_i + \phi_{i-1})$$

$$= \frac{1}{4}(\phi_{i+1} + 2\phi_i + \phi_{i-1}).$$

Therefore,

$$\mu^2 \phi_i = \left(1 + \frac{1}{4}\delta^2\right)\phi_i.$$

As a consequence, $\mu^2 = \left(1 + \frac{1}{4}\delta^2\right)$ and (2.20) follows.

Remark 2. *The first derivative operator can now be expressed as*

$$\frac{d}{dx} = \frac{2}{h}\sinh^{-1}\left(\frac{\delta}{2}\right). \tag{2.21}$$

In fact,

$$\frac{1}{2}\delta\phi_i = \frac{1}{2}(\phi_{i+1/2} - \phi_{i-1/2})$$

$$= \frac{1}{2}(\exp^{\frac{h}{2}\frac{d}{dx}} - \exp^{-\frac{h}{2}\frac{d}{dx}})$$

$$= \left[\sinh\left(\frac{h}{2}\frac{d}{dx}\right)\right]\phi_i.$$

This implies

$$\frac{\delta}{2} = \sinh\left(\frac{h}{2}\frac{d}{dx}\right).$$

Then, by taking the inverse of sinh and solving for $\dfrac{d}{dx}$, equation (2.21) is obtained.

In Kopal, pp. 552, the coefficients of Padé rational approximations for the first derivative operator divided by the operator μ are listed. A summary of how the approximations are obtained is given in the following lines.

Remark 3. *The first derivative operator can be written as the infinite series*

$$
\frac{d}{dx} = \frac{2}{h} \sinh^{-1}\left(\frac{\delta}{2}\right)
$$

$$
= \frac{2}{h}\left[\frac{\delta}{2} - \left(\frac{1}{2}\right)\frac{\delta^3}{2^3 \cdot 3} + \left(\frac{1 \cdot 3}{2 \cdot 4}\right)\frac{\delta^5}{2^5 \cdot 5} - \cdots - \left(\frac{1 \cdot 3 \cdot 5 \cdot 7 \cdot 9}{2 \cdot 4 \cdot 6 \cdot 8 \cdot 10}\right)\frac{\delta^{11}}{2^{11} \cdot 11} + \cdots\right]
$$

$$
= \frac{1}{h}\left[\delta - \left(\frac{1}{2^3 \cdot 3}\right)\delta^3 + \left(\frac{1 \cdot 3}{2^5 \cdot 4 \cdot 5}\right)\delta^5 - \cdots - \left(\frac{1 \cdot 3 \cdot 5 \cdot 7 \cdot 9}{2^{11} \cdot 4 \cdot 6 \cdot 8 \cdot 10 \cdot 11}\right)\delta^{11} + \cdots\right]
$$

The Taylor series expansion of $\sinh^{-1} x$ is

$$
\sinh^{-1} x = \sum_{n=0}^{\infty}\left(\frac{(-1)^n (2n)!}{2^{2n}(n!)^2}\right)\frac{x^{2n+1}}{2n+1}
$$

$$
= x - \left(\frac{1}{2}\right)\frac{x^3}{3} + \left(\frac{1 \cdot 3}{2 \cdot 4}\right)\frac{x^5}{5} - \left(\frac{1 \cdot 3 \cdot 5}{2 \cdot 4 \cdot 6}\right)\frac{x^7}{7} + \cdots.
$$

Thus, substituting this expansion into (2.21), the above expression for the derivative operator is obtained.

The odd powers of δ in the expansion do not give difference formulas with integer subscripts. As it will be shown below, Kopal modified this expansion by dividing it by the centered finite difference approximation of the first derivative of a discrete function, ϕ_i, given by $\mu\delta\phi_i = \frac{1}{2}\left(\phi_{i+1} - \phi_{i-1}\right) = \delta\mu\phi_i$. The commutativity of μ and δ is straightforward to prove. Kopal then constructed rational approximations of the new expansion to obtain formulas for compact centered finite difference schemes of various orders. The following remark begins this construction.

Remark 4. *The first derivative operator can be expanded as the following infinite series times the centered difference operator $\mu\delta$*

$$
\frac{d}{dx} = \frac{1}{h}\left[1 - \frac{1}{6}\delta^2 + \frac{1}{30}\delta^4 - \frac{1}{140}\delta^6 + \frac{1}{630}\delta^8 - \frac{1}{2772}\delta^{10} + \cdots\right]\mu\delta \qquad (2.22)
$$

To show this statement, the expansion on Remark 3 is divided by the centered

23

operator $\mu\delta$ followed by a substitution using the equivalence operator (2.20):

$$
\begin{aligned}
\frac{2}{h\,\mu\delta}\sinh^{-1}\left(\frac{\delta}{2}\right) &= \frac{2}{h\,\delta}\sinh^{-1}\left(\frac{\delta}{2}\right)\mu^{-1} \\
&= \frac{1}{h}\left[\frac{2}{\delta}\sinh^{-1}\left(\frac{\delta}{2}\right)\right]\left[\left(1+\frac{1}{4}\delta^2\right)^{-1/2}\right] \\
&= \left[1 - \frac{1}{2^3\cdot 3}\delta^2 + \frac{1\cdot 3}{2^5\cdot 4\cdot 5}\delta^4 + \cdots\right]\left[1 - \frac{1}{2\cdot 4}\delta^2 + \frac{1\cdot 3}{2^3\cdot 4^2}\delta^4 + \cdots\right] \\
&= \frac{1}{h}\left[1 - \frac{1}{6}\delta^2 + \frac{1}{30}\delta^4 + \cdots\right].
\end{aligned}
\tag{2.23}
$$

Therefore, (2.22) follows after multiplication by $\mu\delta$.

Theorem 4. *The tridiagonal centered compact schemes (1.3) and (2.7) of fourth and sixth order respectively, can be obtained from the rational Padé approximation of the infinite series (2.23).*

Proof. The rational function approximation (as outlined in [5]) of the product of the two operators

$$
\left[\frac{2}{\delta}\sinh^{-1}\left(\frac{\delta}{2}\right)\right]\left[\left(1+\frac{1}{4}\delta^2\right)^{-1/2}\right]
$$

with a polynomial of degree zero in the numerator and a first degree polynomial in the denominator is given by

$$
\frac{P(\delta^2)}{Q(\delta^2)} = \frac{p_0}{1+q_1\delta^2}.
\tag{2.24}
$$

The coefficients p_0 and q_1 are found by solving the system of equations

$$
1 - p_0 = 0, \qquad q_1 - \frac{1}{6} = 0
$$

Thus, the approximation of (2.23) for polynomials of the given order is

$$
\frac{P(\delta^2)}{Q(\delta^2)} = \frac{1}{1+\frac{1}{6}\delta^2}.
\tag{2.25}
$$

Substituting this rational approximation into (2.22), and by acting the resulting op-

24

erator on ϕ_i leads to

$$\phi_i' \approx \frac{1}{h}\left(\frac{1}{1+\frac{1}{6}\delta^2}\right)\mu\delta\phi_i = \left(\frac{1}{1+\frac{1}{6}\delta^2}\right)\frac{(\phi_{i+1}-\phi_{i-1})}{2h}.$$

By cross multiplying this operator in the denominator to the left-hand side, the numerical approximation formula

$$(1+\frac{1}{6}\delta^2)\phi_i' = \frac{1}{6}\phi_{i-1}' + \frac{2}{3}\phi_i' + \frac{1}{6}\phi_{i+1}' = \frac{(\phi_{i+1}-\phi_{i-1})}{2h}$$

is obtained. Multiplication of this equation by $\frac{6}{4}$ yields the tridiagonal centered fourth order compact scheme (1.3).

A compact scheme of sixth order can be obtained by employing polynomials of degree one in both numerator and denominator of the rational approximations:

$$\frac{P(\delta^2)}{Q(\delta^2)} = \frac{p_0 + p_1\delta^2}{1 + q_1\delta^2}. \tag{2.26}$$

The coefficients are determined by solving the system of equations

$$1 - p_0 = 0, \qquad q_1 - \frac{1}{6} - p_1 = 0, \qquad -\frac{1}{6}q_1 + \frac{1}{30} = 0$$

and it results the difference operator

$$\frac{P(\delta^2)}{Q(\delta^2)} = \frac{1+\frac{1}{30}\delta^2}{1+\frac{1}{5}\delta^2}. \tag{2.27}$$

Substituting this rational approximation into (2.22) and by applying the resulting operator to ϕ_i leads to the tridiagonal sixth order scheme T6 given by

$$\frac{1}{3}\phi_{i-1}' + \phi_i' + \frac{1}{3}\phi_{i+1}' = \frac{7}{9h}(\phi_{i+1}-\phi_{i-1}) + \frac{1}{36h}(\phi_{i+2}-\phi_{i-2}).$$

25

Table 4 shows the Padé approximations of the derivative operator for each of the first derivative interior compact schemes presented in Section 2.1.

Scheme	Numerator	Denominator
T4	1	$1 + \frac{1}{6}\delta^2$
T6	$1 + \frac{1}{30}\delta^2$	$1 + \frac{1}{5}\delta^2$
T8	$1 + \frac{1}{21}\delta^2 - \frac{1}{420}\delta^4$	$1 + \frac{3}{14}\delta^2$
T10	$1 + \frac{1}{18}\delta^2 - \frac{1}{270}\delta^4 + \frac{1}{3780}\delta^6$	$1 + \frac{2}{9}\delta^2$
P6	1	$1 + \frac{1}{6}\delta^2 - \frac{1}{180}\delta^4$
P8	$1 + \frac{5}{42}\delta^2$	$1 + \frac{2}{7}\delta^2 + \frac{1}{70}\delta^4$
P10	$1 + \frac{1}{6}\delta^2 + \frac{1}{630}\delta^4$	$1 + \frac{1}{3}\delta^2 + \frac{1}{42}\delta^4$
S8	1	$1 + \frac{1}{6}\delta^2 - \frac{1}{180}\delta^4 + \frac{1}{1512}\delta^6$
S10	$1 + \frac{23}{150}\delta^2$	$1 + \frac{8}{25}\delta^2 + \frac{1}{50}\delta^4 - \frac{1}{5250}\delta^6$

Table 4: Padé approximations of first derivative operator for compact schemes

2.3 One-Sided Boundary and Near Boundary Schemes

Most physical problems are defined on bounded domains. Their formulation requires boundary conditions. For instance, suppose the domain of the problem consists of the interval $[a, b]$. Then physical boundary conditions appropriate to the particular problem should be imposed at the boundary points a and b respectively. To obtain the approximate solution, the interval $[a, b]$ is partitioned in N equally spaced subintervals with nodes $a = x_1, x_2, \ldots, x_{N-1}, x_N = b$. An application of any of the centered compact schemes derived in the previous sections at the boundary points $x_1 = a$ or $x_N = b$ requires points out the bounded interval $[a, b]$, some to the right of x_N and others to the left of x_1. For larger stencils, not only the boundary grid points x_1 and x_N present this behavior but also near boundary points such as x_2, x_{N-1}, or others depending on the stencil size.

For problems posed with periodic boundary conditions, the interior scheme suffices. At the boundary point x_1 and other near boundary points, any schemes with stencils that protrude the domain can substitute the appropriate boundary points on the other side of the domain. For example, the tridiagonal fourth order scheme for the first derivative (2.9) at x_1 will require one point to the left of the domain. Assuming that the boundary conditions are periodic, the value at x_{N-1} can be used in place of this point. Thus the fourth order compact scheme at x_1 will be

$$\alpha\phi'_{N-1} + \phi'_1 + \alpha\phi'_2 = \frac{a}{2h}(\phi_2 - \phi_{N-1}).$$

A similar formula,

$$\alpha\phi'_{N-1} + \phi'_N + \alpha\phi'_2 = \frac{a}{2h}(\phi_{N-1} - \phi_2),$$

determine the approximation at x_N.

For non-periodic boundary conditions, one-sided compact schemes can be defined at boundary points to avoid using points outside the domain. They can be constructed such that the banded (tridiagonal, pentadiagonal, etc) form of the interior scheme is maintained. Also, their stencil size can be adjusted to match the formal order of accuracy of the corresponding interior scheme.

Various one-sided compact formulas for the first derivative can be obtained from the following general formulas at the boundary and near boundary grid points.

First derivative boundary point 1

$$
\begin{aligned}
&\phi'_1 + \alpha_1\phi'_2 + \beta_1\phi'_3 \\
&= \frac{1}{h}(a_1\phi_1 + b_1\phi_2 + c_1\phi_3 + d_1\phi_4 + \cdots + i_1\phi_9 + j_1\phi_{10} + k_1\phi_{11})
\end{aligned}
\tag{2.28}
$$

27

First derivative boundary point 2

$$\alpha_{2,1}\phi'_1 + \phi'_2 + \alpha_{2,2}\phi'_3 + \beta_2\phi'_4$$
$$= \frac{1}{h}(a_2\phi_1 + b_2\phi_2 + c_2\phi_3 + d_2\phi_4 + \cdots + h_2\phi_8 + i_2\phi_9 + j_{10}\phi_{10})$$

(2.29)

First derivative boundary point 3

$$\beta_{3,1}\phi'_1 + \alpha_{3,1}\phi'_2 + \phi'_3 + \alpha_{3,2}\phi'_4 + \beta_{3,2}\phi'_5$$
$$= \frac{1}{h}(a_3\phi_1 + b_3\phi_2 + c_3\phi_3 + d_3\phi_4 + \cdots + g_3\phi_7 + h_3\phi_8 + i_3\phi_9)$$

First derivative boundary point 4

$$\beta_{4,1}\phi'_2 + \alpha_{4,1}\phi'_3 + \phi'_4 + \alpha_{4,2}\phi'_5 + \beta_{4,2}\phi'_6$$
$$= \frac{1}{h}(a_4\phi_1 + b_4\phi_2 + c_4\phi_3 + d_4\phi_4 + \cdots + g_4\phi_7 + h_4\phi_8 + i_4\phi_9)$$

First derivative boundary point $N-3$

$$\beta_{N-3,1}\phi'_{N-5} + \alpha_{N-3,1}\phi'_{N-4} + \phi'_{N-3} + \alpha_{N-3,2}\phi'_{N-2} + \beta_{N-3,2}\phi'_{N-1}$$
$$= \frac{1}{h}(a_{N-3}\phi_N + b_{N-3}\phi_{N-1} + c_{N-3}\phi_{N-2} + \cdots + g_{N-3}\phi_{N-6} + h_{N-3}\phi_{N-7} + i_{N-3}\phi_{N-8})$$

First derivative boundary point $N-2$

$$\beta_{N-2,1}\phi'_{N-4} + \alpha_{N-2,1}\phi'_{N-3} + \phi'_{N-2} + \alpha_{N-2,2}\phi'_{N-1} + \beta_{N-2,2}\phi'_N$$
$$= \frac{1}{h}(a_{N-2}\phi_N + b_{N-2}\phi_{N-1} + c_{N-2}\phi_{N-2} + \cdots + g_{N-2}\phi_{N-6} + h_{N-2}\phi_{N-7} + i_{N-2}\phi_{N-8})$$

First derivative boundary point $N-1$

$$\beta_{N-1}\phi'_{N-3} + \alpha_{N-1,1}\phi'_{N-2} + \phi'_{N-1} + \alpha_{N-1,2}\phi'_N$$
$$= \frac{1}{h}(a_{N-1}\phi_N + b_{N-1}\phi_{N-1} + c_{N-1}\phi_{N-2} + \cdots + g_{N-1}\phi_{N-6} + h_{N-1}\phi_{N-7} + i_{N-1}\phi_{N-8})$$

First derivative boundary point N

$$\beta_N \phi'_{N-2} + \alpha_N \phi'_{N-1} + \phi'_N$$
$$= \frac{1}{h}(a_N \phi_N + b_N \phi_{N-1} + c_N \phi_{N-2} + \cdots + g_N \phi_{N-6} + h_N \phi_{N-7} + i_N \phi_{N-8})$$

The left-hand side of the boundary formulas above have been chosen such that fewer right-hand side terms are required, that is, there is no requirement of symmetry of the α and β terms. Maintaining the symmetry in the left-hand side of the boundary schemes keeps the symmetry of the complete linear system but reduces the degrees of freedom. Therefore, to obtain differencing formulas of higher order, the stencil of grid points in the right-hand side must be increased.

The Taylor series matching procedure, already employed in the construction of the interior schemes, applied to the boundary formula (2.28) at node 1 results in a system of equations for the unknowns parameters: α_1, β_1, a_1, b_1, c_1, etc. This system of equations is presented in Appendix C. By requiring the coefficients to satisfy the successive equations results in a sequence of higher order schemes. The maximum order for the family of one-sided boundary schemes represented by (2.28) when all equations are simultaneously satisfied is twelve. A list of coefficients values for tridiagonal and pentadiagonal one-sided boundary compact schemes at node 1 is given in Table 5.

	β	α	a	b	c	d	e	f	g	h	i	j	k	Order
T4		3	$\frac{-17}{6}$	$\frac{3}{2}$	$\frac{3}{2}$	$\frac{-1}{6}$								4
T6		5	$\frac{-197}{60}$	$\frac{-5}{12}$	5	$\frac{-5}{3}$	$\frac{5}{12}$	$\frac{-1}{20}$						6
T8		7	$\frac{-503}{140}$	$\frac{-63}{20}$	$\frac{21}{2}$	$\frac{-35}{6}$	$\frac{35}{12}$	$\frac{-21}{20}$	$\frac{7}{30}$	$\frac{-1}{42}$				8
T10		9	$\frac{-2485}{649}$	$\frac{-1809}{280}$	18	-14	$\frac{21}{2}$	$\frac{-63}{10}$	$\frac{14}{5}$	$\frac{-6}{7}$	$\frac{9}{56}$	$\frac{-1}{72}$		10
P6	6	8	$\frac{-43}{12}$	$\frac{-20}{3}$	9	$\frac{4}{3}$	$\frac{-1}{12}$							6
P8	15	12	$\frac{-79}{20}$	$\frac{-77}{5}$	$\frac{55}{4}$	$\frac{20}{3}$	$\frac{-5}{4}$	$\frac{1}{5}$	$\frac{-1}{60}$					8
P10	28	16	$\frac{-1181}{280}$	$\frac{-892}{35}$	$\frac{77}{5}$	$\frac{56}{3}$	$\frac{-35}{6}$	$\frac{28}{15}$	$\frac{-7}{15}$	$\frac{8}{105}$	$\frac{-1}{168}$			10
P12	45	20	$\frac{-1590}{359}$	$\frac{-4609}{126}$	$\frac{711}{56}$	40	$\frac{-35}{2}$	$\frac{42}{5}$	$\frac{-7}{2}$	$\frac{8}{7}$	$\frac{-15}{56}$	$\frac{5}{126}$	$\frac{-1}{360}$	12

Table 5: Coefficients of boundary schemes for first derivative at node 1

29

For the one-sided compact scheme approximating the first derivative at the second boundary point (2.29), the system of equations to be solved changes in the left-hand side due to one additional term. The right-hand side is altered due to the fact that the function is now centered about the second node as opposed to the first. The system of equations for node 2 resulting after the matching of Taylor expansions is also given in Appendix C.

All other one-sided compact schemes for the first derivative at boundary or near boundary points are found using the same matching procedure. Tables 6 through 8 list values for tridiagonal and pentadiagonal schemes at nodes 2, 3, and 4.

	β	α_1	α_2	a	b	c	d	e	f	g	h	i	j	Order
T6	$\frac{1}{8}$	$\frac{3}{4}$		$\frac{-43}{96}$	$\frac{-5}{6}$	$\frac{9}{8}$	$\frac{1}{6}$	$\frac{-1}{96}$						6
T8	$\frac{1}{12}$	$\frac{5}{4}$		$\frac{-79}{240}$	$\frac{-77}{60}$	$\frac{55}{48}$	$\frac{5}{9}$	$\frac{-5}{48}$	$\frac{1}{60}$	$\frac{-1}{720}$				8
T10	$\frac{1}{16}$	$\frac{7}{4}$		$\frac{-1181}{4480}$	$\frac{-223}{140}$	$\frac{77}{80}$	$\frac{7}{6}$	$\frac{-35}{96}$	$\frac{7}{60}$	$\frac{-7}{240}$	$\frac{1}{210}$	$\frac{-1}{2688}$		10
P8	$\frac{1}{15}$	2	$\frac{2}{3}$	$\frac{-247}{900}$	$\frac{-19}{12}$	$\frac{1}{3}$	$\frac{13}{9}$	$\frac{1}{12}$	$\frac{-1}{300}$					8
P10	$\frac{5}{3}$	$\frac{1}{21}$	3	$\frac{-544}{2581}$	$\frac{-39}{20}$	$\frac{-17}{20}$	$\frac{95}{36}$	$\frac{5}{12}$	$\frac{-1}{20}$	$\frac{1}{180}$	$\frac{-1}{2940}$			10
P12	$\frac{28}{9}$	$\frac{1}{27}$	4	$\frac{-857}{4963}$	$\frac{-621}{280}$	$\frac{-83}{35}$	$\frac{511}{135}$	$\frac{7}{6}$	$\frac{-7}{30}$	$\frac{7}{135}$	$\frac{-1}{105}$	$\frac{1}{840}$	$\frac{-1}{13608}$	12

Table 6: Coefficients of boundary schemes for first derivative at node 2

	β_1	β_2	α_1	α_2	a	b	c	d	e	f	g	h	i	Order
T8			$\frac{13}{55}$	$\frac{6}{11}$	$\frac{-1}{66}$	$\frac{-2051}{3300}$	$\frac{-53}{132}$	$\frac{31}{33}$	$\frac{7}{66}$	$\frac{-1}{132}$	$\frac{1}{3300}$			8
T10			$\frac{1}{7}$	1	$\frac{-1}{168}$	$\frac{-433}{980}$	$\frac{-19}{20}$	$\frac{21}{20}$	$\frac{5}{12}$	$\frac{-1}{20}$	$\frac{1}{60}$	$\frac{-1}{420}$	$\frac{1}{5880}$	10
P10	$\frac{1}{90}$	1	$\frac{4}{15}$	$\frac{8}{9}$	$\frac{-34}{675}$	$\frac{-127}{225}$	$\frac{-7}{12}$	$\frac{20}{27}$	$\frac{4}{9}$	$\frac{1}{75}$	$\frac{-1}{2700}$			10
P12	$\frac{1}{168}$	$\frac{5}{12}$	$\frac{4}{21}$	$\frac{4}{3}$	$\frac{-115}{4024}$	$\frac{-1019}{2205}$	$\frac{-19}{20}$	$\frac{23}{45}$	$\frac{125}{144}$	$\frac{1}{15}$	$\frac{-1}{180}$	$\frac{1}{2205}$	$\frac{-1}{47040}$	12

Table 7: Coefficients of boundary schemes for first derivative at node 3

	β_1	β_2	α_1	α_2	a	b	c	d	e	f	g	h	i	Order
T10			$\frac{1}{4}$	$\frac{5}{8}$	$\frac{1}{1344}$	$\frac{-1}{42}$	$\frac{-49}{80}$	$\frac{-9}{20}$	$\frac{15}{16}$	$\frac{1}{6}$	$\frac{-1}{48}$	$\frac{1}{420}$	$\frac{-1}{6720}$	10
P12	$\frac{1}{42}$	$\frac{1}{6}$	$\frac{1}{3}$	$\frac{5}{6}$	$\frac{-1}{1680}$	$\frac{-193}{2205}$	$\frac{-107}{180}$	$\frac{-9}{20}$	$\frac{25}{36}$	$\frac{19}{45}$	$\frac{1}{60}$	$\frac{-1}{1260}$	$\frac{1}{35280}$	12

Table 8: Coefficients of boundary schemes for first derivative at node 4

The coefficients for the one-sided boundary compact schemes for the first derivative at nodes $N, N-1, N-2$, and $N-3$ are also determined with the same matching

procedure. These schemes have right-hand side coefficients that are the negative of the coefficients obtained for nodes 1, 2, 3, and 4, that is, $a_N = -a_1, b_N = -b_1$, etc.

The one-sided boundary compact schemes for the second derivative are similar to those of the first derivative. For example, the boundary formula at node 1 is given by

$$\phi_1'' + \alpha \phi_2'' + \beta \phi_3'' = \frac{1}{h^2}(a\phi_1 + b\phi_2 + \cdots + i\phi_9 + j\phi_{10}).$$

Coefficients of boundary compact schemes at other nodes for the second derivative are listed in Appendix D. These boundary compact schemes at nodes $N-3, N-2, N-1$, and N have the same coefficients as the schemes for nodes 1, 2, 3, and 4, that is, $a_N = a_1, b_N = b_1$, etc.

2.4   Matrix Representation

Having defined the interior centered compact schemes in Section 2.1 and the one-sided boundary compact schemes in Section 2.3, it is possible to determine values of the first and higher order derivatives from known values of the function on a given partition of the domain. Consider a partition of the interval $[a, b]$ in N equally spaced subintervals with nodes $a = x_1, x_2, \ldots, x_{N-1}, x_N = b$ for the one-dimensional case. Then the first derivative values can be calculated by compact schemes of the same formal order of accuracy at every grid point.

Any compact scheme can be represented as a linear system of equations given by

$$A\phi' = \frac{1}{h}B\phi. \tag{2.30}$$

In particular, a sixth order tridiagonal scheme is shown in explicitly in Figure 3.

The first equation of this linear system corresponds to the one-sided compact scheme of sixth order whose coefficients are listed in the second row of Table 5. Similarly, the second equation also comes from a sixth order boundary scheme whose

$$
\begin{bmatrix}
1 & 5 & 0 & 0 & 0 & 0 & \cdots & & \\
\frac{1}{8} & 1 & \frac{3}{4} & 0 & 0 & 0 & \cdots & & \\
0 & \frac{1}{3} & 1 & \frac{1}{3} & 0 & 0 & \cdots & & \\
0 & 0 & \frac{1}{3} & 1 & \frac{1}{3} & 0 & \cdots & & \\
\vdots & \vdots & \ddots & \ddots & \ddots & \ddots & \ddots & \vdots & \vdots \\
& & \cdots & 0 & \frac{1}{3} & 1 & \frac{1}{3} & 0 & 0 \\
& & \cdots & 0 & 0 & \frac{1}{3} & 1 & \frac{1}{3} & 0 \\
& & \cdots & 0 & 0 & 0 & \frac{3}{4} & 1 & \frac{1}{8} \\
& & \cdots & 0 & 0 & 0 & 0 & 5 & 1
\end{bmatrix}
\begin{bmatrix}
\phi'_1 \\ \phi'_2 \\ \phi'_3 \\ \phi'_4 \\ \vdots \\ \phi'_{N-3} \\ \phi'_{N-2} \\ \phi'_{N-1} \\ \phi'_N
\end{bmatrix}
$$

$$
= \frac{1}{h}
\begin{bmatrix}
\frac{-197}{60} & -\frac{5}{12} & 5 & -\frac{5}{3} & \frac{5}{12} & -\frac{1}{20} & 0 & & \\
-\frac{43}{96} & -\frac{5}{6} & \frac{9}{8} & \frac{1}{6} & -\frac{1}{96} & 0 & 0 & & \\
-\frac{1}{36} & -\frac{14}{18} & 0 & \frac{14}{18} & \frac{1}{36} & 0 & 0 & & \\
0 & -\frac{1}{36} & -\frac{14}{18} & 0 & \frac{14}{18} & \frac{1}{36} & 0 & & \\
\vdots & \ddots & \ddots & \ddots & \ddots & \ddots & \ddots & \ddots & \vdots \\
& 0 & -\frac{1}{36} & -\frac{14}{18} & 0 & \frac{14}{18} & \frac{1}{36} & 0 & \\
& 0 & 0 & -\frac{1}{36} & -\frac{14}{18} & 0 & \frac{14}{18} & \frac{1}{36} & \\
& 0 & 0 & \frac{1}{96} & -\frac{1}{6} & -\frac{9}{8} & \frac{5}{6} & \frac{43}{96} & \\
& 0 & \frac{1}{20} & -\frac{5}{12} & \frac{5}{3} & -5 & \frac{5}{12} & \frac{197}{60} &
\end{bmatrix}
\begin{bmatrix}
\phi_1 \\ \phi_2 \\ \phi_3 \\ \phi_4 \\ \vdots \\ \phi_{N-3} \\ \phi_{N-2} \\ \phi_{N-1} \\ \phi_N
\end{bmatrix}
$$

Figure 3: Complete sixth order matrix system

coefficients are listed in the first row of Table 6. The following intermediate rows all correspond to sixth order centered compact schemes at the interior nodes which are listed in the second row of Table 1. Finally, the last two rows of Figure 3 correspond to one-sided sixth order compact schemes which are applied at x_{N-1} and x_N respectively.

When the boundary conditions include values of the unknown function at $x_1 = a$ or $x_N = b$ (Dirichlet boundary conditions), two different approaches may be taken. The simplest approach as suggested by Lele [15] is to exclude the boundary equations at node 1 or node N. This means that the first row and column or the last row and column of the matrices in (2.30) should be eliminated. A more appropriate method is to substitute the known boundary value into the boundary formula at node 1 or N and then combine the derivative value at that node with the adjacent boundary formula as demonstrated by Carpenter *et al.* [4]. To maintain the stability of the scheme with this approach, the boundary formula were the boundary value is known must be at most one degree less than the interior scheme. The reduction of formal order of accuracy maintains stability and generally does not diminish the order of convergence of the scheme.

Computation of the first derivative with a higher order of formal accuracy requires that more rows of the linear system correspond to boundary formulas as shown in the matrix representation (2.31) on the following page. Depending on the parameter choices, every equation of the following linear system represents a maximum tenth order scheme with at most a seven point stencil.

For a two-dimensional problem, both partial derivatives in x and y may need to be approximated. By using an equal number of grid points in both directions, this is accomplished quite readily. For a fixed y value, the compact scheme is used to approximate all partial derivatives with respect to x. This is done for all y values. The partial derivatives with respect to y are approximated in a similar fashion for all fixed x. The stencil diagram for a two-dimensional problem is shown in Figure 4.

$$
\begin{bmatrix}
1 & \alpha_1 & \beta_1 & 0 & 0 & 0 & 0 & 0 & 0 & \cdots & & & \\
\alpha_{2,1} & 1 & \alpha_{2,2} & \beta_2 & 0 & 0 & 0 & 0 & 0 & \cdots & & & \\
\beta_{3,1} & \alpha_{3,1} & 1 & \alpha_{3,2} & \beta_{3,2} & 0 & 0 & 0 & 0 & \cdots & & & \\
0 & \beta & \alpha & 1 & \alpha & \beta & 0 & 0 & 0 & \cdots & & & \\
0 & 0 & \beta & \alpha & 1 & \alpha & \beta & 0 & 0 & \cdots & & & \\
0 & 0 & 0 & \beta & \alpha & 1 & \alpha & \beta & 0 & \cdots & & & \\
\vdots & \vdots & \vdots & \ddots & \ddots & \ddots & \ddots & \ddots & \ddots & \ddots & \vdots & \vdots & \vdots \\
& & & \cdots & 0 & \beta & \alpha & 1 & \alpha & \beta & 0 & 0 & 0 \\
& & & \cdots & 0 & 0 & \beta & \alpha & 1 & \alpha & \beta & 0 & 0 \\
& & & \cdots & 0 & 0 & 0 & \beta & \alpha & 1 & \alpha & \beta & 0 \\
& & & \cdots & 0 & 0 & 0 & 0 & \beta_{3,2} & \alpha_{3,2} & 1 & \alpha_{3,1} & \beta_{3,1} \\
& & & \cdots & 0 & 0 & 0 & 0 & 0 & \beta_2 & \alpha_{2,2} & 1 & \alpha_{2,1} \\
& & & \cdots & 0 & 0 & 0 & 0 & 0 & 0 & \beta_1 & \alpha_1 & 1
\end{bmatrix}
\begin{bmatrix}
\phi'_1 \\ \phi'_2 \\ \phi'_3 \\ \phi'_4 \\ \phi'_5 \\ \phi'_6 \\ \vdots \\ \phi'_{N-5} \\ \phi'_{N-4} \\ \phi'_{N-3} \\ \phi'_{N-2} \\ \phi'_{N-1} \\ \phi'_N
\end{bmatrix}
$$

$$
= \frac{1}{h}
\begin{bmatrix}
a_1 & b_1 & c_1 & d_1 & e_1 & f_1 & g_1 & h_1 & i_1 & 0 & \cdots & & \\
a_2 & b_2 & c_2 & d_2 & e_2 & f_2 & g_2 & h_2 & 0 & 0 & \cdots & & \\
a_3 & b_3 & c_3 & d_3 & e_3 & f_3 & g_3 & 0 & 0 & 0 & \cdots & & \\
-\frac{c}{6} & -\frac{b}{4} & -\frac{a}{2} & 0 & \frac{a}{2} & \frac{b}{4} & \frac{c}{6} & 0 & 0 & 0 & \cdots & & \\
0 & -\frac{c}{6} & -\frac{b}{4} & -\frac{a}{2} & 0 & \frac{a}{2} & \frac{b}{4} & \frac{c}{6} & 0 & 0 & \cdots & & \\
0 & 0 & -\frac{c}{6} & -\frac{b}{4} & -\frac{a}{2} & 0 & \frac{a}{2} & \frac{b}{4} & \frac{c}{6} & 0 & \cdots & & \\
\vdots & \vdots & \ddots & \ddots & \ddots & \ddots & \ddots & \ddots & \ddots & \ddots & \ddots & \vdots & \vdots \\
& \cdots & 0 & -\frac{c}{6} & -\frac{b}{4} & -\frac{a}{2} & 0 & \frac{a}{2} & \frac{b}{4} & \frac{c}{6} & 0 & 0 \\
& \cdots & 0 & 0 & -\frac{c}{6} & -\frac{b}{4} & -\frac{a}{2} & 0 & \frac{a}{2} & \frac{b}{4} & \frac{c}{6} & 0 \\
& \cdots & 0 & 0 & 0 & -\frac{c}{6} & -\frac{b}{4} & -\frac{a}{2} & 0 & \frac{a}{2} & \frac{b}{4} & \frac{c}{6} \\
& \cdots & 0 & 0 & 0 & -g_3 & -f_3 & -e_3 & -d_3 & -c_3 & -b_3 & -a_3 \\
& \cdots & 0 & 0 & -h_2 & -g_2 & -f_2 & -e_2 & -d_2 & -c_2 & -b_2 & -a_2 \\
& \cdots & 0 & -i_1 & -h_1 & -g_1 & -f_1 & -e_1 & -d_1 & -c_1 & -b_1 & -a_1
\end{bmatrix}
\begin{bmatrix}
\phi_1 \\ \phi_2 \\ \phi_3 \\ \phi_4 \\ \phi_5 \\ \phi_6 \\ \vdots \\ \phi_{N-5} \\ \phi_{N-4} \\ \phi_{N-3} \\ \phi_{N-2} \\ \phi_{N-1} \\ \phi_N
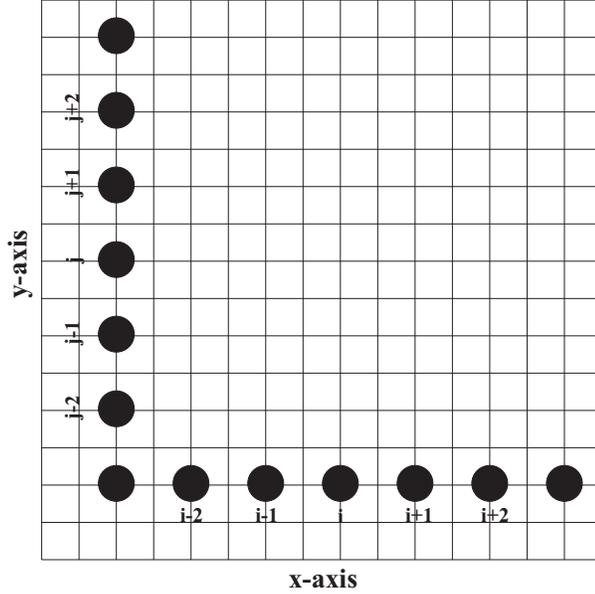\end{bmatrix}
\tag{2.31}
$$

Figure 4: Stencil for two-dimensional problem

The sample MATLAB code given in Appendix B readily computes both partial derivatives with respect to x and y. The code as given will compute y derivatives for all nodes. To compute x derivatives, the transpose of the solution must be input and the code will then give the transpose of the x derivative values at each node.

As it has been said before, the computational time increment, when implicit algorithms such as the compact schemes are implemented, are marginal due to the banded nature of the matrix to be inverted. There exists very efficient algorithms for this type of sparse matrix. For compact schemes implemented in time marching methods, the matrix equation does not need to be solved at each time level. In fact, both left and right-hand side matrices remain unchanged at each time iteration. Therefore, the matrix $\frac{1}{h}A^{-1}B = Q$ may be stored before the time iteration begins. The compact scheme is then implemented with a matrix-vector or matrix-matrix product at each time level. The computational savings by applying the compact scheme in this way is very noteworthy.

Although the matrix Q is defined in term of the inverse of the matrix A, it should

35

be noted that in the computation of Q the matrix A is not to be inverted. The solution of the matrix equation $AQ = B$ is found using a well-known algorithm such as the Thomas algorithm for the tridiagonal case. The matrix Q is then stored and used at each time step to determine the derivative values.

2.5   Matrix Stability Analysis

A stability analysis of some of the compact schemes, constructed in the previous sections, is now performed. For completeness, this section includes the most common definition of stability for finite difference approximations of initial value problems attributed to Lax [8]. First, consider the one-dimensional IVP defined by

$$u_t(x, t) = \mathcal{L}u(x, t), \qquad 0 < x < L, \quad 0 < t < T, \tag{2.32}$$

$$u(x, 0) = f(x), \qquad 0 < x < L, \tag{2.33}$$

where $\mathcal{L}$ is a spatial differential operator and $\boldsymbol{f}$ is periodic on the interval $[0, L]$. Uniform partitions $x_1, x_2, \ldots, x_{M-1}, x_M = L$ and $t_0, t_1, \ldots, t_N = T$ with step sizes Δx for the space variable and Δt for the time variable, respectively, are defined. The values of the numerical approximation to the exact solution at the points (x_i, t_n) are denoted by U_i^n. By employing finite difference formulas to approximate the time and space derivatives a finite difference scheme is obtained. It may be represented as a matrix equation of the form:

$$\boldsymbol{U}^{n+1} = \mathcal{L}_\Delta \boldsymbol{U}^n, \qquad \boldsymbol{U}^0 = \boldsymbol{f}, \tag{2.34}$$

where $\mathcal{L}_\Delta$ is a finite difference operator that depends on the particular finite difference approximations used, $\boldsymbol{U}^n$ is a vector with components U_i^n, and $\boldsymbol{f}$ is a vector whose components are $f_i = f(x_i)$, $i = 1, 2, \ldots, M$.

Definition 5. *Let $\boldsymbol{U}^n$ and $\boldsymbol{V}^n$ satisfy the finite difference scheme (2.34) with different initial conditions $\boldsymbol{U}^0 = \boldsymbol{f}$ and $\boldsymbol{V}^0 = \boldsymbol{g}$, respectively. Then the finite difference scheme (2.34) is stable if there exists a positive constant C independent of the mesh spacing and initial data such that*

$$||\boldsymbol{U}^n - \boldsymbol{V}^n|| \leq C||\boldsymbol{U}^0 - \boldsymbol{V}^0||, \quad n \to \infty, \quad \Delta x \to 0, \quad \Delta t \to 0, \quad n\Delta t \leq T. \quad (2.35)$$

Extension of this definition to higher spatial dimensions is straightforward. As mentioned above, this definition of stability is due to Lax. Strikwerda [21] studied the stability or well-posedness property of initial boundary value problems for the method of lines applied to hyperbolic and parabolic partial differential equations in one space dimension. The method of lines consists of the approximation of IBVP for partial differential equations by IVP for systems of ordinary differential equations. As a result, a semi-discrete approximations of the original IBVP is obtained. In particular, consider an IBVP modeled by the advection equation

$$\frac{\partial u}{\partial t}(x,t) + c\frac{\partial u}{\partial x}(x,t), \quad 0 < x < L, \quad t > 0 \quad c > 0, \quad (2.36)$$

$$u(x,0) = f(x), \quad 0 < x < L, \quad (2.37)$$

$$u(0,t) = g(t), \quad t > 0. \quad (2.38)$$

If a partition $0 = x_1, x_2, \ldots, x_M = L$ is defined in the interval $[0, L]$, then the following system of differential equations results

$$\frac{\partial u}{\partial t}(x_i,t) + c\frac{\partial u}{\partial x}(x_i,t), \quad i = 1,2,3\ldots,M, \quad t > 0. \quad (2.39)$$

$$u(x_i,0) = f(x_i), \quad u(x_1,t) = g(t). \quad (2.40)$$

If a higher order compact scheme is used to approximate $\frac{\partial u}{\partial x}(x_i,t)$ at the grid points $x_1, x_2, \ldots, x_M$, then as stated in Section 2.4, the vector formed from its approxima-

37

tions at every grid point, $\frac{\partial \boldsymbol{U}}{\partial x}(t)$, satisfies the matrix equation.

$$A\frac{\partial \boldsymbol{U}}{\partial x}(t) = \frac{1}{h}B\,\boldsymbol{U}(t) = D\boldsymbol{U}(t), \tag{2.41}$$

where $\boldsymbol{U}(t) = (U(x_1,t), U(x_2,t),\ldots,U(x_M,t))^T = (U_1(t), U_2(t),\ldots,U_M(t))^T$. Substitution of this approximation into (2.39) - (2.40) leads to a system of ordinary differential equations:

$$\frac{d\boldsymbol{U}}{dt}(t) = c(A^{-1}D)\,\boldsymbol{U}(t) = Q\boldsymbol{U}(t), \tag{2.42}$$

$$\boldsymbol{U}(0) = \boldsymbol{f}. \tag{2.43}$$

The exact solution for this problem can be written as $\boldsymbol{U}(t) = e^{tQ}\boldsymbol{f}(x)$. The stability (or well-posedness) of the IVP (2.42) - (2.43) depends on the properties of Q, which includes information from the spatial interior scheme and boundary discretizations [21].

In [13], it was found that stability of the semi-discrete problem implies Lax-stability of the fully discrete problem under certain conditions for the time discretization. This is the content of the following theorem.

Theorem 5. *Under mild restrictions, if a semi-discrete approximation is stable in a generalized sense and a Runge-Kutta method that is locally stable is used to time march the semi-discretization, then the resulting totally discrete approximation is stable in the same sense as long as the stability region of the R-K method encompasses the norm of the semi-discretization.*

Since stability analysis is easier to perform for the semi-discrete approximation than Lax-stability analysis for the fully discrete numerical scheme, Carpenter *et al.* [4] showed stability of this IVP when the spatial discretization is performed using the fourth order interior compact scheme (1.3) combined with the one-sided fourth order

38

compact scheme for the first derivative at node 1, found in the first row of Table 5. To do this, they applied an extension of the stability theory of Gustafson, Kreiss, and Sundstrom (G-K-S) to semi-discrete problems [13]. It consists of breaking the original finite domain modal analysis of the G-K-S stability theory into three equivalent but simpler modal problems.

A fully discrete problem can be obtained from the semi-discrete problem (2.42) - (2.43) by using a conventional Runge-Kutta algorithm of third or fourth order to advance in time. Then, numerical stability for this fully discrete approximation is established from the stability of the corresponding semi-discrete problem by means of the previous theorem due to Kreiss [13].

The Lax-stability definition deals with the "boundedness" behavior of the numerical solution when the mesh size $\Delta x \to 0$ for a fixed time t_0. Lax's equivalence theorem establishes that stable and consistent schemes converges at a fixed time t^* to the analytical solution when the mesh size is refined ($\Delta x \to 0$). As pointed out in [1, 18], nothing in the above definition excludes error growth in time, and it specifically allows exponential growth of the error in time. However, for long time numerical simulation, it is desirable that the numerical solution remain bounded for a fixed spatial mesh ($\Delta x =$ constant) as the time $t \to \infty$.

This property was studied by Abarbanel *et al.* in [1]. They called it "strict stability." In the case of semi-discrete approximations, strict stability implies that for a fixed spatial discretization of size Δx, all eigenvalues of the matrix defining the system of ordinary differential equations have non-positive real part.

In this case, the matrix to be analyzed is the matrix $Q = cA^{-1}D$. It includes the spatial step size Δx so the eigenvalues depends on the step size. For each step size, these eigenvalues can be numerically approximated using the subroutine 'eig' of MATLAB or any other numerical library with a numerical eigenvalue solver.

For the complete compact scheme presented by combining the interior and bound-

ary schemes from sections 2.1 and 2.3, the eigenvalue plots are shown in Figures 5 - 7. It is observed that some of the eigenvalues are located in the right half complex plane for certain schemes. As a consequence, strict stability is not verified and for a fixed grid the solution is expected to blow up for a long time run. However, as discussed before this combined compact scheme is stable in the Lax sense.

Shown in figures 5 and 6 are the eigenvalue spectrum for the tridiagonal fourth and sixth order schemes as well as the pentadiagonal sixth order scheme and septadiagonal eight order scheme. These plots are formed by using the approach of Lele [15] by eliminating the first row and column for a supposed known boundary condition. For each scheme, the eigenvalues were determined using the MATLAB 'eig' command for a 49×49 matrix.
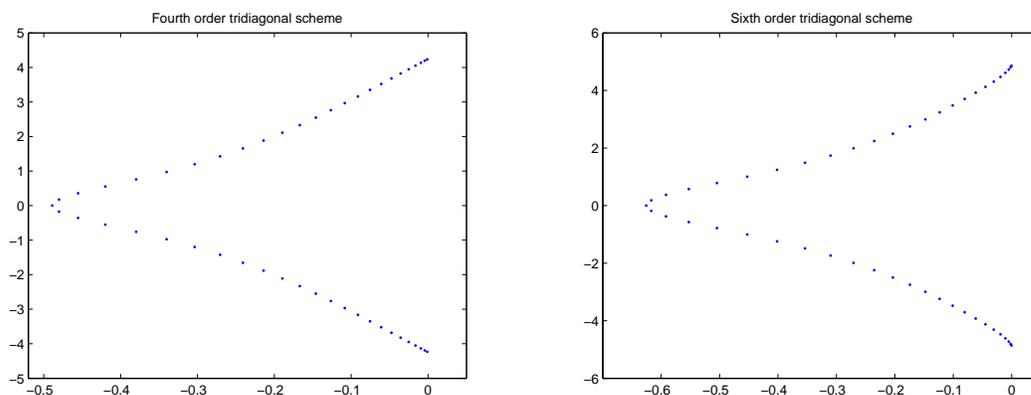

Figure 5: Eigenvalue spectra for T4 and T6 schemes

For the T8 scheme, the eigenvalues with the largest positive real part are $\lambda = 0.0224518 \pm 4.7187805i$. The P8 scheme has eigenvalues $\lambda = 0.0533402 \pm 4.8228221i$. These schemes as given here are therefore unstable. The eighth order tridiagonal and pentadiagonal schemes are implemented in the following section even though they are unstable. It will be shown that the schemes do appear stable for a short time but they do eventually blow up.

The eigenvalue spectrum for the fourth order tridiagonal scheme is shown in Figure
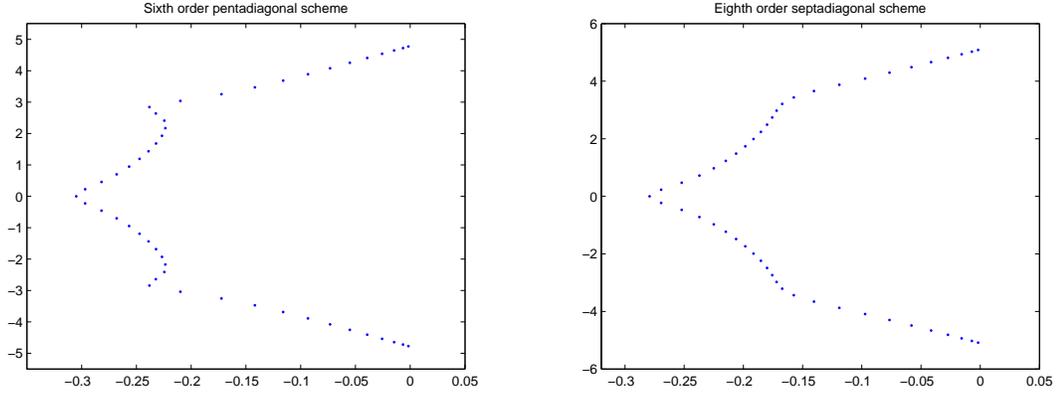
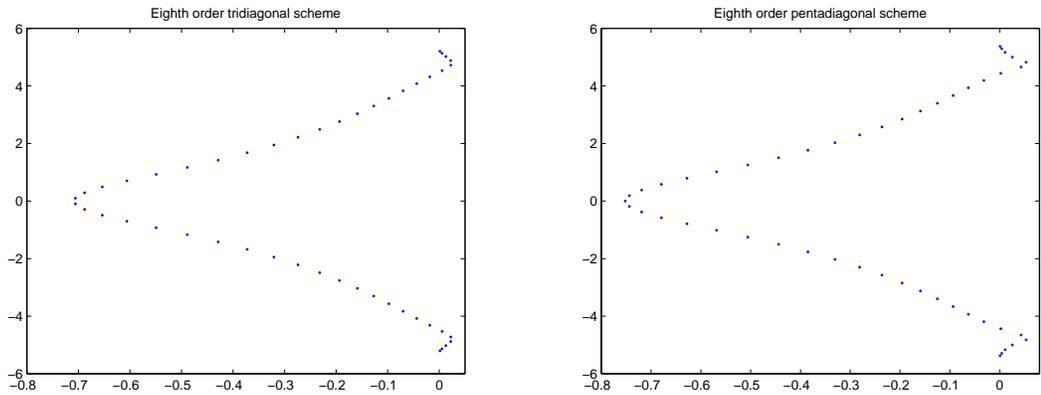Figure 6: Eigenvalue spectra for P6 and S8 schemes

Figure 7: Eigenvalue spectra for T8 and P8 schemes

8 for several different step sizes. As discussed by Lele [15], the eigenvalues with the smallest negative real part approach the imaginary axis at the rate of N^{-3} where N is the size of the matrix. The compact schemes therefore remain stable as $h \to 0$. The largest real part of the eigenvalues for the various matrix sizes is shown in Table 9.
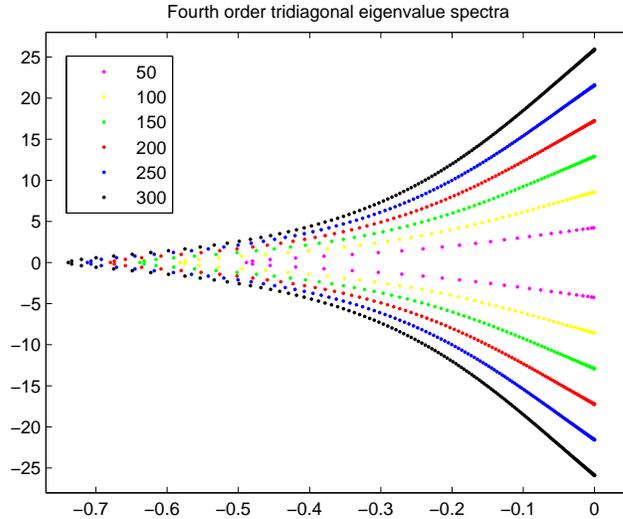
Figure 8: Eigenvalue spectrum of T4 scheme with $N = 50, 100, 150, 200, 250, 300$

N	$\Re(\lambda)$
50	-0.0010
100	-2.4566e-004
150	-1.0687e-004
200	-5.9469e-005
250	-3.7815e-005
300	-2.6147e-005

Table 9: Largest real part in eigenvalue spectrum for T4 schemes

2.6 One-Dimensional Wave Equation

The compact schemes presented here will now be used to solve the spatial derivative of the one-dimensional wave equation

$$\phi_t + c\phi_x = 0 \tag{2.44}$$

in the domain $[0, 1]$. The domain will be partitioned into 100 equally spaced intervals and solved with wave speed $c = 0.05$ and the boundary condition $\phi(0, t) = 0$. Euler time integration is used with a time step $\Delta t = 0.001$. The CFL stability condition

for this problem is based on the computation of the Courant number $C = \frac{c\Delta t}{\Delta x}$. For the given step sizes in space and time, the CFL number is $C = 0.005$, well within any necessary range for stability. More detailed requirements for stability based on the CFL condition will be given in section 7.

The numerical scheme to be solved is given by

$$\frac{\phi_i^{n+1} - \phi_i^n}{\Delta t} = -c(\phi_i^n)_x. \tag{2.45}$$

First, introduce a new function $F_i^n = (\phi_i^n)_x$. The values of F_i^n are then determined using a compact scheme such as the fourth order

$$\frac{1}{4}F_{i-1}^n + F_i^n + \frac{1}{4}F_{i+1}^n = \frac{3}{4h}\left(\phi_{i+1}^n - \phi_{i-1}^n\right).$$

The solution is then updated at each node i by the update formula $\phi_i^{n+1} = \phi_i^n - 0.05\Delta t(F_i^n)$.

The initial profile that is to be propagated through the domain is given by $\phi(x,0) = \sin(10\pi x)$. The exact solution as time progresses should see the initial profile shifted to the right undisturbed. To the left of the initial profile, the solution is zero. The compact scheme solutions are presented for several different orders of accuracy at time steps T = 10s, T = 25s, and T = 60s in Figures 9 - 18.

The sixth order schemes show a slight improvement over the fourth order scheme where the eighth order schemes seem to begin a breakdown in accuracy to the left of the initial profile. Increasing the order of accuracy beyond eight has no improvement and in some cases the spurious oscillations introduced by the approximation scheme are amplified.

Among the eighth order schemes, increasing the band width or decreasing the right-hand stencil does not seem to have a systematic effect on the solution of the wave equation. The eighth order tridiagonal scheme is quite comparable to the sixth
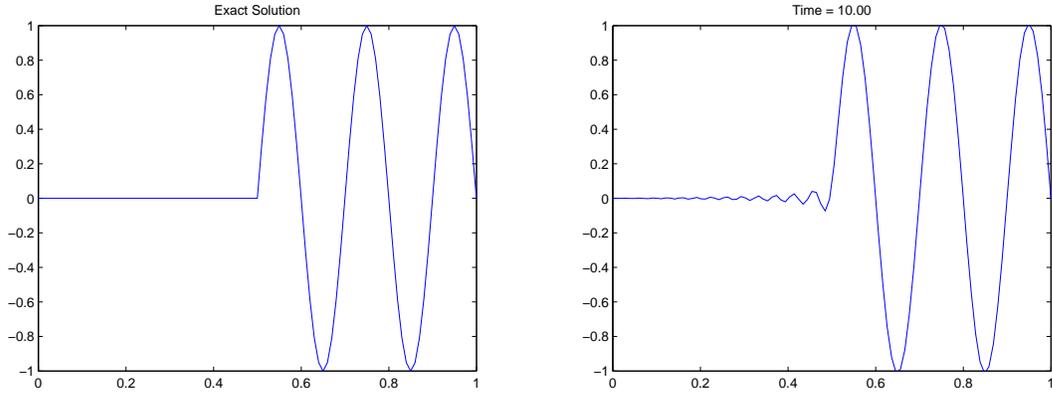
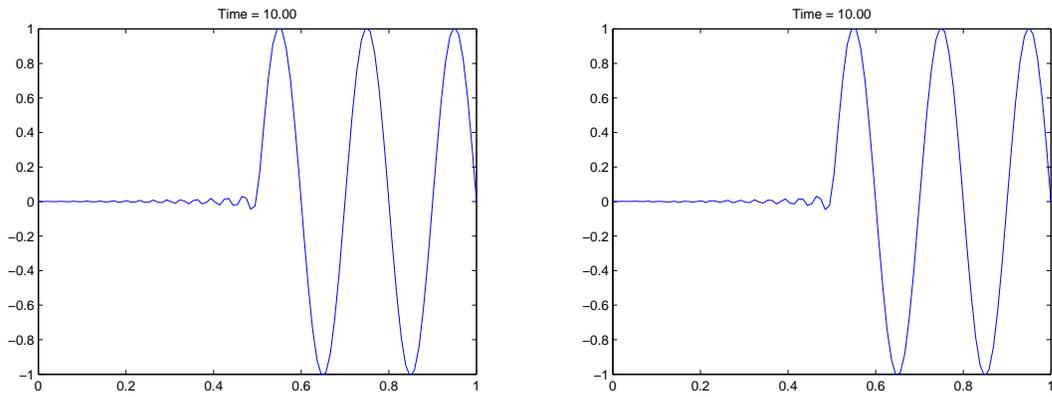Figure 9: Exact solution and compact scheme T4 at T = 10s

Figure 10: Compact schemes T6 and P6 at T = 10s
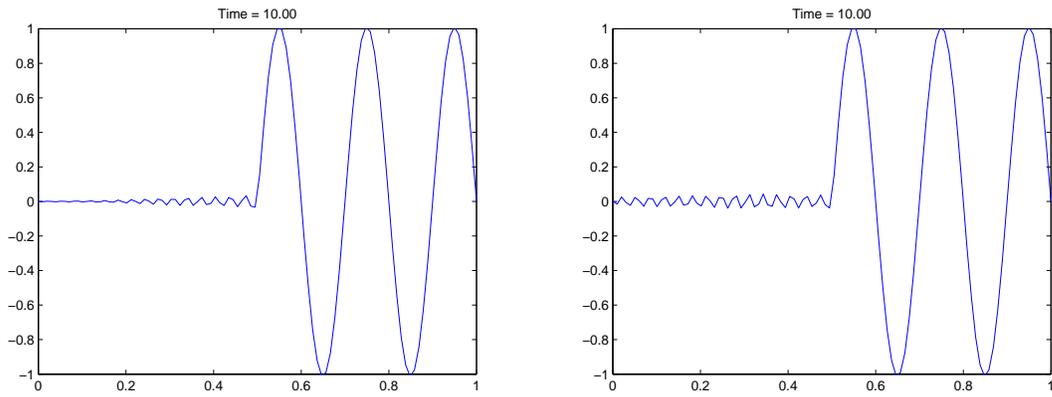
Figure 11: Compact schemes T8 and P8 at T = 10s
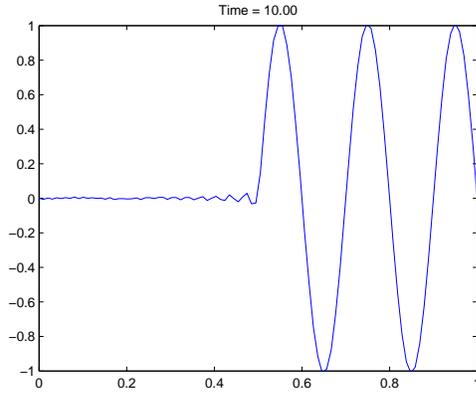
Figure 12: Compact scheme S8 at T = 10s

order schemes but the spurious oscillations of the eighth order pentadiagonal scheme are not diminished at the same rate. The septadiagonal scheme however shows some improvement over the sixth order schemes.

At T = 20s, the initial solution shall have passed through the domain and the solution should thereafter be zero. The range of the graphs vary depending on the maximum distance from zero of the approximation for the T = 25s and T = 60s cases. Figures 13 through 15 show the compact scheme result five seconds after the solution has passed through the domain.
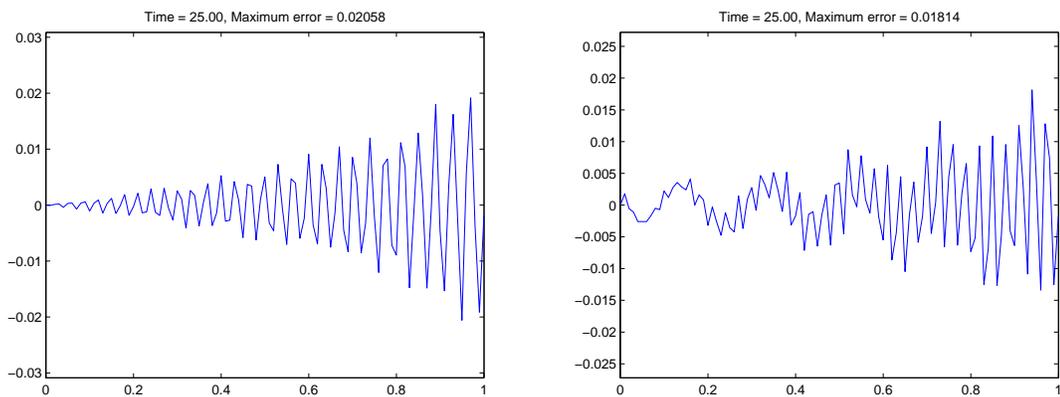
Figure 13: Spurious oscillations from T4 and S8 schemes at T = 25s

In each case the oscillations seems to be diminishing as time passes. Figures 16

Figure 14: Spurious oscillations from T6 and P6 schemes at T = 25s
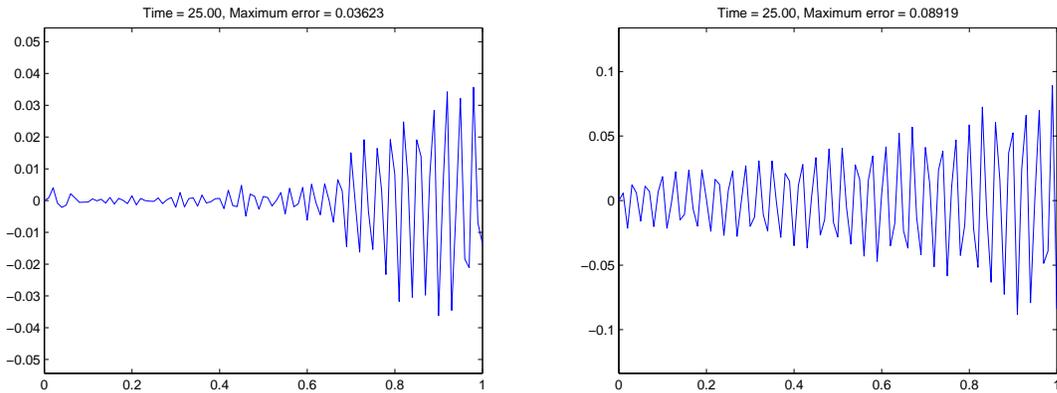
Figure 15: Spurious oscillations from T8 and P8 schemes at T = 25s

through 18 show the wave equation solutions at T = 60s, contradicting the assumption that the oscillations die down. One case in fact shows an amplification of the waves as a consequence of the instability of the scheme.

The pentadiagonal eighth order scheme oscillations have grown in amplitude and are now greater than the original profile, thus verifying the instability suggested by the eigenvalue spectrum. These results suggest that the order-optimized compact scheme is not necessarily the best method of approximation. Increased order of accuracy does not guarantee the best solution. The spectral schemes will be shown to be much more accurate. To discuss these, it is first necessary to discuss the Fourier error analysis of

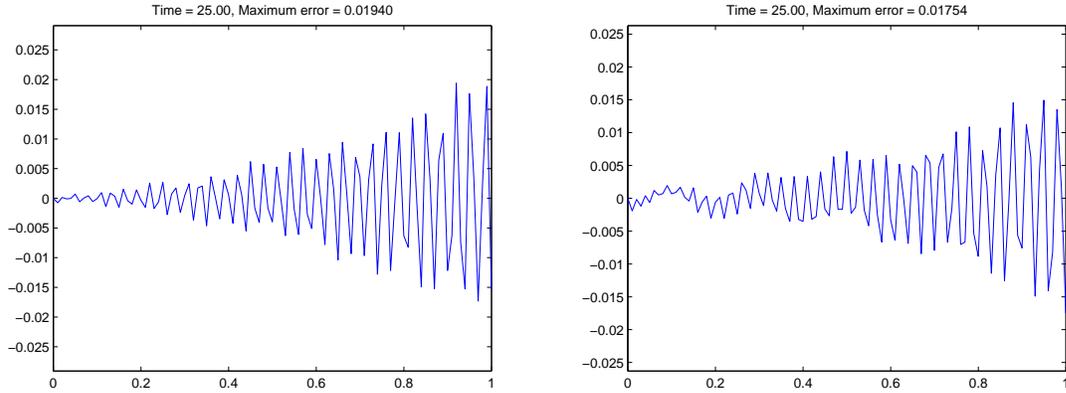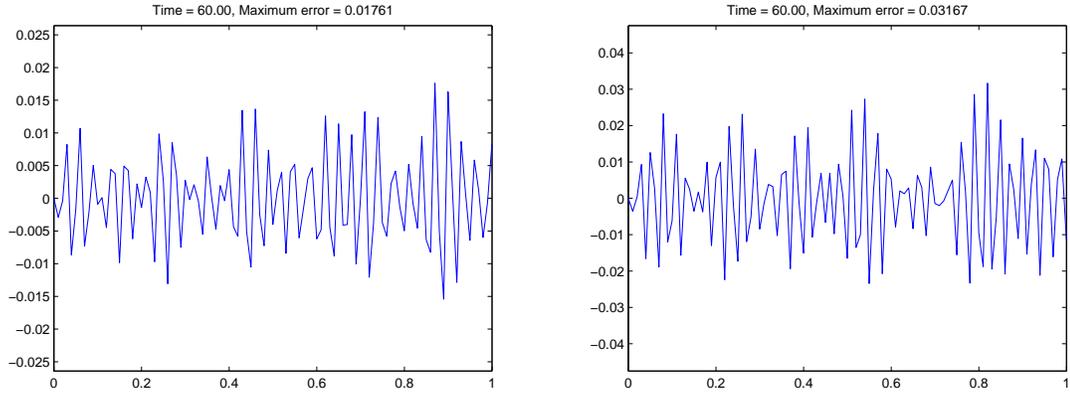Figure 16: Spurious oscillations from T4 and S8 schemes at T = 60s
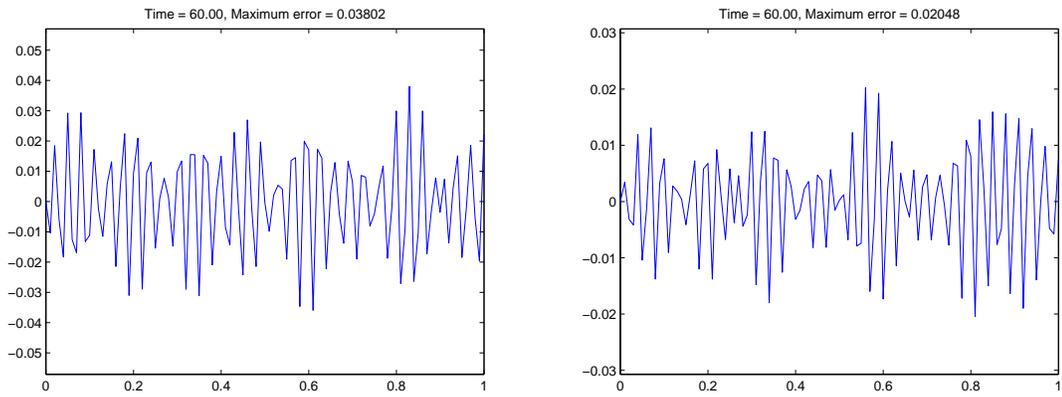
Figure 17: Spurious oscillations from T6 and P6 schemes at T = 60s
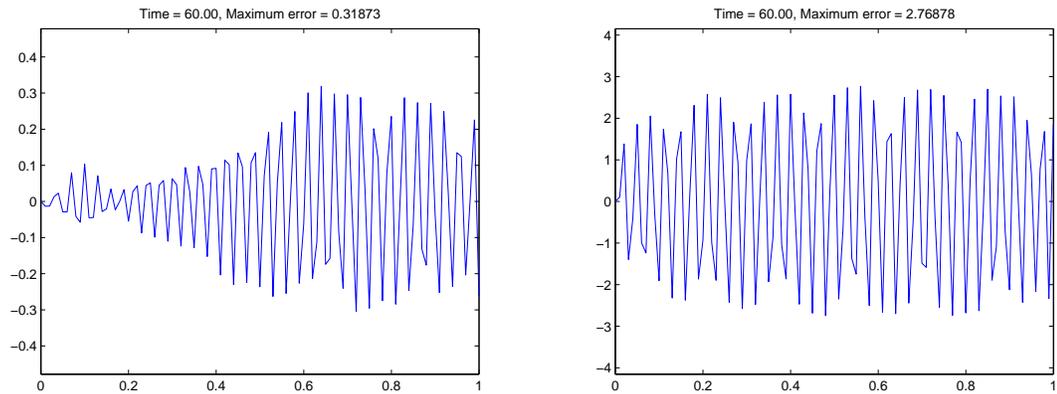
Figure 18: Spurious oscillations from T8 and P8 schemes at T = 60s

the compact schemes.

Before moving to the next section, it is worth noting the computation time using the compact scheme. The MATLAB code given in Appendix B can be optimized to approximate the one-dimensional wave equation solution for a long time run (T = 60s) in about 2.5 seconds. The computation time can be made to be reasonably small by performing as many operations outside of the time loop as possible.

3 Spectral function

Analysis of dispersion and dissipation errors can be achieved in part by considering the spectral function associated with the compact schemes.

Assuming that the dependent variables are periodic over $[0, L]$ and introducing the step size $h = L/N$ where N is the number of discretization points, the Fourier coefficients are

$$\phi(x) = \sum_{k=-N/2}^{N/2} \hat{\phi}_k \exp\left(\frac{2\pi i k x}{L}\right). \tag{3.1}$$

These coefficients satisfy $\hat{\phi}_k = \hat{\phi}_{-k}^*$ for $k = 0, 1, \ldots, \frac{N}{2}$ where $*$ indicates complex conjugation.

Scaling the spatial coordinates by a factor of $1/h$ gives a new spatial variable $s = x/h$. Introducing the wave number $\omega = \dfrac{2\pi k h}{L} = \dfrac{2\pi k}{N}$, the Fourier coefficients reduce to

$$\phi(x) = \sum_{k=-N/2}^{N/2} \hat{\phi}_k e^{i\omega s} \tag{3.2}$$

where $\omega \in [0, \pi]$.

Upon substitution of this expression into the compact scheme (2.9), the result is

$$\beta i\omega \sum_{k=-N/2}^{N/2} \hat{\phi}_k e^{i\omega s} e^{-2i\omega} + \alpha i\omega \sum_{k=-N/2}^{N/2} \hat{\phi}_k e^{i\omega s} e^{-i\omega} + i\omega \sum_{k=-N/2}^{N/2} \hat{\phi}_k e^{i\omega s}$$

$$+\alpha i\omega \sum_{k=-N/2}^{N/2} \hat{\phi}_k e^{i\omega s} e^{i\omega} + \beta i\omega \sum_{k=-N/2}^{N/2} \hat{\phi}_k e^{i\omega s} e^{2i\omega}$$

$$= \frac{a}{2h} \sum_{k=-N/2}^{N/2} \left(\hat{\phi}_k e^{i\omega s} e^{i\omega} - \hat{\phi}_k e^{i\omega s} e^{-i\omega} \right) + \frac{b}{4h} \sum_{k=-N/2}^{N/2} \left(\hat{\phi}_k e^{i\omega s} e^{2i\omega} - \hat{\phi}_k e^{i\omega s} e^{-2i\omega} \right)$$

$$+\frac{c}{6h} \sum_{k=-N/2}^{N/2} \left(\hat{\phi}_k e^{i\omega s} e^{3i\omega} - \hat{\phi}_k e^{i\omega s} e^{-3i\omega} \right) + \frac{d}{8h} \sum_{k=-N/2}^{N/2} \left(\hat{\phi}_k e^{i\omega s} e^{4i\omega} - \hat{\phi}_k e^{i\omega s} e^{-4i\omega} \right).$$

Combining summation terms and factoring out the common $i\omega$ term from the left-hand side gives

$$i\omega \sum_{k=-N/2}^{N/2} \left[\beta\hat{\phi}_k e^{i\omega s} e^{-2i\omega} + \alpha\hat{\phi}_k e^{i\omega s} e^{-i\omega} + \hat{\phi}_k e^{i\omega s} + \alpha\hat{\phi}_k e^{i\omega s} e^{i\omega} + \beta\hat{\phi}_k e^{i\omega s} e^{2i\omega} \right]$$

$$= \sum_{k=-N/2}^{N/2} \left[\frac{a}{2h} (\hat{\phi}_k e^{i\omega s} e^{i\omega} - \hat{\phi}_k e^{i\omega s} e^{-i\omega}) + \frac{b}{4h} (\hat{\phi}_k e^{i\omega s} e^{2i\omega} - \hat{\phi}_k e^{i\omega s} e^{-2i\omega}) \right.$$

$$\left. + \frac{c}{6h} (\hat{\phi}_k e^{i\omega s} e^{3i\omega} - \hat{\phi}_k e^{i\omega s} e^{-3i\omega}) + \frac{d}{8h} (\hat{\phi}_k e^{i\omega s} e^{4i\omega} - \hat{\phi}_k e^{i\omega s} e^{-4i\omega}) \right].$$

Factoring and collecting like terms leads to

$$h\omega \sum_{k=-N/2}^{N/2} \hat{\phi}_k e^{i\omega s} \left[1 + 2\alpha \left(\frac{e^{i\omega} + e^{-i\omega}}{2} \right) + 2\beta \left(\frac{e^{2i\omega} + e^{-2i\omega}}{2} \right) \right]$$

$$= \sum_{k=-N/2}^{N/2} \hat{\phi}_k e^{i\omega s} \left[a \left(\frac{e^{i\omega} - e^{-i\omega}}{2i} \right) + \frac{b}{2} \left(\frac{e^{2i\omega} - e^{-2i\omega}}{2i} \right) \right.$$

$$\left. + \frac{c}{3} \left(\frac{e^{3i\omega} - e^{-3i\omega}}{2i} \right) + \frac{d}{4} \left(\frac{e^{4i\omega} - e^{-4i\omega}}{2i} \right) \right].$$

A new variable $\tilde{\omega}$ is introduced which is called the modified wave number. This variable is the wave number ω scaled by a factor of h, or thus $\tilde{\omega} = h\omega$. Canceling the

49

$\hat{\phi}_k e^{i\omega s}$ terms from each side, it is noted that the summations will be equal only upon equality of the terms

$$
\tilde{\omega}\left[1 + 2\alpha\left(\frac{e^{i\omega} + e^{-i\omega}}{2}\right) + 2\beta\left(\frac{e^{2i\omega} + e^{-2i\omega}}{2}\right)\right]
$$
$$
= \left[a\left(\frac{e^{i\omega} - e^{-i\omega}}{2i}\right) + \frac{b}{2}\left(\frac{e^{2i\omega} - e^{-2i\omega}}{2i}\right) + \frac{c}{3}\left(\frac{e^{3i\omega} - e^{-3i\omega}}{2i}\right) + \frac{d}{4}\left(\frac{e^{4i\omega} - e^{-4i\omega}}{2i}\right)\right].
$$

Solving for the modified wave number $\tilde{\omega}$ in terms of the wave number ω and using the relations

$$
\sin\omega = \frac{e^{i\omega} - e^{-i\omega}}{2i} \quad \text{and} \quad \cos\omega = \frac{e^{i\omega} + e^{-i\omega}}{2}
$$

gives the spectral function for the interior compact scheme

$$
\mathcal{SF}(\omega) = \tilde{\omega}(\omega) = \frac{a\sin(\omega) + \frac{b}{2}\sin(2\omega) + \frac{c}{3}\sin(3\omega) + \frac{d}{4}\sin(4\omega)}{1 + 2\alpha\cos(\omega) + 2\beta\cos(2\omega)}. \tag{3.3}
$$

It should be noted that the spectral function corresponding to exact differentiation is $\tilde{\omega}(\omega) = \omega$. For a given interior scheme, the spectral function plotted against the exact derivative function will show the percentage of wave numbers where the compact scheme reasonably approximates the exact derivative. The spectral functions for the interior schemes are purely real. All centered schemes are therefore non-dissipative and the corresponding error shown in the real part of the spectral function describes strictly the dispersive characteristics of the scheme.

The graphs of the spectral functions for tridiagonal and pentadiagonal schemes in Figure 19 show that the pentadiagonal schemes generally have better resolution characteristics. However, the exact degree to which the resolution characteristics compare for the different schemes will be discussed in Section 4.1. It is also clear that the resolution improves as higher order schemes are considered.

While the interior compact schemes have spectral functions that are entirely real valued, the spectral functions for the boundary schemes are in general complex. Again

50
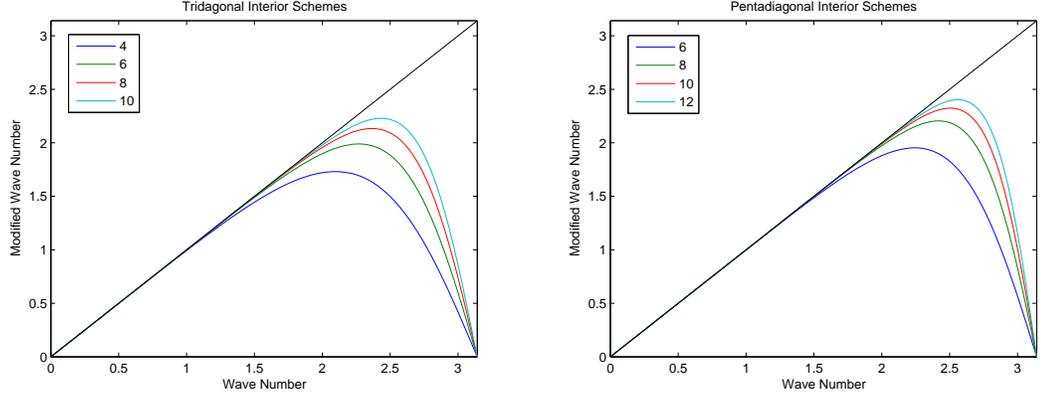
Figure 19: Spectral functions for tridiagonal and pentadiagonal interior schemes

the real part of the spectral functions will describe the dispersive error while the imaginary part projects the dissipative error. Therefore, the presence of necessary boundary formulas for non-periodic problems introduces some level of dissipation into the scheme.

For the first derivative boundary formula at node 1, the spectral function is found using a similar procedure. Substitution of the Fourier coefficients gives

$$
i\omega \left[\hat{\phi}_1 e^{i\omega s} + \alpha \hat{\phi}_1 e^{i\omega s} e^{i\omega} + \beta \hat{\phi}_1 e^{i\omega s} e^{2i\omega} \right]
$$
$$
= \frac{1}{h} \left[a_1 \hat{\phi}_1 e^{i\omega s} + a_2 \hat{\phi}_1 e^{i\omega s} e^{i\omega} + a_3 \hat{\phi}_1 e^{i\omega s} e^{2i\omega} + \cdots + a_{10} \hat{\phi}_1 e^{i\omega s} e^{9i\omega} + a_{11} \hat{\phi}_1 e^{i\omega s} e^{10i\omega} \right].
$$

Canceling common terms gives

$$
i\omega \left[1 + \alpha e^{i\omega} + \beta e^{2i\omega} \right] = \frac{1}{h} \left[a_1 + a_2 e^{i\omega} + a_3 e^{2i\omega} + \cdots + a_{10} e^{9i\omega} + a_{11} e^{10i\omega} \right].
$$

Solving for $\tilde{\omega}$ gives the spectral function for the first boundary point of the first derivative scheme

$$
\tilde{\omega}(\omega) = \frac{a_1 + a_2 e^{i\omega} + a_3 e^{2i\omega} + \cdots + a_{10} e^{9i\omega} + a_{11} e^{10i\omega}}{i(1 + \alpha e^{i\omega} + \beta e^{2i\omega})}. \tag{3.4}
$$

51

The real and imaginary parts of the spectral functions for the first derivative boundary formula at node 1 is shown in Figures 20 and 21 for the tridiagonal and pentadiagonal boundary formulas given in Table 5. The spectral functions for other boundary nodes are similar.

Figure 20: Real part of spectral functions for node 1 schemes

Figure 21: Imaginary part of spectral functions for node 1 schemes

After analyzing the spectral function, it is possible to derive another type of compact scheme: the spectral scheme.

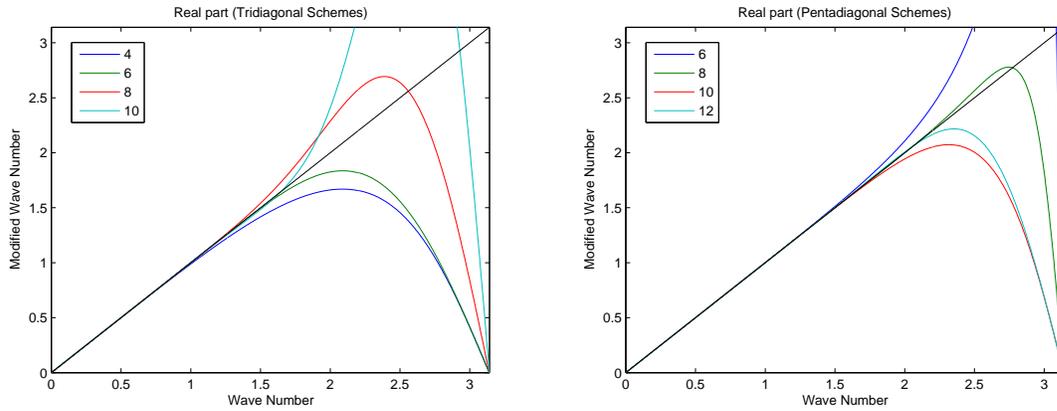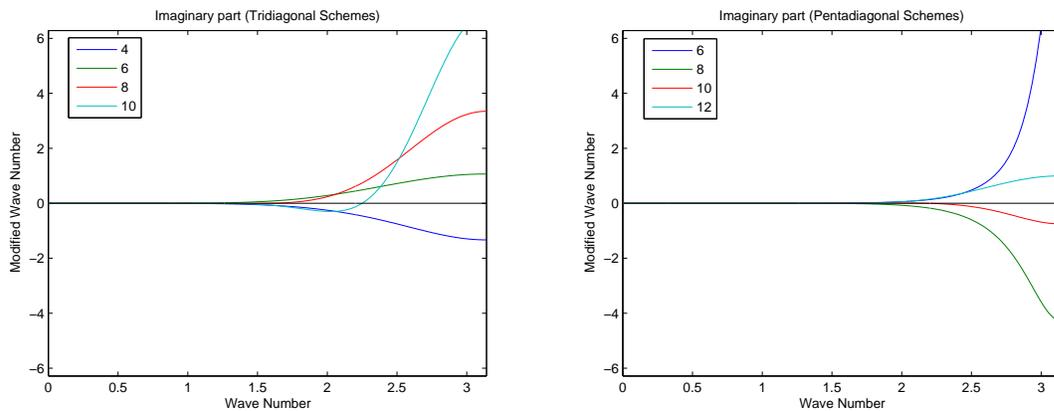# 4   Spectral schemes

The spectral compact scheme is derived by not requiring the maximum order of formal accuracy. Spectral schemes are somewhat more complicated to derive but possess certain properties that are advantageous over the Padé schemes.

For the first derivative scheme (2.9), the spectral scheme is developed by requiring less than maximum formal accuracy such as fourth or sixth order. The coefficients are also subjected to specific conditions in the spectral function. If fourth order accuracy is guaranteed by requiring the first two equations (2.13) - (2.14) of the matching procedure, then the remaining conditions needed to uniquely determine the coefficients are found by requiring $\tilde{\omega}(\omega_1) = \omega_1, \tilde{\omega}(\omega_2) = \omega_2, \tilde{\omega}(\omega_3), \ldots$ in the spectral function (3.3) for specific wave numbers $\omega_1, \omega_2, \omega_3, \ldots$ on $(0, \pi)$.

As is shown in the graphs of the spectral functions in the previous section, the compact schemes generally have poor resolution characteristics on the interval $(\frac{\pi}{2}, \pi)$ and this is generally where the values of ω_i are chosen. These wave numbers may be chosen arbitrarily but the hope is that the choice of wave numbers improves the resolution characteristics of the scheme.

Coefficients of spectral schemes of both fourth order and sixth order accuracy are presented in Table 10 and 11. The specific choice of wave numbers in the derivation of the coefficients is also shown. However, no attempt was made to improve the resolution characteristics of these schemes. The procedure for finding the best resolution characteristics based on the choice of ω_i will be described briefly in Section 4.1.

ω_1	ω_2	ω_3	a	b	c	α	β
2.2	2.3	2.4	1.2950	1.0121	0.0406	0.5813	0.0925
2.2	2.4	2.6	1.2788	1.0523	0.0468	0.5903	0.0986
2.2	2.5	2.8	1.2597	1.0991	0.0547	0.6007	0.1060
2.2	2.6	3.0	1.2369	1.1537	0.0648	0.6128	0.1149

Table 10: Coefficients of interior spectral schemes of fourth order

ω_1	ω_2	a	b	c	α	β
2.2	2.4	1.3349	0.9129	0.0252	0.5591	0.0775
2.2	2.6	1.3228	0.9458	0.0278	0.5667	0.0815
2.2	2.8	1.3079	0.9864	0.0309	0.5761	0.0864
2.2	3.0	1.2892	1.0369	0.0348	0.5878	0.0926

Table 11: Coefficients of interior spectral schemes of sixth order

Coefficients of optimized spectral schemes for the tridiagonal case are given by Visbal [9] with details and references for the choices of wave numbers. For the pentadiagonal case, Table 12 shows coefficients for both fourth and sixth order formal truncation error. The A6 scheme is the spectral scheme presented in [7]. The B6 scheme is another sixth order scheme with an increased stencil size determined as part of this work.

Scheme	ω_1	ω_2	ω_3	a	b	c	d	α	β
A4	2.0	2.6	2.8	1.2603	1.0974	0.0531		0.6001	0.1503
A6	2.464	2.7171		1.2988	1.00616	0.03354		0.57967	0.0895
B6	2.3	2.6	2.8	1.2236	1.1703	0.0862	-0.0060	0.6169	0.1201

Table 12: Spectral schemes for minimum error

The spectral functions for the two sixth order schemes from Table 12 are plotted together with the spectral functions for the two septadiagonal schemes from Table 1 in Figure 22. The spectral schemes by definition are better at approximating the derivative for a larger percentage of wave numbers than the septadiagonal schemes or any other type of scheme.

The spectral function can also be used to improve the percentage of wave numbers where the boundary formulas accurately approximate the first derivative at the boundary nodes. For simplicity, the spectral schemes A6 and B6 presented here will simply be linked with the sixth order Padé boundary formulas.

The eigenvalue spectra of the A6 and B6 schemes also verifies their stability. The spectra of these two schemes is shown in Figure 23.
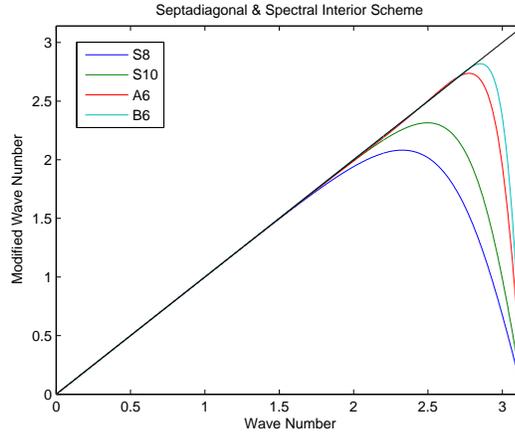
Figure 22: Spectral functions for septadiagonal and sixth order spectral schemes
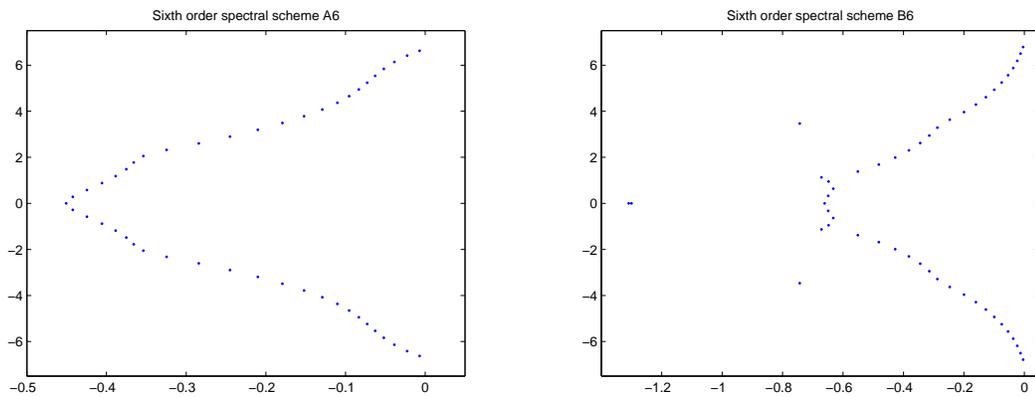
Figure 23: Eigenvalue spectra of the A6 and B6 schemes

The two spectral schemes A6 and B6 prove their accuracy by considering their solutions to the wave equation. Plots of the two approximation schemes at the three time levels T = 10s, T = 25s, and T = 60s is presented in figures 24 through 26.

It is clear in comparison that the spectral schemes yield better solutions over the order optimized schemes. To consider the degree to which the spectral solution improves on the Padé scheme, it may be prudent to analyze the resolving efficiency of the scheme.
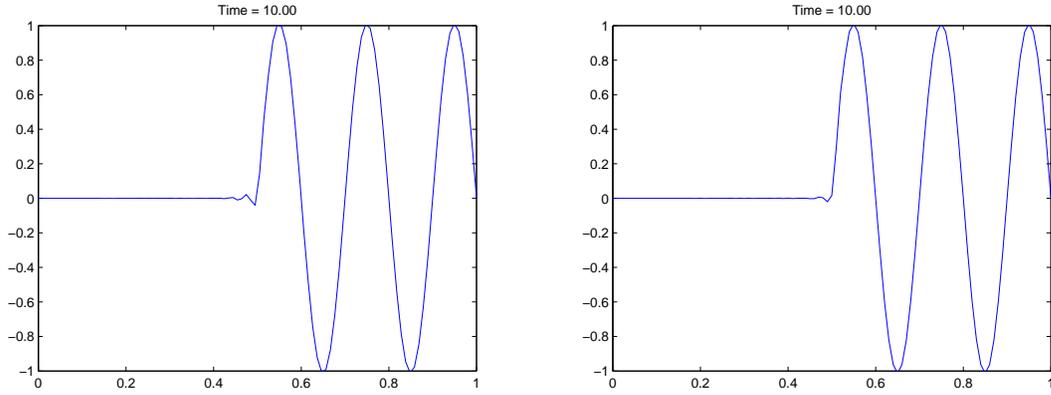
Figure 24: Compact schemes A6 and B6 at T = 10s
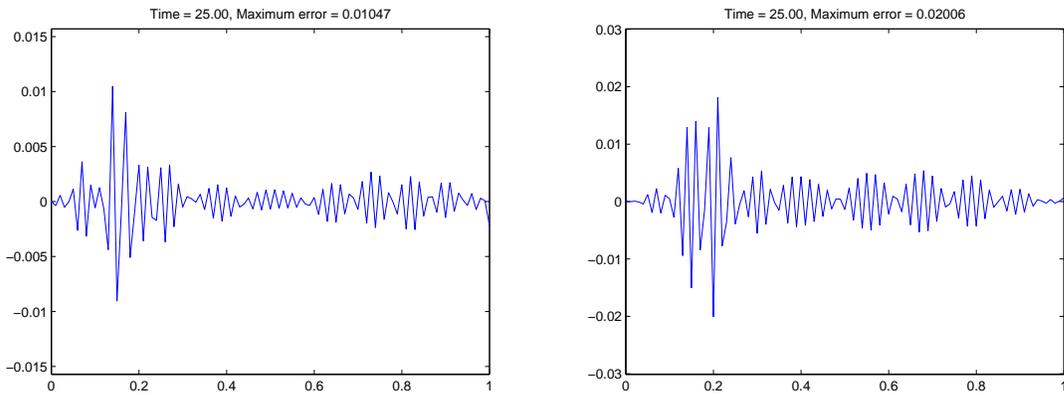
Figure 25: Compact schemes A6 and B6 at T = 25s
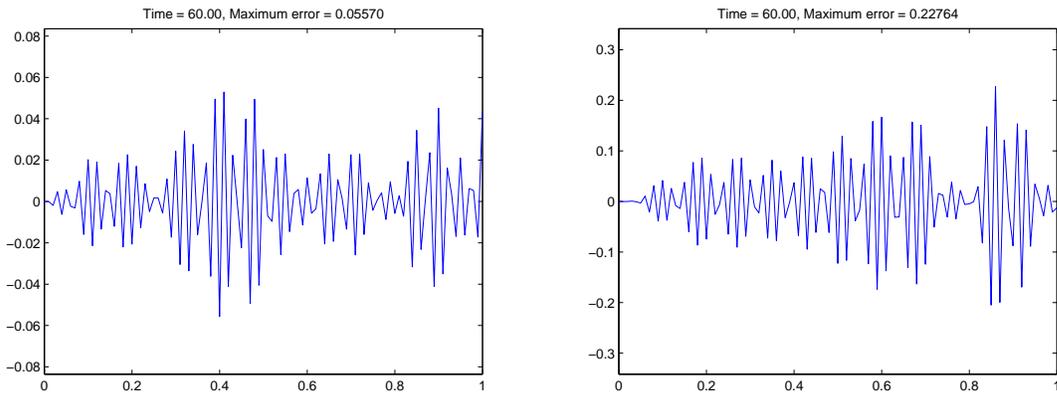
Figure 26: Compact schemes A6 and B6 at T = 60s

4.1 Resolving Efficiency

The resolving efficiency is a measure of the percentage of wave numbers for which the numerical scheme most accurately approximates the exact derivative. The efficiency is determined by the error tolerance

$$\frac{|\tilde{\omega}(\omega) - \omega|}{\omega} \leq \epsilon. \tag{4.1}$$

Scheme	$\epsilon = 0.1$	$\epsilon = 0.01$	$\epsilon = 0.001$
T4	0.65	0.43	0.28
T6	0.73	0.55	0.41
T8	0.78	0.62	0.49
T10	0.80	0.66	0.54
P6	0.72	0.53	0.39
P8	0.80	0.65	0.52
P10	0.83	0.70	0.59
P12	0.85	0.74	0.63
S8	0.76	0.60	0.46
S10	0.83	0.70	0.58
A6	0.92	0.88	0.55
B6	0.94	0.91	0.75

Table 13: Resolving efficiency of interior schemes

Table 13 shows the percentage of wave numbers of several first derivative compact schemes that satisfy the error tolerance (4.1) for the error ϵ. These results show that there is no clear distinction indicating an advantage of the Padé schemes of different band width. That is, the tenth order septadiagonal scheme shows little or no improvement over the pentadiagonal or tridiagonal cases of the same order. It is clear however that the spectral schemes by far are the best at approximating the derivatives for the majority of wave numbers.

The resolving efficiency is one method for which the spectral schemes are optimized. The choice of wave numbers and coefficients are determined by maximizing

the resolving efficiency of the given scheme or by minimizing certain error quantities such as dispersion or isotropy as described by [9].

Despite the obvious improvements with the spectral scheme, there remains a small degree of spurious oscillations that are not damped in the one-dimensional wave equation approximation. To eliminate these, a small amount of damping may be introduced. The filter scheme presented here will help eliminate some of the low-frequency oscillations.

5   Filtering

Stability analysis of the compact scheme is not always a straightforward procedure. Some analysis of the compact scheme can be done by considering the spectral function. Stability is often achieved in a numerical scheme by adding a small amount of damping. A less common method is to filter the updated solution values adding dissipation to the scheme. While explicit filters exists, the schemes presented here are implicit filters that mimic the nature of the compact scheme.

The numerical filtering scheme is an artificial method for introducing dissipation to the compact scheme. For the compact schemes presented above, the filter formula is given by

$$\beta_f \hat{\phi}_{i-2} + \alpha_f \hat{\phi}_{i-1} + \hat{\phi}_i + \alpha_f \hat{\phi}_{i+1} + \beta_f \hat{\phi}_{i+2} = \sum_{k=0}^{M} \frac{a_k}{2} (\phi_{i+k} + \phi_{i-k}), \qquad (5.1)$$

or more explicitly,

$$\beta_f \hat{\phi}_{i-2} + \alpha_f \hat{\phi}_{i-1} + \hat{\phi}_i + \alpha_f \hat{\phi}_{i+1} + \beta_f \hat{\phi}_{i+2}$$
$$= a_0 \phi_i + \frac{a_1}{2} (\phi_{i+1} + \phi_{i-1}) + \frac{a_2}{2} (\phi_{i+2} + \phi_{i-2}) + \cdots + \frac{a_M}{2} (\phi_{i+M} + \phi_{i-M}).$$

The size of M depends on the desired order of the filter. Generally, a filtering

scheme is chosen to be at least two orders higher than the compact scheme that it is coupled with.

The spectral function for a filter scheme is similar to the spectral function for the interior compact schemes. Here the function involves only cosine terms. The domain of the spectral function is again $[0, \pi]$ and the function is

$$\mathcal{SF}(\omega) = \frac{\sum_{k=0}^{M} a_k \cos(k\omega)}{1 + 2\alpha_f \cos(\omega) + 2\beta_f \cos(2\omega)}, \tag{5.2}$$

or more explicitly

$$\mathcal{SF}(\omega) = \frac{a_0 + a_1 \cos(\omega) + a_2 \cos(2\omega) + a_3 \cos(3\omega) + \cdots + a_M \cos(M\omega)}{1 + 2\alpha_f \cos(\omega) + 2\beta_f \cos(2\omega)}.$$

To determine the order of the filter, the Taylor series matching procedure is again used but at least one additional constraint is needed. For any filter, the spectral function at the right endpoint of the domain must be zero, that is $\mathcal{SF}(\pi) = 0$, thus matching the spectral functions of the interior compact schemes.

The Taylor series expansions at all nodes is given by the formula

$$\hat{\phi}_{i+k} = \phi_i + kh \left(\frac{\partial \phi}{\partial x}\right)_i + \frac{k^2 h^2}{2!} \left(\frac{\partial^2 \phi}{\partial x^2}\right)_i + \cdots + \frac{k^n h^n}{n!} \left(\frac{\partial^n \phi}{\partial x^n}\right)_i + R_n(x) \tag{5.3}$$

where

$$R_n(x) = \frac{k^{n+1} h^{n+1}}{(n+1)!} \left(\frac{\partial^{n+1} \phi}{\partial x^{n+1}}\right)_{i+\xi}.$$

For the condition $\mathcal{SF}(\pi) = 0$, the resulting equation is

$$a_0 - a_1 + a_2 - a_3 + a_4 - a_5 + a_6 - a_7 + a_8 = 0.$$

The remainder of the equations come from matching terms for like powers of h. Factorial terms are neglected as they appear in the same magnitude on both sides of

59

the equations. The additional equations from the matching procedure are

$$a_0 + a_1 + a_2 + a_3 + a_4 + a_5 + a_6 + a_7 + a_8 = 2\alpha_f + 2\beta_f + 1$$

$$a_1 + 2^2 a_2 + 3^2 a_3 + 4^2 a_4 + 5^2 a_5 + 6^2 a_6 + 7^2 a_7 + 8^2 a_8 = 2\alpha_f + 2^3 \beta_f$$

$$a_1 + 2^4 a_2 + 3^4 a_3 + 4^4 a_4 + 5^4 a_5 + 6^4 a_6 + 7^4 a_7 + 8^4 a_8 = 2\alpha_f + 2^5 \beta_f$$

$$a_1 + 2^6 a_2 + 3^6 a_3 + 4^6 a_4 + 5^6 a_5 + 6^6 a_6 + 7^6 a_7 + 8^6 a_8 = 2\alpha_f + 2^7 \beta_f$$

$$a_1 + 2^8 a_2 + 3^8 a_3 + 4^8 a_4 + 5^8 a_5 + 6^8 a_6 + 7^8 a_7 + 8^8 a_8 = 2\alpha_f + 2^9 \beta_f$$

$$a_1 + 2^{10} a_2 + 3^{10} a_3 + 4^{10} a_4 + 5^{10} a_5 + 6^{10} a_6 + 7^{10} a_7 + 8^{10} a_8 = 2\alpha_f + 2^{11} \beta_f$$

$$a_1 + 2^{12} a_2 + 3^{12} a_3 + 4^{12} a_4 + 5^{12} a_5 + 6^{12} a_6 + 7^{12} a_7 + 8^{12} a_8 = 2\alpha_f + 2^{13} \beta_f$$

$$a_1 + 2^{14} a_2 + 3^{14} a_3 + 4^{14} a_4 + 5^{14} a_5 + 6^{14} a_6 + 7^{14} a_7 + 8^{14} a_8 = 2\alpha_f + 2^{15} \beta_f.$$

The filter coefficients cannot be optimized for order of accuracy in the same way as the compact scheme. When attempting to determine all coefficients uniquely, the system of equations breaks down and many coefficients become zero. This occurs when attempting to determine any of the left-hand side coefficients uniquely. One approach is therefore to retain all left-hand side coefficients as free parameters and solve the right-hand side coefficients in terms of the left-hand side parameters. These free parameters are then available to adjust the amount of filtering.

The range of values of the free parameters from the left-hand side of the filter scheme are determined by the spectral function. These parameters appear in the denominator of the spectral function and therefore must guarantee a nonzero denominator for all $\omega \in (0, \pi)$. For a tridiagonal filter scheme, the choice of the free parameter must be on the interval $(-0.5, 0.5)$. The pentadiagonal case is less straightforward. Here the choices of α and β should satisfy

$$1 + 2\alpha \cos(\omega) + 2\beta \cos(2\omega) > 0 \tag{5.4}$$

for all $\omega \in (0, \pi)$.

It should be noted that by setting all free parameters to zero in the filter ultimately leaves the solution unaffected.

As is common with the interior compact schemes, filter schemes also require boundary formulas for those points where the stencil protrudes the boundary. Filtering schemes generally have larger stencils and therefore require more boundary formulas. The spectral function for these boundary formulas is derived similarly to the spectral function for interior schemes and the $SF(\pi) = 0$ condition is also required for the boundary schemes. The boundary formulas for the filter are presented in Appendix E for completeness.

As is similar to the second derivative boundary formulas, the coefficients of the filter boundary formulas at nodes 1 through 5 are the same as the coefficients for nodes N through $N - 4$. The coefficients for the interior filter schemes are presented in Table 14. The coefficients for the tridiagonal filter were given by [9]. The boundary formula coefficients are also presented in Appendix E.

	a_0	a_1	a_2	a_3	a_4	a_5
T4	$\frac{5+6\alpha}{8}$	$\frac{1+2\alpha}{2}$	$\frac{-1+2\alpha}{8}$			
T6	$\frac{11+10\alpha}{16}$	$\frac{15+34\alpha}{32}$	$\frac{-3+6\alpha}{16}$	$\frac{1-2\alpha}{32}$		
T8	$\frac{93+70\alpha}{128}$	$\frac{7+18\alpha}{16}$	$\frac{-7+14\alpha}{32}$	$\frac{1-2\alpha}{16}$	$\frac{-1+2\alpha}{128}$	
T10	$\frac{193+126\alpha}{256}$	$\frac{105+302\alpha}{256}$	$\frac{15(-1+2\alpha)}{62}$	$\frac{45(1-2\alpha)}{512}$	$\frac{5(-1+2\alpha)}{256}$	$\frac{1-2\alpha}{512}$
P6	$\frac{11+10\alpha-10\beta}{16}$	$\frac{15+34\alpha+30\beta}{32}$	$\frac{-3+6\alpha+26\beta}{16}$	$\frac{1-2\alpha+2\beta}{32}$		
P8	$\frac{93+70\alpha-70\beta}{128}$	$\frac{7+18\alpha+14\beta}{16}$	$\frac{-7+14\alpha+50\beta}{32}$	$\frac{1-2\alpha+2\beta}{16}$	$\frac{-1+2\alpha-2\beta}{128}$	
P10	$\frac{193+126\alpha-126\beta}{256}$	$\frac{105+302\alpha+210\beta}{256}$	$\frac{-15+30\alpha+98\beta}{64}$	$\frac{45(1-2\alpha+2\beta)}{512}$	$\frac{5(-1+2\alpha-2\beta)}{256}$	$\frac{1-2\alpha+2\beta}{512}$

Table 14: Coefficients of interior filtering schemes

The spectral functions for the boundary filter formulas are in general complex. This indicates that the boundary formulas may introduce some degree of dispersion in addition to the desired dissipation. Also, the real part of the spectral functions for the boundary schemes is greater than one for certain wave numbers with a given choice of the free parameters suggesting that certain wave numbers will be amplified. These

61

concerns can be reduced by appropriate choice of α and β. For a tridiagonal filter scheme, both concerns are minimized as α is chosen as close as possible to 0.5. For a pentadiagonal filter, the choice of α and β must be made with more care to minimize these problems and still satisfy (5.4). One such suitable choice is $\alpha = \beta = 0.4$.
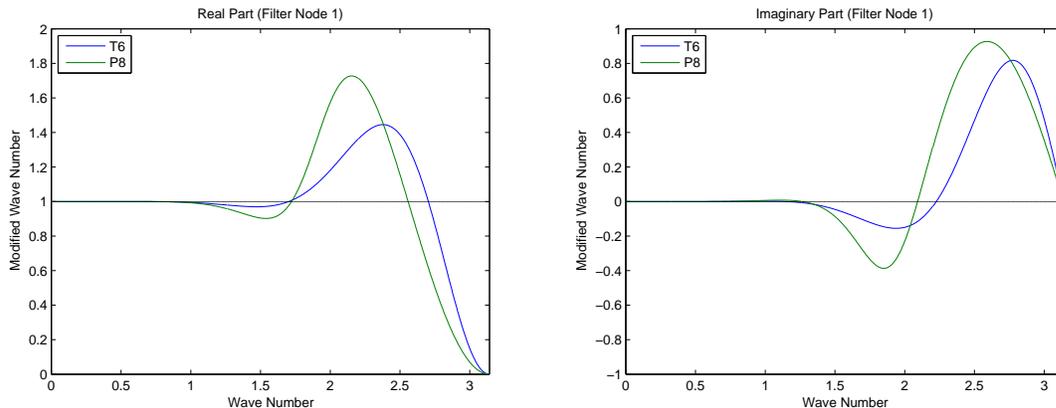
Figure 27: Real/imaginary parts of T6 and P6 spectral functions for filter node 1

The real and imaginary parts of the spectral function for the filter boundary formula at node 1 are shown in Figure 27. The amount of excess over unity of the real parts and the amount of deviation from zero in the imaginary parts is clearly seen.

Although the filtering scheme coefficients have been presented for both the tridiagonal and pentadiagonal filter cases, the tridiagonal filter may be applied in place of larger band width filters with similar results.

5.1   Wave Equation Revisited

The effect of filtering can be most easily seen for the one-dimensional wave equation. Considering the same problem as before, the updated solution filtered at every time step should eliminate the presence of the spurious oscillatory wave frequencies. In Figure 28, tridiagonal filters are applied after each time step for the fourth and sixth order schemes.
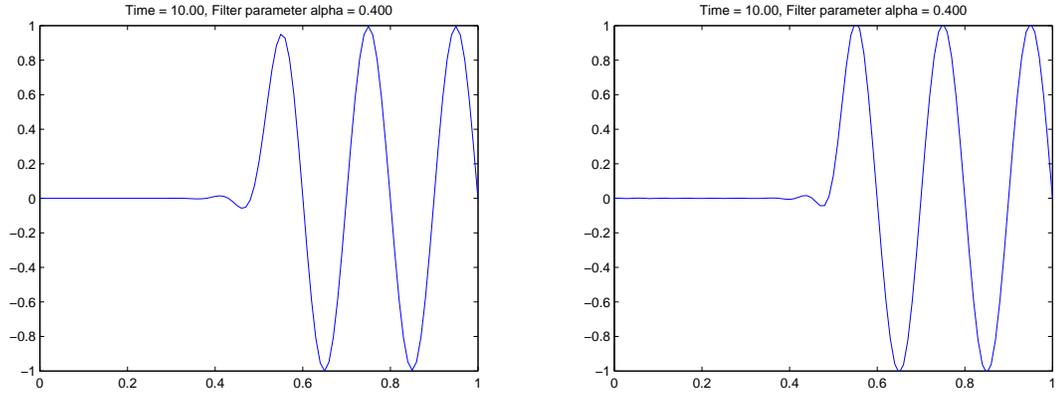
Figure 28: Filtered T4 scheme and filtered T6 scheme ($\alpha = 0.4$) at T = 10s

The filters successfully remove much of the oscillations to the left of the initial profile while leaving the remainder of the wave relatively unaffected. Demonstrating the success of the eighth order pentadiagonal filter, figures 29 and 30 show the filtered solutions at T = 10s, T = 25s and T = 60s for the sixth order pentadiagonal compact scheme.
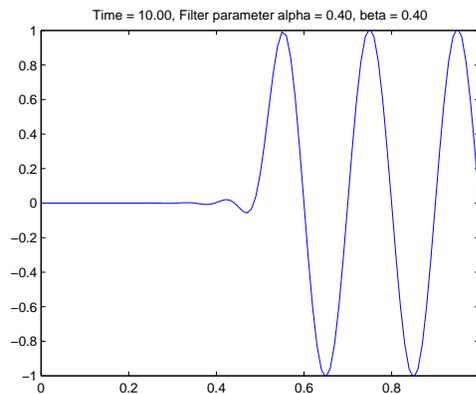
Figure 29: P6 schemes with eighth order filter ($\alpha = \beta = 0.4$) at T = 10s

After 25 seconds, the filtered result appears with a maximum error of order 10^{-3}. After 60 seconds, the filtered solution approximates the exact solution to within 10^{-15}.

Although filtering does produce the desired damping of these low frequency oscillations, it must be used with caution. The degree of filtering may have such an
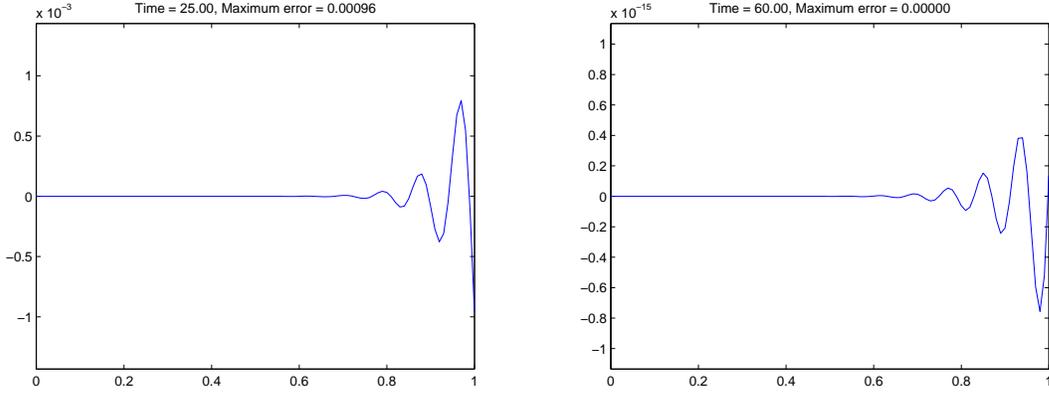
Figure 30: P6 scheme with eighth order filter ($\alpha = \beta = 0.4$) at T = 25s, 60s

impact as to damp the actual solution. Thus the filter must be employed with care to guarantee that only the low frequency oscillations are removed.

6 Boundary Conditions

Dirichlet boundary conditions are easy to implement with compact schemes. Combinations of the boundary condition with the adjacent node approximation formula can then be accomplished as discussed previously. Neumann boundary conditions require more care. For instance, the homogeneous Neumann boundary condition $\frac{\partial \phi}{\partial x} = 0$ can be determined using the one-sided explicit formula

$$\alpha \phi_1 = a_0 \phi_2 + a_1 \phi_3 + a_2 \phi_4 + a_3 \phi_5 + a_4 \phi_6 + a_5 \phi_7 + a_6 \phi_8 + a_7 \phi_9. \qquad (6.1)$$

The Taylor series matching procedure is again used in this process. Each term is expanded about node 1 and like terms are equated to arrive at certain orders of accuracy for the boundary condition. In this case, however, the coefficients of the ϕ' term are set to 1. These coefficients can be set to equal any constant to obtain the same effect and the choice of 1 keeps the algorithm simple. This leaves the ϕ' term as the only nonzero term left over. The system of equations to be solved is given in

Table 15.

$$a_0 + a_1 + a_2 + a_3 + a_4 + a_5 + a_6 + a_7 = \alpha$$
$$a_0 + 2a_1 + 3a_2 + 4a_3 + 5a_4 + 6a_5 + 7a_6 + 8a_7 = 1$$
$$a_0 + 2^2 a_1 + 3^2 a_2 + 4^2 a_3 + 5^2 a_4 + 6^2 a_5 + 7^2 a_6 + 8^2 a_7 = 0$$
$$a_0 + 2^3 a_1 + 3^3 a_2 + 4^3 a_3 + 5^3 a_4 + 6^3 a_5 + 7^3 a_6 + 8^3 a_7 = 0$$
$$a_0 + 2^4 a_1 + 3^4 a_2 + 4^4 a_3 + 5^4 a_4 + 6^4 a_5 + 7^4 a_6 + 8^4 a_7 = 0$$
$$a_0 + 2^5 a_1 + 3^5 a_2 + 4^5 a_3 + 5^5 a_4 + 6^5 a_5 + 7^5 a_6 + 8^5 a_7 = 0$$
$$a_0 + 2^6 a_1 + 3^6 a_2 + 4^6 a_3 + 5^6 a_4 + 6^6 a_5 + 7^6 a_6 + 8^6 a_7 = 0$$
$$a_0 + 2^7 a_1 + 3^7 a_2 + 4^7 a_3 + 5^7 a_4 + 6^7 a_5 + 7^7 a_6 + 8^7 a_7 = 0$$
$$a_0 + 2^8 a_1 + 3^8 a_2 + 4^8 a_3 + 5^8 a_4 + 6^8 a_5 + 7^8 a_6 + 8^8 a_7 = 0.$$

Table 15: System of equations for Neumann boundary formula coefficients

Table 16 lists coefficients for the Neumann boundary condition $\frac{\partial \phi}{\partial x} = 0$. These coefficients are the same for both nodes 1 and N.

Order	a_0	a_1	a_2	a_3	a_4	a_5	a_6	a_7	α
4	48	-36	16	-3					25
6	360	-450	400	-225	72	-10			147
8	6720	-11760	15680	-14700	9408	-3920	960	-105	2283

Table 16: Coefficients for Neumann boundary condition $\frac{\partial \phi}{\partial x} = 0$

7 Temporal Derivatives

The compact scheme approximates spatial derivatives only. For problems such as the wave equation above, the explicit Euler time differencing method can be easily implemented. The higher-order Runge-Kutta methods are also commonly applied for temporal derivatives. This section considers a modified fourth order Runge-Kutta method by incorporating the compact scheme.

It is noted that for any time marching scheme, the Courant-Friedrichs-Lewy (CFL) condition must be satisfied. This type of stability analysis of the compact scheme is

often only verified by numerical experimentation rather than with the detailed von Neumann analysis. This is considered only briefly here.

For the explicit Euler time marching scheme, the necessary conditions are outlined by Vichnevetsky [23] and Lele [15]. When the compact scheme is employed with the Euler time approximation, the requirements are generally more strict [11] than for the low order explicit finite difference schemes.

The von Neumann stability analysis begins by considering the explicit Euler time integration of the semi-discrete equation $\phi_i' = A\phi_i$ where A is the discrete differential operator for the spatial derivatives. The updated solution is given by

$$\phi_i^{n+1} = \phi_i^n + \Delta t A \phi_i^n. \tag{7.1}$$

Substitution of the "trial" solution $\phi_i^n = b^n e^{i\omega x}$ into this scheme yields

$$b^{n+1} = [1 + \Delta t \tilde{\omega}(\omega)] b^n \tag{7.2}$$

where $\tilde{\omega}(\omega)$ is the spectral function of the discrete differential operator A. The ratio $z(\omega) = b^{n+1}/b^n = 1 + \Delta t \tilde{\omega}(\omega)$ is called the amplification factor and the von Neumann stability condition requires that $|z(\omega)| \leq 1$.

Definition 6. *The stability region S for the explicit Euler scheme is defined as the region in the $\Delta t \tilde{\omega}(\omega)$ plane determined by*

$$\Delta t \tilde{\omega}(\omega) = z - 1, \quad |z| \leq 1. \tag{7.3}$$

The stability of the Euler time integration method then corresponds to the step sizes in time and space for which $\Delta t \tilde{\omega}(\omega)$ lies within the stability region S for all ω. This stability region is a disc centered at $-1 + 0i$ in the complex $\Delta t \tilde{\omega}(\omega)$ plane as shown in Figure 1 of [23].

The fourth order first derivative compact scheme has the spectral function $\tilde{\omega}(\omega) = \frac{3\sin(\omega)}{2+\cos(\omega)}$. As the spectral function is entirely real-valued, the segment of the real axis where $\Delta t \tilde{\omega}(\omega)$ lies within the disc of the stability region S will determine the step size ratio for which the Euler scheme is stable in combination with this compact scheme. The spectral function of the fourth order scheme has the bound $\left| \frac{3\sin(\omega)}{2+\cos(\omega)} \right| \leq \sqrt{3}$ and the stability condition for the advection case determined by Hirsh [11] is

$$\frac{c\Delta t}{\Delta x} \leq \sqrt{1/6}, \tag{7.4}$$

showing that the scheme is stable on the interval $[-\sqrt{1/2}, 0]$ of the real axis in the $\Delta t \tilde{\omega}(\omega)$ plane.

For the diffusion case, the stability region of the fourth order second derivative compact scheme is determined in a similar manner. The limitations here are

$$\frac{\nu\Delta t}{\Delta x^2} \leq \frac{1}{3}. \tag{7.5}$$

For the Runge-Kutta time approximation methods, a similar approach proves to be much more difficult. However, Figure 5(d) of [23] shows plots of the stability regions of the Runge-Kutta methods of orders 1, 2, 3, and 4 which assist in determining the stability of these methods.

As discussed by Lele [15], the exact stability limitations in time and space steps depend on segments of the real and imaginary axis where the time advancement scheme is stable. Let σ_r and σ_i denote the segment lengths on the real and imaginary axes respectively. For the advection case,

$$\frac{c\Delta t}{\Delta x} \leq \frac{\sigma_i}{\tilde{\omega}_m} \tag{7.6}$$

where σ_i is from the segment of the imaginary axis $[-i\sigma_i, i\sigma_i]$ where the time advance-

ment scheme is stable. In the diffusion case, the restriction is to

$$\frac{\nu \Delta t}{\Delta x^2} \le \frac{\sigma_r}{\tilde{\omega}_m} \qquad (7.7)$$

where $[-\sigma_r, 0]$ is the segment of the real axis where the time advancement scheme is stable. The value of $\tilde{\omega}_m$ is the maximum value of the modified wave number for the first and second derivative compact schemes respectively. Vichnevetsky [23] also shows that the values of σ_i and σ_r for the fourth order Runge-Kutta method are 2.85 and 2.9 respectively.

For problem with non-periodic boundaries, stability requirements depend on the spectral radius of the matrix of the compact scheme. As this is much more complicated, step size requirements for stability with the use of compact schemes are usually determined by numerical experimentation. The step sizes are then chosen to fall well within the necessary range.

The application of the Runge-Kutta time approximation method to stiff differential equations in conjunction with the compact scheme space derivative approximation has yet to be analyzed or implemented in the current research available.

The modified fourth order Runge-Kutta method is discussed in the remainder of the section. For an initial value problem of the form

$$\begin{cases} \phi'(t) = f(\phi(t)) \\ \phi(0) = \phi^0 \end{cases},$$

the solution at a given time step can be computed with the fourth order Runge-Kutta

method by determining the four values

$$(K_1)_i^n = \Delta t f(\phi_i^n),$$

$$(K_2)_i^n = \Delta t f(\phi_i^n + \frac{1}{2}(K_1)_i^n),$$

$$(K_3)_i^n = \Delta t f(\phi_i^n + \frac{1}{2}(K_2)_i^n),$$

$$(K_4)_i^n = \Delta t f(\phi_i^n + (K_3)_i^n),$$

(7.8)

and then computing

$$\phi_i^{n+1} = \phi_i^n + \frac{1}{6}((K_1)_i^n + 2(K_2)_i^n + 2(K_3)_i^n + (K_4)_i^n)$$

(7.9)

for $i = 1, 2, 3, \ldots, N - 2, N - 1, N$.

For partial differential equations, the function f will be treated simply as a function of ϕ instead of a function of the derivatives of ϕ. For example, applying this method to the one dimensional wave equation begins with $u_t = -cu_x = f(u)$. Now for the given function f, it is straightforward to compute K_1 through K_4:

$$
\begin{aligned}
(K_1)_i^n &= \Delta t f(u_i^n) \\[6pt]
&= -c\Delta t(u_i^n)_x \\[6pt]
(K_2)_i^n &= \Delta t f(u_i^n + \frac{1}{2}(K_1)_i^n) \\[6pt]
&= -c\Delta t(u_i^n + \frac{1}{2}(K_1)_i^n)_x \\[6pt]
&= -c\Delta t(u_i^n)_x - \frac{c\Delta t}{2}((K_1)_i^n)_x \\[6pt]
&= -c\Delta t(u_i^n)_x + \frac{c^2\Delta t^2}{2}(u_i^n)_{xx} \\[6pt]
(K_3)_i^n &= \Delta t f(u_i^n + \frac{1}{2}(K_2)_i^n) \\[6pt]
&= -c\Delta t(u_i^n + \frac{1}{2}(K_2)_i^n)_x \\[6pt]
&= -c\Delta t(u_i^n)_x - \frac{c\Delta t}{2}(K_2)_i^n)_x \\[6pt]
&= -c\Delta t(u_i^n)_x + \frac{c^2\Delta t^2}{2}(u_i^n)_{xx} - \frac{c^3\Delta t^3}{2}(u_i^n)_{xxx} \\[6pt]
(K_4)_i^n &= \Delta t f(u_i^n + (K_3)_i^n) \\[6pt]
&= -c\Delta t(u_i^n + (K_3)_i^n)_x \\[6pt]
&= -c\Delta t(u_i^n)_x - c\Delta t((K_3)_i^n)_x \\[6pt]
&= -c\Delta t(u_i^n)_x + c^2\Delta t^2(u_i^n)_{xx} - \frac{c^3\Delta t^3}{2}(u_i^n)_{xxx} + \frac{c^4\Delta t^4}{2}(u_i^n)_{xxxx}.
\end{aligned}
$$

The updated solution then computed with these values is given by

$$
\begin{aligned}
u_i^{n+1} &= u_i^n + \frac{1}{6}[(K_1)_i^n + 2(K_2)_i^n + 2(K_3)_i^n + (K_4)_i^n] \\[6pt]
&= u_i^n + \frac{1}{6}\left[-6c\Delta t(u_i^n)_x + c^2\Delta t^2(u_i^n)_{xx} + \frac{c^3\Delta t^3}{2}(u_i^n)_{xxx} - \frac{c^4\Delta t^4}{2}(u_i^n)_{xxxx} \right].
\end{aligned}
$$

The difficulty presented here is in computing values of $(u_i^n)_x$, $(u_i^n)_{xx}$, $(u_i^n)_{xxx}$, $(u_i^n)_{xxxx}$. For problems involving higher order derivatives, the Runge-Kutta algorithm requires knowledge of derivatives of order greater than four. The approach taken here is to

approximate $(u_i^n)_x$ using the compact scheme yielding the values of $(K_1)_i^n$. Following this, the values of $(K_2)_i^n = -c\Delta t(u_i^n)_x - \frac{c\Delta t}{2}((K_1)_i^n)_x$ can be computed by using both the values of $(K_1)_i^n$ and the derivative values of $(K_1)_i^n$ which may be obtained by using the compact scheme on $(K_1)_i^n$. $(K_3)_i^n$ is then computed using the values of $(K_1)_i^n$ and the derivative of $(K_2)_i^n$ which again can be found using the compact scheme. $(K_4)_i^n$ is found in a similar manner.

A similar idea is considered in the following section where second derivatives are computed by applying the first derivative scheme once to yield the first derivative values and then the compact scheme is used again on the derivative values to approximate the second derivative. This would likely double the required computation time, but the derivation of compact schemes for higher-order derivatives may therefore be bypassed. Li and Visbal [17] gave an excellent discussion of the effect of successive application of lower-order derivative schemes. The formal order of accuracy appears to be maintained, but the resolution characteristics are diminished in comparison to the direct application of schemes for higher-order derivatives.

An interesting question that arises from such a combination is whether or not such an approach can be used to accurately approximate a mixed partial derivative. Applying the compact scheme over a grid to obtain derivatives in one direction and then running the compact scheme again over those derivative values in the other direction may yield an accurate approximation of such second order mixed partial derivatives.

8   Applications

The compact scheme has been analyzed in the application to the one-dimensional wave equation. Four other application problems will be considered here.

8.1 Heat Equation

The one-dimensional heat equation

$$\phi_t = \sigma \phi_{xx} \tag{8.1}$$

is solved on the domain $[0, 2\pi]$ with 100 grid points for diffusivity $\sigma = 2$. The initial heat distribution is given by $\phi(x, 0) = \sin x$. The exact solution is given by $\phi(x, t) = e^{-2t} \sin(x)$ and the compact scheme solution is compared with the standard forward in time, centered in space (FTCS) method. With a time step $\Delta t = 0.0001$, the solution is iterated 10000 times using the Euler explicit time derivative approximation and the solution is shown after 1 second. The step size in time must be chosen to satisfy the CFL condition

$$C = \frac{2\Delta t}{\Delta x^2} \leq \frac{1}{3}$$

for the fourth order scheme where $\frac{1}{3}$ is the ratio of $\frac{\sigma_r}{\bar{\omega}_m}$ from 7.6. This is more restrictive than the $\frac{1}{2}$ requirement for the forward in time, centered in space second order finite difference scheme. The given step size in time yields $C = 0.0507$ which should be sufficient for the fourth order scheme and other higher order compact schemes.

Two experiments were run in this problem. First, the second derivative scheme was used to approximate the spatial derivative. Then the first derivative compact scheme was run twice in succession to approximate the second derivative. The maximum point-wise error of the second derivative compact scheme in comparison to the exact solution are given in column A of Table 17. Column B represents the maximum point-wise error of the first derivative compact scheme run twice in succession. The maximum point-wise error for the FTCS solution was 0.0138 where this scheme is formally second order accurate in space.

For most of the schemes, the first derivative algorithm applied twice approximates the second derivative with a reasonable degree of accuracy. However, the table shows
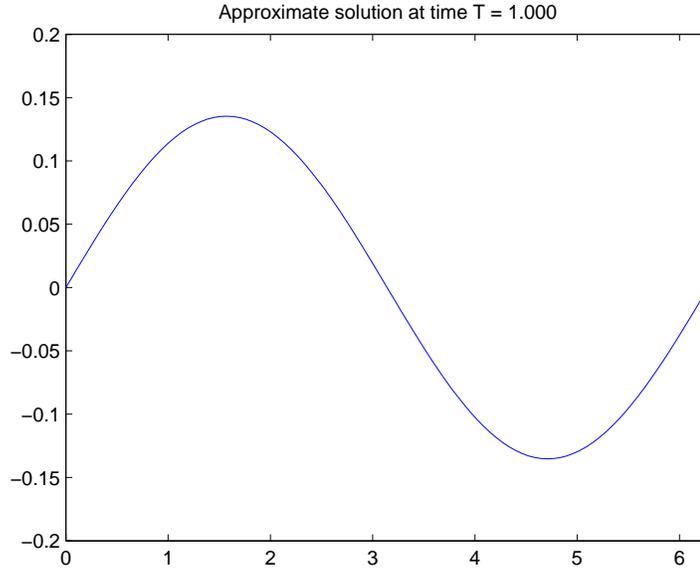
Figure 31: Heat Equation exact solution $\phi(x, t) = e^{-2\pi t} \sin(x)$

Scheme	A	B
T4	2.7046e-005	2.7012e-005
T6	2.7065e-005	2.7065e-005
P6	2.7224e-005	1.9427e-004

Table 17: Point-wise errors in numerical approximation of heat equation at T = 1s

little advantage of this approach in comparison with the second derivative algorithm.

The Neumann boundary condition $\frac{d\phi}{dx} = 0$ was applied for another experiment to determine the effectiveness of the boundary formulas presented in Section 6. The Neumann condition was used for the left boundary and the Dirichlet condition for the right boundary. The initial condition and all other details remain the same from the previous experiment. The graph of the approximation is shown in Figure 32.
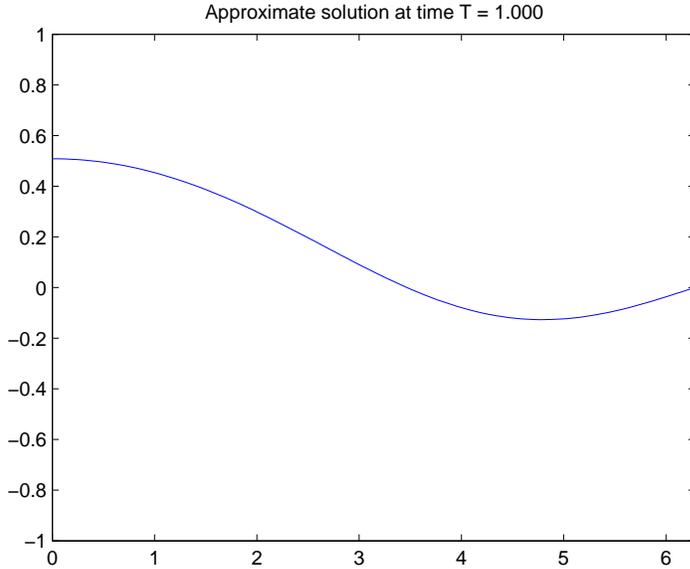
Figure 32: Heat Equation with Neumann boundary condition

8.2 Burgers' Equation

Burgers' equation is a nonlinear convection-diffusion equation that is often used as a standard test for numerical algorithms. The equation given here is

$$\phi_t + \left(\frac{1}{2} - \phi \right) \phi_x = \nu \phi_{xx} \qquad (8.2)$$

where ν represents the viscosity. The problem is to be solved on the physical domain where $\lim_{x \to -\infty} \phi(x, t) = 0$, and $\lim_{x \to \infty} \phi(x, t) = 1$. For the approximation, the simplified domain $[-5, 5]$ is used with assumed boundary conditions $\phi(-5, t) = 0$, and $\phi(5, t) = 1$ and a linear initial profile $\phi(x, 0) = \frac{1}{10}x + \frac{1}{2}$.

With a value of $\nu = \frac{1}{8}$ for the viscosity, the spatial derivatives will be computed using the fourth order compact schemes for both first and second derivatives. The steady-state behavior of the solution will be determined and approximate values will be compared to the actual steady-state solution $\phi(x) = \frac{1}{2} \left(1 + \tanh \frac{x}{4\nu} \right)$. Euler explicit time integration is used to march the solution forward in time with step size $\Delta t = 0.05$.

74

The spatial step size is $\Delta x = 0.2$. These choices yield the ratio $\frac{\nu \Delta t}{\Delta x^2} = 0.3$ which is less than the required $\frac{1}{3}$ necessary for stability of the fourth order scheme. The exact solution is plotted in Figure 33.
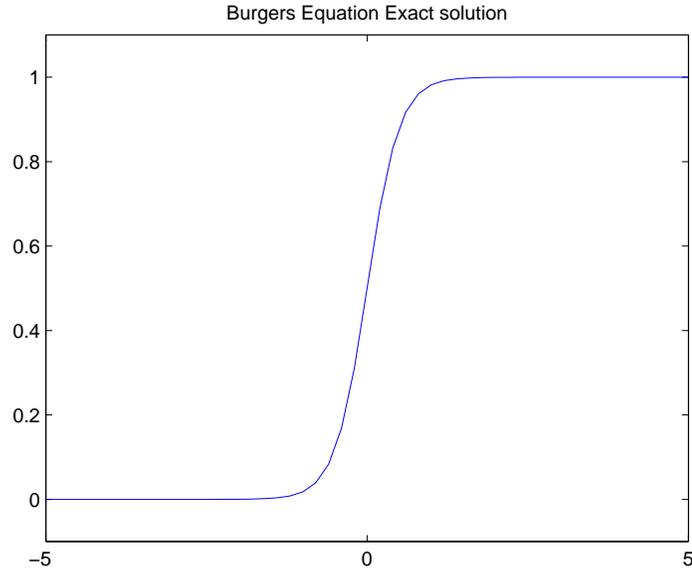
Figure 33: Exact steady-state solution of Burgers' Equation

The results of the experiment are given in Table 18. The scheme was marched in time until a steady state was reached, that is, the time derivative change was less than 10^{-8} (chosen arbitrarily). The infinity norm of the difference of the steady state approximation and the exact solution was 0.00035367.

To determine the correct order of accuracy of the compact scheme, an approach similar to that given by LeVeque [16] and Villamizar [3] is followed. For the steady state solution, the infinity norm error is computed since the exact solution is known. This is done for various step sizes Δx. Table 19 shows the error for various step sizes along with the logarithms of the step sizes and errors.

A linear regression for the two logarithms in Table 19 produces an equation with a slope approximately equal to the exponent in the truncation error of the numerical scheme. The data and regression line are plotted in Figure 34. The linear regression

75

x	Exact	T4
0	0.5	0.5
0.2	0.68997	0.69033
0.4	0.83202	0.83224
0.6	0.91683	0.91687
0.8	0.96083	0.96082
1.0	0.98201	0.98199
1.2	0.99184	0.99182
1.4	0.99632	0.99631
1.6	0.99834	0.99834
1.8	0.99925	0.99925
2.0	0.99966	0.99966

Table 18: Burgers' Equation Solutions

Δx	$-\log(\Delta x)$	Error	$-\log(\text{Error})$
$\frac{1}{5}$	1.6094379	0.00035367	7.947146283
$\frac{1}{6}$	1.7917595	0.00015300	8.785072637
$\frac{1}{7}$	1.9459101	0.00008251	9.402542582
$\frac{1}{8}$	2.0794415	0.00004994	9.904648226
$\frac{1}{9}$	2.1972246	0.00003106	10.37946097
$\frac{1}{10}$	2.3025851	0.00001991	10.82428844

Table 19: Error and convergence analysis for Burgers' Equation

equation is $y = 4.0931x + 1.4046$ with a correlation coefficient of $R^2 = 0.999$ showing the expected rate of convergence.

8.3 Convection Equation

The compact schemes are used here to solve the convection-diffusion equation

$$\phi_t + u\phi_x + v\phi_y = \alpha(\phi_{xx} + \phi_{yy}) \tag{8.3}$$
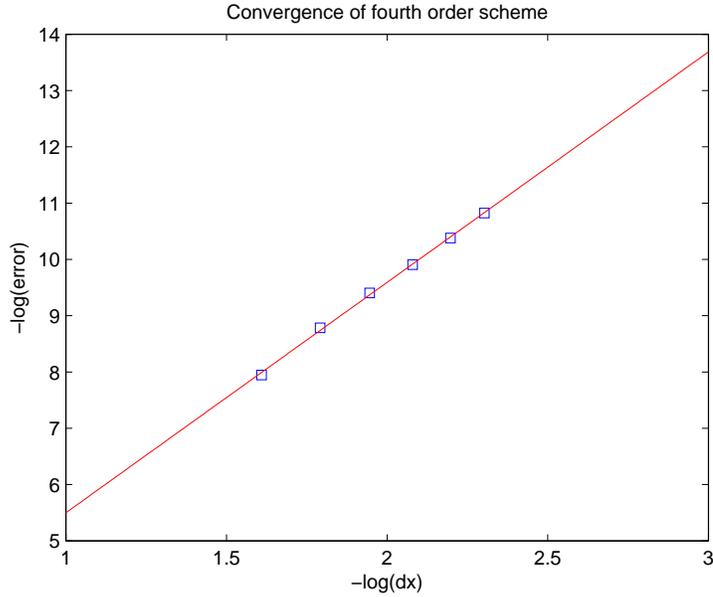
Figure 34: Convergence rate of fourth order scheme for Burgers' Equation

on the domain $x \in [-\frac{1}{2}, \frac{1}{2}], y \in [-\frac{1}{2}, \frac{1}{2}]$ over a grid 100×100 grid. The initial condition is given by

$$\phi(x, y, 0) = 5 \exp\left(-1500 \left[\left(x - \frac{1}{4}\right)^2 + y^2\right]\right). \qquad (8.4)$$

The velocity components are taken to be $u = -y, v = x$ and $\alpha = 0$. The time derivative is solved using the Runge-Kutta fourth order method with $\Delta t = 1.0 \times 10^{-3}$. This is a re-creation of the experiment analyzed by [7]. The choice of step sizes in the x and y direction along with the time step size is sufficient for the stability requirements as discussed earlier.

The Runge-Kutta system of equations is given by

$$(K_1)^n_{ij} = \Delta t f(\phi^n_{ij})$$

$$= \Delta t (y(\phi^n_{ij})_x - x(\phi^n_{ij})_y)$$

$$(K_2)^n_{ij} = \Delta t f(\phi^n_{ij} + \frac{1}{2}(K_1)^n_{ij})$$

$$= \Delta t (y(\phi^n_{ij})_x - x(\phi^n_{ij})_y + \frac{1}{2}(y((K_1)^n_{ij})_x - x((K_1)^n_{ij})_y))$$

$$(K_3)^n_{ij} = \Delta t f(\phi^n_{ij} + \frac{1}{2}(K_2)^n_{ij})$$

$$= \Delta t (y(\phi^n_{ij})_x - x(\phi^n_{ij})_y + \frac{1}{2}(y((K_2)^n_{ij})_x - x((K_2)^n_{ij})_y))$$

$$(K_4)^n_{ij} = \Delta t f(\phi^n_{ij} + (K_3)^n_{ij})$$

$$= \Delta t (y(\phi^n_{ij})_x - x(\phi^n_{ij})_y + y((K_3)^n_{ij})_x - x((K_3)^n_{ij})_y)$$

$$\phi^{n+1}_{ij} = \phi^n_{ij} + \frac{1}{6}((K_1)^n_{ij} + 2(K_2)^n_{ij} + 2(K_3)^n_{ij} + (K_4)^n_{ij}).$$

The initial condition is a sharp Gaussian profile with a peak at five. The cone will be convected in a circular pattern around the origin. Without the diffusive term, the initial profile should be undistorted when it returns to the initial position. Each figure lists the minimum and maximum values of the approximate solution after one full rotation. The initial profile is plotted in Figure 35.

With a discretized domain, the peak of the initial condition is not rendered exactly at the value of 5 but at 4.76649. As the cone rotates around the circle, the peak of the cone is rendered at different grid points and the maximum value fluctuates. With the refined mesh size 100×100, any significant loss introduced by the approximation scheme should be apparent. The approximations for several different schemes are shown in figures 36 and 37.

For the spectral scheme A6, the solution was again approximated after four full rotations to determine if the initial peak is diminished after a longer time simulation. The results given in Figure 38 show that there is only a minimal loss. All other fourth and sixth order schemes used here showed a significant loss after two full rotations.
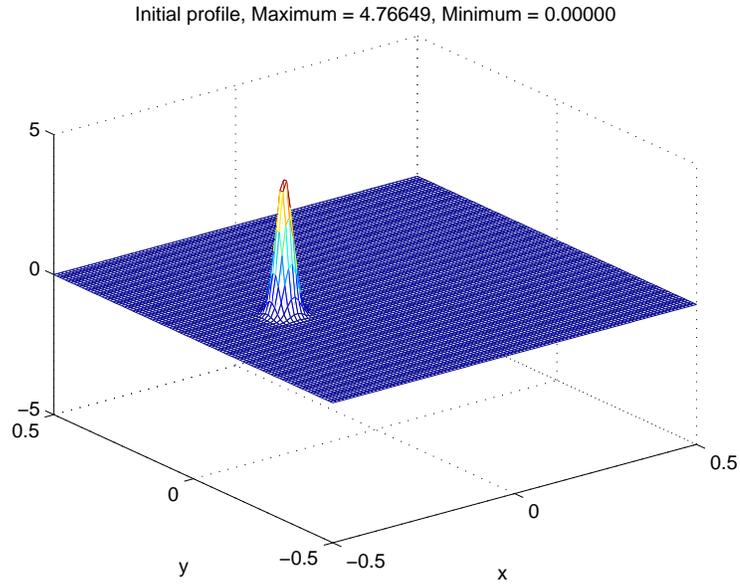
Figure 35: Initial profile for convection equation

Maximum = 4.49247, Minimum = −0.36307   Maximum = 4.81397, Minimum = −0.02857
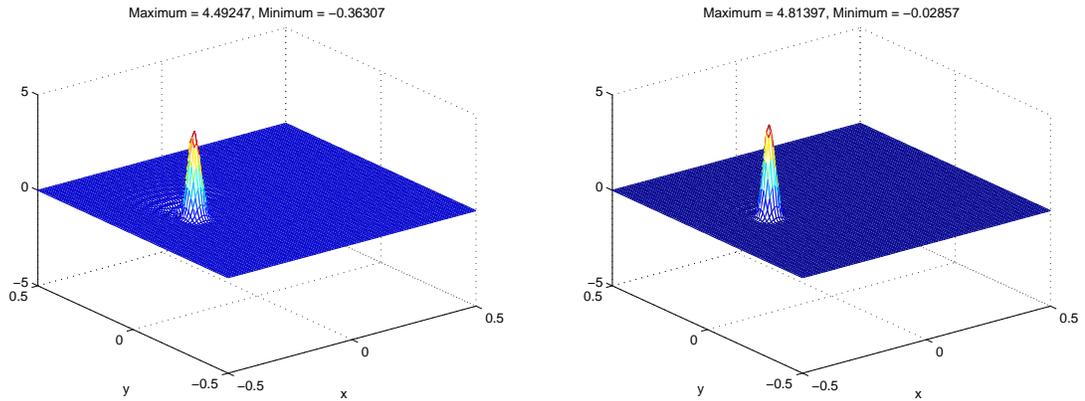
Figure 36: Convection solution at T = 2π with the T4 and T6 schemes

As was suggested earlier, the Runge-Kutta method applied to the partial differential equations considered here incorporates the compact scheme in computing spatial derivatives. All previous experiments on the convection equation (8.3) used the Runge-Kutta method for the time derivative approximation. The values of K_1 through K_4 were all computed using the compact scheme with the same order of accuracy as was used for the derivatives ϕ_x and ϕ_y.
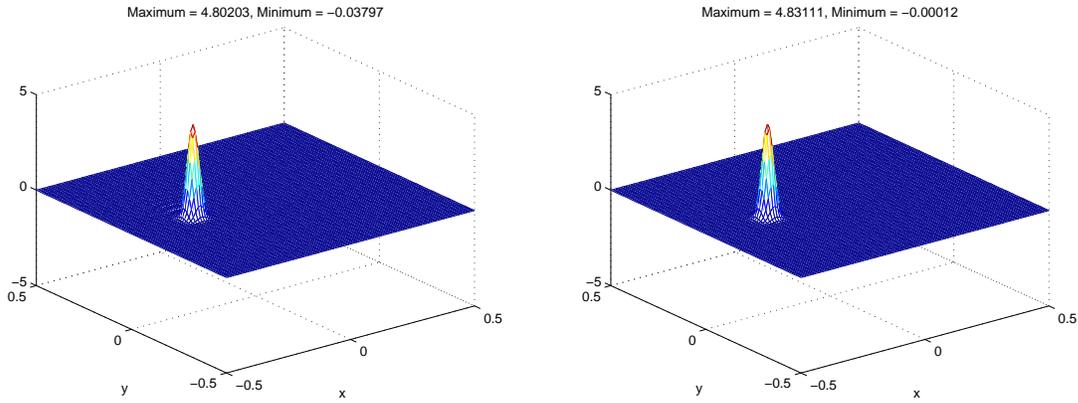
Figure 37: Convection solution at T $= 2\pi$ with the P6 and A6 schemes
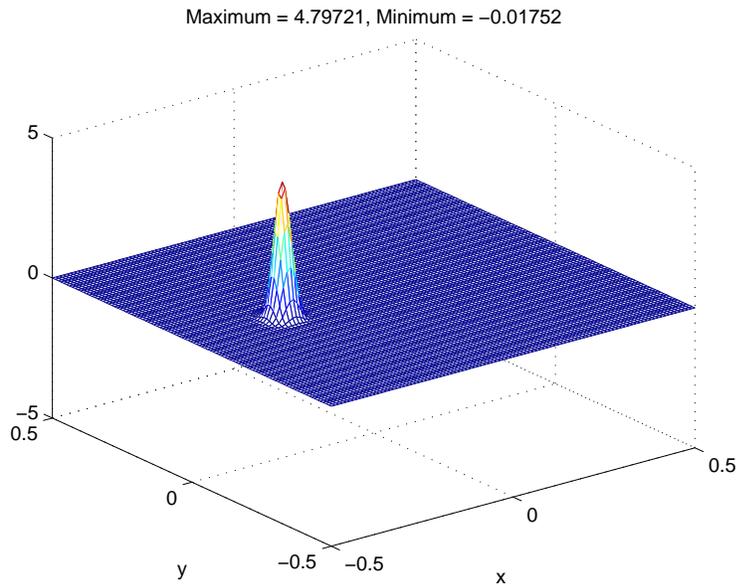
Figure 38: Convection solution at T $= 8\pi$ with the A6 scheme

Another experiment was run using both the T4 and T6 schemes for the spatial derivatives. This time the Runge-Kutta method employed various compact schemes in the approximations of K_1 through K_4. The results are shown in Table 20.

Table 20 shows both maximum and minimum values obtained for both the T4 and T6 schemes used for the spatial derivative. That is, the solution depended more on which compact scheme was incorporated into the Runge-Kutta algorithm than the

RK4		
scheme	max	min
T4	4.4925	-0.3631
T6	4.8140	-0.0286
P6	4.8020	-0.0380
A6	4.8311	-0.0001

Table 20: Convection max and min at $T = 2\pi$ for (8.3) with compact schemes scheme used for the spatial derivatives.

8.4 Korteweg-de Vries (KdV) Equation

As demonstrated by [17], the compact scheme may be applied to the standard Korteweg-de Vries (KdV) equation

$$\phi_t + 3(\phi^2)_x + \phi_{xxx} = 0. \tag{8.5}$$

This is a nonlinear equation with a third derivative term. Li and Visbal claim that [17] is the first known implementation of a third derivative compact scheme. Such schemes have been considered for several years, yet implementation for third derivatives has generally been performed by successive use of the first derivative scheme.

With the initial condition

$$\phi(x, 0) = -2\text{sech}^2 x, \tag{8.6}$$

the exact solution is

$$\phi(x, t) = -2\text{sech}^2(x - 4t). \tag{8.7}$$

The numerical solution is obtained by applying the sixth order compact scheme with periodic boundary conditions. The solution is approximated on the interval $[-10, 12]$ with $N = 41, 81, 161$ equally spaced grid points. The time step $\Delta t = 0.01\Delta x^2$ is suggested by [17]. Numerical results show the scheme to be unstable for $\frac{\Delta t}{\Delta x^2} > 0.05$.

81

The solution is filtered with an eighth order tridiagonal filter ($\alpha = 0.4$)

The maximum point-wise error is computed for the three grid spacings. The effect of the frequency of the filter is shown in Table 21. The first column shows the maximum point-wise error when the filter is run every time step and the second column shows the error with the filter applied every 10 time steps. The third column shows the effect of the filter run every 100 time steps. For comparison, the last column shows the maximum point-wise error when the filter is not applied.

N	filter 1	filter 10	filter 100	no filter
41	0.1865	0.0201	0.0491	0.0544
81	0.0116	0.0118	0.0138	0.0139
161	0.0024	0.0034	0.0035	0.0035

Table 21: Maximum point-wise errors for KdV equation

As the grid is refined, the frequency of the filter application appears to become less important in considering the maximum point-wise error. It is also interesting to note the effect of the filter application for the $N = 41$ case. The filter applied at every time step produced a result that was worse than the approximation without filtering. If the order of the filter is increased to eight, the approximation is still worse than all other results for this case. Only when the filter is increased to tenth order is the maximum point-wise error (0.0543) better than no application of the filter for this grid spacing. A plot of the approximate solution after 0.5 seconds for the $N = 81$ case is shown in Figure 39 and the point-wise error is shown in Figure 40.

A similar analysis as before is done to determine the order of accuracy of the compact scheme in this application. The sixth order compact scheme with periodic boundary formulas was used for the first and third derivative. A tenth order tridiagonal filter was implemented with $\alpha = 0.4$. Table 22 shows the point-wise error for several different grid spacings. The least squares line from this data set is $y = 4.1566x + 0.294$ with a correlation coefficient of $R^2 = 0.9939$ showing that there
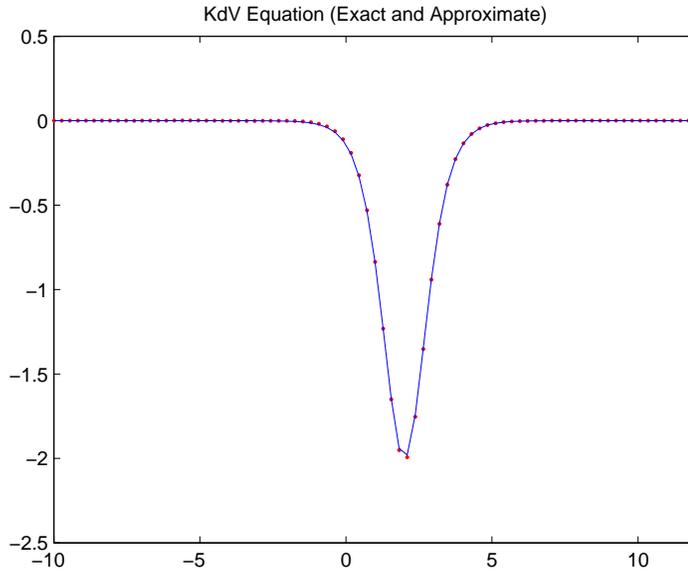
Figure 39: KdV approximate solution after 0.5s with filtered sixth order scheme
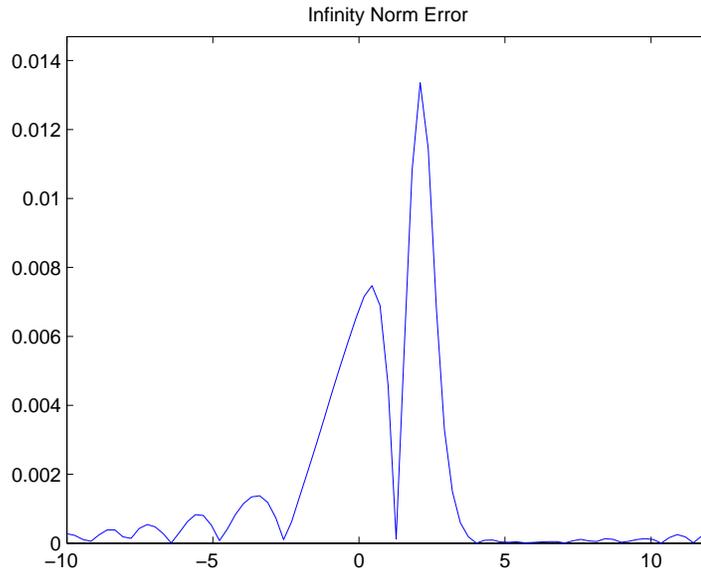
Figure 40: Point-wise error in KdV equation approximation after 0.5 seconds

is approximately fourth order convergence rather than sixth order. Since there was no steady state to be reached with this problem, the solution was simply marched in time for 1.5 seconds and the approximation was compared with the exact solution at

that time.

Δx	$-\log(\Delta x)$	Error	$-\log(\text{Error})$
$\frac{22}{60}$	0.435729	0.1136	2.1750718
$\frac{22}{80}$	0.5606673	0.0772	2.5613558
$\frac{22}{100}$	0.6575773	0.0508	2.9798589
$\frac{22}{120}$	0.7367586	0.0354	3.3410435
$\frac{22}{140}$	0.8037054	0.0260	3.6496587
$\frac{22}{160}$	0.8616973	0.0199	3.9170355

Table 22: Error and convergence for KdV Equation

The error and least squares line are plotted together in Figure 41.
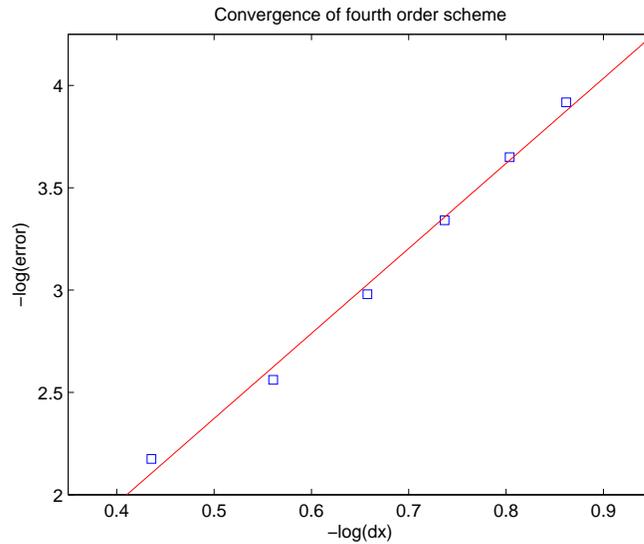
Figure 41: Convergence rate of sixth order scheme for KdV Equation

If the filter coefficient α is increased to 0.45, the least squares line for the error is $y = 4.424x + 0.0859$ with a correlation coefficient $R^2 = 0.9988$. With a filter coefficient of 0.495, the regression line becomes $y = 4.6423x - 0.084$ with a correlation coefficient $R^2 = 1$.

9 Summary

The development of the high order compact schemes was done in several parts. Interior point formulas of the Padé type were derived using the Taylor series matching procedure. Boundary formulas of the same type were also derived. Comparison of these schemes with the explicit finite difference methods of the same order showed several advantages of the compact scheme. Necessary conditions of stability and convergence were discussed and the eigenvalue analysis showed some of the schemes to be strictly stable.

The resolving efficiency of the schemes were determined by considering the spectral functions of the compact schemes. The spectral functions were also used to derive coefficients for the spectral type schemes. Comparison of Padé and spectral schemes in approximation of the one-dimensional wave equation showed the spectral schemes to be considerably better. Filter formulas were derived and implemented. The Euler explicit and fourth-order Runge-Kutta temporal approximation methods were considered in conjunction with the compact schemes.

Several test problems were considered. The order of convergence was shown to be higher than the typical second order explicit method. The method of implementation of the compact schemes in MATLAB showed that the compact schemes may be used with relatively good efficiency. The compact schemes perform well in the examples considered here and merit further analysis and consideration in more general two dimensional and three dimensional initial/boundary value problems.

Appendix A

The algorithm used to solve a differential equation with the compact scheme is simple. Assuming that all the details of the numerical scheme have already been determined, such as mesh size, time integration method, time step size, and initial profile, the

procedure is as follows:

- Choose degree of accuracy

- Choose stencil sizes

- Determine necessary coefficients

- Generate implicit left-hand side matrix

- Generate right-hand side matrix

- Solve system to obtain necessary derivative matrices

- Update solution with time integration method

The matrices involved in the computation do not change at each time level. Therefore it is best to code the algorithm with the matrices predetermined and defined. These matrices can then be called at the necessary step in the algorithm without having to be reproduced.

Appendix B

The following MATLAB codes are designed to run the compact scheme for one and two dimensional problems.

The function 'compactLHS' saved as a '.m' file with the input 'N' generates the square matrix of size N×N for the left hand side of the sixth order tridiagonal scheme.

function A = compactLHS(N)

A = zeros(N,N); B = ones(N,3);

%Interior scheme

B(:,1) = 1 / 3; B(:,3) = 1 / 3; %alpha

%Boundary formulation

B(2,3) = 5; B(N-1,1) = 5; %Nodes 1 and N

B(1,1) = 1 / 8; B(3,3) = 3 / 4; %Node 2

B(N-2,1) = 3 / 4; B(N,3) = 1 / 8; %Node N-1

%Sparse matrix generation

A = spdiags(B,[-1 0 1],A);

The function 'compactRHS' saved as a '.m' file with the same input as 'compactLHS' generates the right-hand side matrix of the compact scheme.

function B = compactRHS(N)

B = zeros(N,N); C = zeros(N,5);

C(:,1) = -1 / 36;

C(:,2) = -14 / 18;

C(:,4) = 14 / 18;

C(:,5) = 1 / 36;

B = spdiags(C,[-2 -1 0 1 2],B);

B(1,1) = -197/60; B(1,2) = -5/12; B(1,3) = 5;

B(1,4) = -5/3; B(1,5) = 5/12; B(1,6) = -1/20;

B(2,1) = -43/96; B(2,2) = -5/6; B(2,3) = 9/8; B(2,4) = 1/6;

B(2,5) = -1/96;

B(N-1,N) = 43/96; B(N-1,N-1) = 5/6; B(N-1,N-2) = -9/8; B(N-1,N-3) = -1/6;

B(N-1,N-4) = 1/96;

B(N,N) = 197/60; B(N,N-1) = 5/12; B(N,N-2) = -5; B(N,N-3) = 5/3;

B(N,N-4) = -5/12; B(N,N-5) = 1/20;

The matrices A and B from 'compactLHS' and 'compactRHS', initial value of the solution u, spatial step size dx, and 'int1' and 'int2' are the inputs for the 'compact' function where 'int1' and 'int2' are the first and last node required for computation. The function then approximates the values of the first derivative at all nodes from 'int1' to 'int2' solving the matrix equation (2.30).

function z = compact(A,B,u,dx,int1,int2);

[m n] = size(u);

if m> 1 && n > 1

    m = int1; n = int2;

else

    m = 1; n = 1;

end

rhs = B * (u / dx);

z = A(int1:int2,int1:int2) \ rhs(int1:int2,m:n);

For a two dimensional problem, the code readily computes the y derivatives for all mesh points. The same code can be used to determine the x derivatives by substituting the transpose of the matrix u. The solution z then returns the transpose of the matrix of x derivatives. Similar codes can be written for compact schemes of all orders.

The code presented here for the compact scheme does not optimize the computation time. As noted earlier, the matrix equation solution X of $AX = B$ may be pre-determined outside of the time loop for a given scheme. This new matrix X may therefore be multiplied with the previous time solution to obtain the approximate derivative values at the current time iteration. Thus the matrix system to be solved at each time level reduces to matrix-vector or matrix-matrix multiplication.

The filter scheme can be accomplished in a similar manner as the compact scheme. There is one code which generates the implicit left hand side and another to generate the right hand side. Again the functions 'filterLHS' and 'filterRHS' should be saved as '.m' files. The input is similar to that of the compact schemes. Here the free parameter 'alpha' is necessary is input for both functions. The function 'filterLHS' is shown here.

function C = filterLHS(N,alpha)

C = zeros(N,N); D = ones(N,3);

D(:,1) = alpha; D(:,3) = alpha;

C = spdiags(D,[-1 0 1],C);

The function 'filterRHS' is shown here.

function D = filterRHS(order,N,alpha)

D = zeros(N,N);

a = (93 + 70 * alpha) / 128;

b = (7 + 18 * alpha) / 16;

c = (-7 + 14 * alpha) / 32;

d = (1 - 2 * alpha) / 16;

e = (-1 + 2 * alpha) / 128;

B = zeros(N,9);

B(:,1) = e / 2; B(:,2) = d / 2; B(:,3) = c / 2; B(:,4) = b / 2;

B(:,5) = a;

B(:,6) = b / 2; B(:,7) = c / 2; B(:,8) = d / 2; B(:,9) = e / 2;

D = spdiags(B,[-4 -3 -2 -1 0 1 2 3 4],D);

D(1,1) = (255 + alpha) / 256; D(1,2) = (1 + 31 * alpha) / 32;

D(1,3) = (-7 + 7 * alpha) / 64; D(1,4) = (7 - 7 * alpha) / 32;

D(1,5) = 7 * (-5 + 5 * alpha) / 128; D(1,6) = (7 - 7 * alpha) / 32;

D(1,7) = 7 * (-1 + alpha) / 64; D(1,8) = (1 - alpha) / 32;

D(1,9) = (-1 + alpha) / 256;

D(2,1) = (1 + 254 * alpha) / 256; D(2,2) = (31 + 2 * alpha) / 32;

D(2,3) = (7 + 50 * alpha) / 64; D(2,4) = (-7 + 14 * alpha) / 32;

D(2,5) = 7 * (5 - 10 * alpha) / 128; D(2,6) = (-7 + 14 * alpha) / 32;

D(2,7) = (7 - 14 * alpha) / 64; D(2,8) = (-1 + 2 * alpha) / 32;

D(2,9) = (1 - 2 * alpha) / 256;

D(3,1) = (-1 + 2 * alpha) / 256; D(3,2) = (1 + 30 * alpha) / 32;

D(3,3) = (57 + 14 * alpha) / 64; D(3,4) = (7 + 18 * alpha) / 32;

D(3,5) = 7 * (-5 + 10 * alpha) / 128; D(3,6) = (7 - 14 * alpha) / 32;

D(3,7) = (-7 + 14 * alpha) / 64; D(3,8) = (1 - 2 * alpha) / 32;

D(3,9) = (-1 + 2 * alpha) / 256;

D(4,1) = (1 - 2 * alpha) / 256; D(4,2) = (-1 + 2 * alpha) / 32;

D(4,3) = (7 + 50 * alpha) / 64; D(4,4) = (25 + 14 * alpha) / 32;

D(4,5) = (35 + 58 * alpha) / 128; D(4,6) = (-7 + 14 * alpha) / 32;

D(4,7) = (7 - 14 * alpha) / 64; D(4,8) = (-1 + 2 * alpha) / 32;

D(4,9) = (1 - 2 * alpha) / 256;

D(N-3,N) = (1 - 2 * alpha) / 256; D(N-3,N-1) = (-1 + 2 * alpha) / 32;

D(N-3,N-2) = (7 + 50 * alpha) / 64; D(N-3,N-3) = (25 + 14 * alpha) / 32;

D(N-3,N-4) = (35 + 58 * alpha) / 128; D(N-3,N-5) = (-7 + 14 * alpha) / 32;

D(N-3,N-6) = (7 - 14 * alpha) / 64; D(N-3,N-7) = (-1 + 2 * alpha) / 32;

D(N-3,N-8) = (1 - 2 * alpha) / 256;

D(N-2,N) = (-1 + 2 * alpha) / 256; D(N-2,N-1) = (1 + 30 * alpha) / 32;

D(N-2,N-2) = (57 + 14 * alpha) / 64; D(N-2,N-3) = (7 + 18 * alpha) / 32;

D(N-2,N-4) = 7 * (-5 + 10 * alpha) / 128; D(N-2,N-5) = (7 - 14 * alpha) / 32;

D(N-2,N-6) = (-7 + 14 * alpha) / 64; D(N-2,N-7) = (1 - 2 * alpha) / 32;

D(N-2,N-8) = (-1 + 2 * alpha) / 256;

D(N-1,N) = (1 + 254 * alpha) / 256; D(N-1,N-1) = (31 + 2 * alpha) / 32;

D(N-1,N-2) = (7 + 50 * alpha) / 64; D(N-1,N-3) = (-7 + 14 * alpha) / 32;

D(N-1,N-4) = 7 * (5 - 10 * alpha) / 128; D(N-1,N-5) = (-7 + 14 * alpha) / 32;

D(N-1,N-6) = (7 - 14 * alpha) / 64; D(N-1,N-7) = (-1 + 2 * alpha) / 32;

D(N-1,N-8) = (1 - 2 * alpha) / 256;

D(N,N) = (255 + alpha) / 256; D(N,N-1) = (1 + 31 * alpha) / 32;

D(N,N-2) = (-7 + 7 * alpha) / 64; D(N,N-3) = (7 - 7 * alpha) / 32;

D(N,N-4) = 7 * (-5 + 5 * alpha) / 128; D(N,N-5) = (7 - 7 * alpha) / 32;

D(N,N-6) = 7 * (-1 + alpha) / 64; D(N,N-7) = (1 - alpha) / 32;

D(N,N-8) = (-1 + alpha) / 256;

The the left-hand side and right-hand side matrices generated, the solution X of the matrix equation $CX = D$ encodes all the necessary information about the filter. At any time step, the filter can be accomplished by multiplying this matrix by the solution vector or matrix.

Appendix C

The derivation of compact schemes relies heavily upon Taylor's theorem.

Theorem 6. *If f is an $n+1$ times differentiable function on an interval I containing x_0, then for each x in I there exists ξ between x and x_0 such that*

$$f(x) = \quad f(x_0) + f'(x_0)(x - x_0) + \frac{f''(x_0)}{2!}(x - x_0)^2 + \frac{f'''(x_0)}{3!}(x - x_0)^3 + \cdots +$$

$$\frac{f^{(n)}(x_0)}{n!}(x - x_0)^n + R_n(x) \tag{9.1}$$

where

$$R_n(x) = \frac{f^{(n+1)}(\xi)}{(n + 1)!}(x - x_0)^{n+1}.$$

The proof of Taylor's theorem can be found in many Calculus texts such as [14].

If a partition, $x = x_0 + ih$, $i = 0, 1, \ldots, J$, is defined in the interval I containing x_0, x_i, and x_{i+j} then, (9.1) can be used to obtain a representation of $f_{i+j} = f(x_{i+j})$ ($x_{i+j} = x_0 + (i + j)h$) as a Taylor series centered at x_i. In fact,

$$f_{i+j} = f_i + jhf_i' + \frac{j^2 h^2}{2!} f_i'' + \cdots \frac{j^n h^n}{n!} f_i^{(n)} + R_{n_{i+j}},$$

where $f_i^{(n)} = f^{(n)}(x_i)$, $n = 0, 1, \ldots, n$.

For functions of two or more variables as for example, $\phi(x, t)$, having $n+1$ partial derivatives with respect to x in the interval I , the above Taylor series expansion can be written as

$$\phi_{i+j} = \phi_i + jh \left(\frac{\partial \phi}{\partial x} \right)_i + \frac{j^2 h^2}{2!} \left(\frac{\partial^2 \phi}{\partial x^2} \right)_i + \cdots + \frac{j^n h^n}{n!} \left(\frac{\partial^n \phi}{\partial x^n} \right)_i + R_{n_{i+j}} \tag{9.2}$$

where the error term R_n is given by

$$R_{n_{i+j}} = \frac{j^{n+1} h^{n+1}}{(n + 1)!} \left(\frac{\partial^{n+1} \phi}{\partial x^{n+1}} \right)_{i+\xi}, \qquad 0 < \xi < j. \tag{9.3}$$

Assuming that ϕ has $n+2$ derivatives with respect to x in the interval I, the Taylor

92

$$
\begin{aligned}
0 &= a+b+c+d+e+f+g \\
1+\alpha+\beta &= b+2c+3d+4e+5f+6g \\
2!(\alpha+2\beta) &= b+2^2c+3^2d+4^2e+5^2f+6^2g \\
\frac{3!}{2!}(\alpha+2^2\beta) &= b+2^3c+3^3d+4^3e+5^3f+6^3g \\
\frac{4!}{3!}(\alpha+2^3\beta) &= b+2^4c+3^4d+4^4e+5^4f+6^4g \\
\frac{5!}{4!}(\alpha+2^4\beta) &= b+2^5c+3^5d+4^5e+5^5f+6^5g \\
\frac{6!}{5!}(\alpha+2^5\beta) &= b+2^6c+3^6d+4^6e+5^6f+6^6g \\
\frac{7!}{6!}(\alpha+2^6\beta) &= b+2^7c+3^7d+4^7e+5^7f+6^7g \\
\frac{8!}{7!}(\alpha+2^7\beta) &= b+2^8c+3^8d+4^8e+5^8f+6^8g
\end{aligned}
$$

Table 23: System of equations for first derivative node 1 coefficients

series expansion of $\dfrac{\partial \phi}{\partial x}$ centered at x_i is given by

$$
\left(\frac{\partial \phi}{\partial x}\right)_{i+j} = \left(\frac{\partial \phi}{\partial x}\right)_i + jh\left(\frac{\partial^2 \phi}{\partial x^2}\right)_i + \frac{j^2 h^2}{2!}\left(\frac{\partial^3 \phi}{\partial x^3}\right)_i + \cdots + \frac{j^n h^n}{n!}\left(\frac{\partial^{n+1} \phi}{\partial x^{n+1}}\right)_i + \mathcal{R}_{n_{i+j}} \quad (9.4)
$$

where

$$
\mathcal{R}_{n_{i+j}} = \frac{j^{n+1} h^{n+1}}{(n+1)!}\left(\frac{\partial^{n+2} \phi}{\partial x^{n+2}}\right)_{i+\xi}, \qquad 0 < \xi < j.
$$

These formulas and their analogs for higher order derivatives are the basis for deriving finite difference schemes and are used extensively in this work.

The system of equations for determining the first derivative boundary formula at node 1 is shown in Table 23.

A systematic adding of more variables and equations will increase the formal accuracy of the boundary formula. Shown also in Table 24 is the system of equations for the first derivative boundary formula at node 2.

Of note is the change in the left and right hand sides of these systems. The number

93

$$0 = a+b+c+d+e+f$$

$$\alpha_1 + 1 + \alpha_2 + \beta = -a+c+2d+3e+4f$$

$$2!(-\alpha_1+\alpha_2+2\beta) = a+c+2^2d+3^2e+4^2f$$

$$\frac{3!}{2!}(\alpha_1+\alpha_2+2^2\beta) = -a+c+2^3d+3^3e+4^3f$$

$$\frac{4!}{3!}(-\alpha_1+\alpha_2+2^3\beta) = a+c+2^4d+3^4e+4^4f$$

$$\frac{5!}{4!}(\alpha_1+\alpha_2+2^4\beta) = -a+c+2^5d+3^5e+4^5f$$

$$\frac{6!}{5!}(-\alpha_1+\alpha_2+2^5\beta) = a+c+2^6d+3^6e+4^6f$$

$$\frac{7!}{6!}(\alpha_1+\alpha_2+2^6\beta) = -a+c+2^7d+3^7e+4^7f$$

$$\frac{8!}{7!}(-\alpha_1+\alpha_2+2^7\beta) = a+c+2^8d+3^8e+4^8f$$

Table 24: System of equations for first derivative node 2 coefficients

of points needed on the right hand side decreases as an additional point become available for the left hand side. Similarly a shift in the values of the coefficients of the right hand side indicates the change for the center of the Taylor series expansions at each node.

Appendix D

The coefficients of the second derivative boundary formulas are listed here in Tables 25 through 31.

	α	a	b	c	d	e	f	g	h	i	j	k
T4	10	$\frac{145}{12}$	$\frac{-76}{3}$	$\frac{29}{2}$	$\frac{-4}{3}$	$\frac{1}{12}$						
T6	$\frac{126}{11}$	$\frac{2077}{157}$	$\frac{-2943}{110}$	$\frac{573}{44}$	$\frac{167}{99}$	$\frac{-18}{11}$	$\frac{57}{110}$	$\frac{131}{1980}$				
T8	$\frac{3044}{223}$	$\frac{2515}{171}$	$\frac{-5075}{187}$	$\frac{3996}{733}$	$\frac{4636}{301}$	$\frac{-2658}{191}$	$\frac{4483}{578}$	$\frac{-4112}{1465}$	$\frac{1221}{2023}$	$\frac{-137}{2335}$		
T10	$\frac{6710}{419}$	$\frac{1432}{89}$	$\frac{-3878}{151}$	$\frac{-1689}{166}$	$\frac{5681}{119}$	$\frac{17776}{329}$	$\frac{9619}{221}$	$\frac{7447}{289}$	$\frac{3715}{339}$	$\frac{-1456}{459}$	$\frac{1310}{2339}$	$\frac{517}{11351}$

Table 25: Tridiagonal coefficients of second derivative at nodes 1 and N

	β	α	a	b	c	d	e	f	g	h	i	j
P6	$\frac{-131}{4}$	$\frac{11}{2}$	$\frac{177}{16}$	$\frac{-507}{8}$	$\frac{783}{8}$	$\frac{-201}{4}$	$\frac{81}{16}$	$\frac{-3}{8}$				
P8	$\frac{10073}{86}$	$\frac{7999}{238}$	$\frac{5546}{257}$	$\frac{11427}{110}$	$\frac{-16102}{55}$	$\frac{20492}{107}$	$\frac{-15403}{535}$	$\frac{1751}{333}$	$\frac{-3720}{5081}$	$\frac{232}{4421}$		
P10	$\frac{3987}{37}$	$\frac{18025}{564}$	$\frac{9743}{464}$	$\frac{7937}{85}$	$\frac{-40827}{152}$	$\frac{10786}{61}$	$\frac{-3445}{128}$	$\frac{1567}{319}$	$\frac{-532}{891}$	$\frac{-79}{5935}$	$\frac{61}{3175}$	$\frac{-115}{48923}$

Table 26: Pentadiagonal coefficients of second derivative at nodes 1 and N

	α_1	α_2	a	b	c	d	e	f	g	h	i	j
T6	$\frac{2}{11}$	$\frac{-131}{22}$	$\frac{177}{88}$	$\frac{-507}{44}$	$\frac{783}{44}$	$\frac{-201}{22}$	$\frac{81}{88}$	$\frac{-3}{44}$				
T8	$\frac{238}{7999}$	$\frac{2206}{633}$	$\frac{1001}{1559}$	$\frac{7211}{2333}$	$\frac{-2500}{287}$	$\frac{2285}{401}$	$\frac{-1906}{2225}$	$\frac{217}{1387}$	$\frac{-127}{5830}$	$\frac{24}{15371}$		
T10	$\frac{343}{12956}$	$\frac{1830}{479}$	$\frac{843}{1391}$	$\frac{1530}{431}$	$\frac{-9017}{948}$	$\frac{3216}{535}$	$\frac{-554}{799}$	$\frac{-86}{24291}$	$\frac{399}{6271}$	$\frac{-242}{8755}$	$\frac{55}{9259}$	$\frac{-4}{7291}$

Table 27: Tridiagonal coefficients of second derivative at nodes 2 and $N-1$

	β	α_1	α_2	a	b	c	d	e	f	g
P8	$\frac{1150}{1339}$	$\frac{23}{688}$	$\frac{2335}{688}$	$\frac{1607}{2376}$	$\frac{1943}{701}$	$\frac{-1421}{201}$	$\frac{955}{308}$	$\frac{459}{851}$	$\frac{-212}{11191}$	$\frac{12}{25283}$
P10	$\frac{-1062}{1297}$	$\frac{155}{4886}$	$\frac{4725}{1508}$	$\frac{1165}{1754}$ $\frac{1502}{545}$	$\frac{-283}{31}$	$\frac{4879}{642}$	$\frac{-934}{423}$	$\frac{1060}{2823}$	$\frac{-209}{3160}$	$\frac{114}{13543}$

Table 28: Pentadiagonal coefficients of second derivative at nodes 2 and $N-1$

	α_1	α_2	a	b	c	d	e	f	g	h	i	k
T8	$\frac{9}{38}$	$\frac{-563}{342}$	$\frac{1313}{15199}$	$\frac{1165}{867}$	$\frac{-2969}{570}$	$\frac{3082}{487}$	$\frac{-1969}{684}$	$\frac{851}{2280}$	$\frac{-223}{4663}$	$\frac{23}{6840}$		
T10	$\frac{151}{3108}$	$\frac{2467}{859}$	$\frac{132}{19553}$	$\frac{6575}{9089}$	$\frac{1265}{593}$	$\frac{-2967}{425}$	$\frac{14435}{3039}$	$\frac{-198}{257}$	$\frac{467}{2821}$	$\frac{-107}{3451}$	$\frac{80}{19827}$	$\frac{-11}{42057}$

Table 29: Tridiagonal coefficients of second derivative at nodes 3 and $N-2$

	β_1	β_2	α_1	α_2	a	b	c	d	e	f	g	h
P10	$\frac{-82}{12267}$	$\frac{1185}{931}$	$\frac{-235}{2263}$	$\frac{1451}{320}$	$\frac{-355}{3002}$	$\frac{2803}{3935}$	$\frac{814}{181}$	$\frac{-17489}{1775}$	$\frac{5035}{1284}$	$\frac{504}{575}$	$\frac{-174}{4631}$	$\frac{31}{22718}$

Table 30: Pentadiagonal coefficients of second derivative at nodes 3 and $N-2$

	α_1	α_2	a	b	c	d	e	f	g	h	i	k
T10	$\frac{8}{29}$	$\frac{-151}{232}$	$\frac{-218}{62217}$	$\frac{287}{1882}$	$\frac{597}{551}$	$\frac{-3793}{1044}$	$\frac{1112}{311}$	$\frac{-3563}{2629}$	$\frac{166}{781}$	$\frac{-658}{18037}$	$\frac{37}{8049}$	$\frac{-14}{47587}$

Table 31: Tridiagonal coefficients of second derivative at nodes 4 and $N-3$

Appendix E

Listed here are the boundary formulas for the filtering scheme. They are listed here for completeness at nodes 1, 2, ..., 5, $N-4, N-3, \ldots, N$. Following the filter formulas in Tables 32 through 36 are the coefficients of the boundary filter formulas.

Filter formula at boundary point 1

$$\hat{\phi}_1 + \alpha_f \hat{\phi}_2 + \beta_f \hat{\phi}_3 = a_1 \phi_1 + a_2 \phi_2 + a_3 \phi_3 + \cdots + a_9 \phi_9 + a_{10} \phi_{10} + a_{11} \phi_{11}$$

Filter formula at boundary point 2

$$\alpha_f \hat{\phi}_1 + \hat{\phi}_2 + \alpha_f \hat{\phi}_3 + \beta_f \hat{\phi}_4 = a_1 \phi_1 + a_2 \phi_2 + a_3 \phi_3 + \cdots + a_9 \phi_9 + a_{10} \phi_{10} + a_{11} \phi_{11}$$

Filter formula at boundary point 3

$$\beta_f \hat{\phi}_1 + \alpha_f \hat{\phi}_2 + \hat{\phi}_3 + \alpha_f \hat{\phi}_4 + \beta_f \hat{\phi}_5 = a_1 \phi_1 + a_2 \phi_2 + a_3 \phi_3 + \cdots + a_9 \phi_9 + a_{10} \phi_{10} + a_{11} \phi_{11}$$

Filter formula at boundary point 4

$$\beta_f \hat{\phi}_2 + \alpha_f \hat{\phi}_3 + \hat{\phi}_4 + \alpha_f \hat{\phi}_5 + \beta_f \hat{\phi}_6 = a_1 \phi_1 + a_2 \phi_2 + a_3 \phi_3 + \cdots + a_9 \phi_9 + a_{10} \phi_{10} + a_{11} \phi_{11}$$

Filter formula at boundary point 5

$$\beta_f \hat{\phi}_3 + \alpha_f \hat{\phi}_4 + \hat{\phi}_5 + \alpha_f \hat{\phi}_6 + \beta_f \hat{\phi}_7 = a_1 \phi_1 + a_2 \phi_2 + a_3 \phi_3 + \cdots + a_9 \phi_9 + a_{10} \phi_{10} + a_{11} \phi_{11}$$

Filter formula at boundary point $N-4$

$$\beta_f \hat{\phi}_{N-6} + \alpha_f \hat{\phi}_{N-5} + \hat{\phi}_{N-4} + \alpha_f \hat{\phi}_{N-3} + \beta_f \hat{\phi}_{N-2}$$
$$= a_N \phi_N + a_{N-1} \phi_{N-1} + a_{N-2} \phi_{N-2} + \cdots + a_{N-8} \phi_{N-8} + a_{N-9} \phi_{N-9} + a_{N-10} \phi_{N-10}$$

Filter formula at boundary point $N-3$

$$\beta_f \hat{\phi}_{N-5} + \alpha_f \hat{\phi}_{N-4} + \hat{\phi}_{N-3} + \alpha_f \hat{\phi}_{N-2} + \beta_f \hat{\phi}_{N-1}$$
$$= a_N \phi_N + a_{N-1} \phi_{N-1} + a_{N-2} \phi_{N-2} + \cdots + a_{N-8} \phi_{N-8} + a_{N-9} \phi_{N-9} + a_{N-10} \phi_{N-10}$$

Filter formula at boundary point $N - 2$

$$\beta_f \hat{\phi}_{N-4} + \alpha_f \hat{\phi}_{N-3} + \hat{\phi}_{N-2} + \alpha_f \hat{\phi}_{N-1} + \beta_f \hat{\phi}_N$$

$$= a_N \phi_N + a_{N-1} \phi_{N-1} + a_{N-2} \phi_{N-2} + \cdots + a_{N-8} \phi_{N-8} + a_{N-9} \phi_{N-9} + a_{N-10} \phi_{N-10}$$

Filter formula at boundary point $N - 1$

$$\beta_f \hat{\phi}_{N-3} + \alpha_f \hat{\phi}_{N-2} + \hat{\phi}_{N-1} + \alpha_f \hat{\phi}_N$$

$$= a_N \phi_N + a_{N-1} \phi_{N-1} + a_{N-2} \phi_{N-2} + \cdots + a_{N-8} \phi_{N-8} + a_{N-9} \phi_{N-9} + a_{N-10} \phi_{N-10}$$

Filter formula at boundary point N

$$\beta_f \hat{\phi}_{N-2} + \alpha_f \hat{\phi}_{N-1} + \hat{\phi}_N$$

$$= a_N \phi_N + a_{N-1} \phi_{N-1} + a_{N-2} \phi_{N-2} + \cdots + a_{N-8} \phi_{N-8} + a_{N-9} \phi_{N-9} + a_{N-10} \phi_{N-10}$$

	a_0	a_1	a_2	a_3	a_4	a_5	a_6	a_7	a_8	a_9	a_{10}
T6	$\frac{63+\alpha}{64}$	$\frac{3+29\alpha}{32}$	$\frac{15(-1+\alpha)}{64}$	$\frac{5(1-\alpha)}{16}$	$\frac{15(-1+\alpha)}{64}$	$\frac{3(1-\alpha)}{32}$	$\frac{-1+\alpha}{64}$				
T8	$\frac{255+\alpha}{256}$	$\frac{1+31\alpha}{32}$	$\frac{7(-1+\alpha)}{64}$	$\frac{7(1-\alpha)}{32}$	$\frac{35(-1+\alpha)}{128}$	$\frac{7(1-\alpha)}{32}$	$\frac{7(-1+\alpha)}{64}$	$\frac{1-\alpha}{32}$	$\frac{-1+\alpha}{256}$		
T10	$\frac{1023+\alpha}{1024}$	$\frac{5+507\alpha}{512}$	$\frac{45(-1+\alpha)}{1024}$	$\frac{15(1-\alpha)}{128}$	$\frac{105(-1+\alpha)}{512}$	$\frac{63(1-\alpha)}{256}$	$\frac{105(-1+\alpha)}{512}$	$\frac{15(1-\alpha)}{128}$	$\frac{45(-1+\alpha)}{1024}$	$\frac{5(1-\alpha)}{512}$	$\frac{-1+\alpha}{1024}$
P6	$\frac{63+\alpha-\beta}{64}$	$\frac{3+29\alpha+3\beta}{32}$	$\frac{-15+15\alpha+49\beta}{64}$	$\frac{5(1-\alpha+\beta)}{16}$	$\frac{15(-1+\alpha-\beta)}{64}$	$\frac{3(1-\alpha+\beta)}{32}$	$\frac{-1+\alpha-\beta}{64}$				
P8	$\frac{255+\alpha-\beta}{256}$	$\frac{1+31\alpha+\beta}{32}$	$\frac{-7+7\alpha+57\beta}{64}$	$\frac{7(1-\alpha+\beta)}{32}$	$\frac{35(-1+\alpha-\beta)}{128}$	$\frac{7(1-\alpha+\beta)}{32}$	$\frac{7(-1+\alpha-\beta)}{64}$	$\frac{1-\alpha+\beta}{32}$	$\frac{-1+\alpha-\beta}{256}$		
P10	$\frac{1023+\alpha-\beta}{1024}$	$\frac{5+507\alpha+5\beta}{512}$	$\frac{-45+45\alpha+979\beta}{1024}$	$\frac{15(1-\alpha+\beta)}{128}$	$\frac{105(-1+\alpha-\beta)}{512}$	$\frac{63(1-\alpha+\beta)}{256}$	$\frac{105(-1+\alpha-\beta)}{512}$	$\frac{15(1-\alpha+\beta)}{128}$	$\frac{45(-1+\alpha-\beta)}{1024}$	$\frac{5(1-\alpha+\beta)}{512}$	$\frac{-1+\alpha-\beta}{1024}$

Table 32: Coefficients of filtering schemes at node 1

	a_0	a_1	a_2	a_3	a_4	a_5	a_6	a_7	a_8	a_9	a_{10}
T6	$\frac{1+62\alpha}{64}$	$\frac{29+6\alpha}{32}$	$\frac{15+34\alpha}{64}$	$\frac{-5+10\alpha}{16}$	$\frac{15(1-2\alpha)}{64}$	$\frac{3(-1+2\alpha)}{32}$	$\frac{1-2\alpha}{64}$				
T8	$\frac{1+254\alpha}{256}$	$\frac{31+2\alpha}{32}$	$\frac{7+50\alpha}{64}$	$\frac{7(-1+2\alpha)}{32}$	$\frac{35(1-2\alpha)}{128}$	$\frac{7(-1+2\alpha)}{32}$	$\frac{7(1-2\alpha)}{64}$	$\frac{-1+2\alpha}{32}$	$\frac{1-2\alpha}{256}$		
T10	$\frac{1+1022\alpha}{1024}$	$\frac{507+10\alpha}{512}$	$\frac{45+934\alpha}{1024}$	$\frac{15(-1+2\alpha)}{128}$	$\frac{105(1-2\alpha)}{512}$	$\frac{63(-1+2\alpha)}{256}$	$\frac{105(1-2\alpha)}{512}$	$\frac{15(-1+2\alpha)}{128}$	$\frac{45(1-2\alpha)}{1024}$	$\frac{5(-1+2\alpha)}{512}$	$\frac{1-2\alpha}{1024}$
P6	$\frac{1+62\alpha+\beta}{64}$	$\frac{29+6\alpha-3\beta}{32}$	$\frac{15+34\alpha+15\beta}{64}$	$\frac{-5+10\alpha+11\beta}{16}$	$\frac{15(1-2\alpha+\beta)}{64}$	$\frac{3(-1+2\alpha-\beta)}{32}$	$\frac{1-2\alpha+\beta}{64}$				
P8	$\frac{1+254\alpha+\beta}{256}$	$\frac{31+2\alpha-\beta}{32}$	$\frac{7+50\alpha+7\beta}{64}$	$\frac{-7+14\alpha+25\beta}{32}$	$\frac{35(1-2\alpha+\beta)}{128}$	$\frac{7(-1+2\alpha-\beta)}{32}$	$\frac{7(1-2\alpha+\beta)}{64}$	$\frac{-1+2\alpha-\beta}{32}$	$\frac{1-2\alpha+\beta}{256}$		
P10	$\frac{1+1022\alpha+\beta}{1024}$	$\frac{507+10\alpha-5\beta}{512}$	$\frac{45+934\alpha+45\beta}{1024}$	$\frac{(-15+30\alpha+113\beta)}{128}$	$\frac{105(1-2\alpha+\beta)}{512}$	$\frac{63(-1+2\alpha-\beta)}{256}$	$\frac{105(1-2\alpha+\beta)}{512}$	$\frac{15(-1+2\alpha-\beta)}{128}$	$\frac{45(1-2\alpha+\beta)}{1024}$	$\frac{5(-1+2\alpha-\beta)}{512}$	$\frac{1-2\alpha+\beta}{1024}$

Table 33: Coefficients of filtering schemes at node 2

	a_0	a_1	a_2	a_3	a_4	a_5	a_6	a_7	a_8	a_9	a_{10}
T6	$\frac{-1+2\alpha}{64}$	$\frac{3+26\alpha}{32}$	$\frac{49+30\alpha}{64}$	$\frac{5+6\alpha}{16}$	$\frac{15(-1+2\alpha)}{64}$	$\frac{3(1-2\alpha)}{32}$	$\frac{-1+2\alpha}{64}$				
T8	$\frac{-1+2\alpha}{256}$	$\frac{1+30\alpha}{32}$	$\frac{57+14\alpha}{64}$	$\frac{7+18\alpha}{32}$	$\frac{35(-1+2\alpha)}{128}$	$\frac{7(1-2\alpha)}{32}$	$\frac{7(-1+2\alpha)}{64}$	$\frac{1-2\alpha}{32}$	$\frac{-1+2\alpha}{256}$		
T10	$\frac{-1+2\alpha}{1024}$	$\frac{5+502\alpha}{512}$	$\frac{979+90\alpha}{1024}$	$\frac{15+98\alpha}{128}$	$\frac{105(-1+2\alpha)}{512}$	$\frac{63(1-2\alpha)}{256}$	$\frac{105(-1+2\alpha)}{512}$	$\frac{15(1-2\alpha)}{128}$	$\frac{45(-1+2\alpha)}{1024}$	$\frac{5(1-2\alpha)}{512}$	$\frac{-1+2\alpha}{1024}$
P6	$\frac{-1+2\alpha+62\beta}{64}$	$\frac{3+26\alpha+6\beta}{32}$	$\frac{49+30\alpha-30\beta}{64}$	$\frac{5+6\alpha+10\beta}{16}$	$\frac{-15+30\alpha+34\beta}{64}$	$\frac{3(1-2\alpha+2\beta)}{32}$	$\frac{-1+2\alpha-2\beta}{64}$				
P8	$\frac{-1+2\alpha+254\beta}{256}$	$\frac{1+30\alpha+2\beta}{32}$	$\frac{57+14\alpha-14\beta}{64}$	$\frac{7+18\alpha+14\beta}{32}$	$\frac{-35+70\alpha+58\beta}{128}$	$\frac{7(1-2\alpha+2\beta)}{32}$	$\frac{7(-1+2\alpha-2\beta)}{64}$	$\frac{1-2\alpha+2\beta}{32}$	$\frac{-1+2\alpha-2\beta}{256}$		
P10	$\frac{-1+2\alpha+1022\beta}{1024}$	$\frac{5+502\alpha+10\beta}{512}$	$\frac{979+90\alpha-90\beta}{1024}$	$\frac{15+98\alpha+30\beta}{128}$	$\frac{-105+210\alpha+302\beta}{512}$	$\frac{63(1-2\alpha+2\beta)}{256}$	$\frac{105(-1+2\alpha-2\beta)}{512}$	$\frac{15(1-2\alpha+2\beta)}{128}$	$\frac{45(-1+2\alpha-2\beta)}{1024}$	$\frac{5(1-2\alpha+2\beta)}{512}$	$\frac{-1+2\alpha-2\beta}{1024}$

Table 34: Coefficients of filtering schemes at node 3

	a_0	a_1	a_2	a_3	a_4	a_5	a_6	a_7	a_8	a_9	a_{10}
T8	$\frac{1-2\alpha}{256}$	$\frac{-1+2\alpha}{32}$	$\frac{7+50\alpha}{64}$	$\frac{25+14\alpha}{32}$	$\frac{35+58\alpha}{128}$	$\frac{7(-1+2\alpha)}{32}$	$\frac{7(1-2\alpha)}{64}$	$\frac{-1+2\alpha}{32}$	$\frac{1-2\alpha}{256}$		
T10	$\frac{1-2\alpha}{1024}$	$\frac{5(-1+2\alpha)}{512}$	$\frac{45+934\alpha}{1024}$	$\frac{113+30\alpha}{128}$	$\frac{105+302\alpha}{512}$	$\frac{63(-1+2\alpha)}{256}$	$\frac{105(1-2\alpha)}{512}$	$\frac{15(-1+2\alpha)}{128}$	$\frac{45(1-2\alpha)}{1024}$	$\frac{5(-1+2\alpha)}{512}$	$\frac{1-2\alpha}{1024}$
P8	$\frac{1-2\alpha+2\beta}{256}$	$\frac{-1+2\alpha+30\beta}{32}$	$\frac{7+50\alpha+14\beta}{64}$	$\frac{25+14\alpha-14\beta}{32}$	$\frac{35+58\alpha+70\beta}{128}$	$\frac{-7+14\alpha+18\beta}{32}$	$\frac{7(1-2\alpha+2\beta)}{64}$	$\frac{-1+2\alpha-2\beta}{32}$	$\frac{1-2\alpha+2\beta}{256}$		
P10	$\frac{1-2\alpha+2\beta}{1024}$	$\frac{-5+10\alpha+502\beta}{512}$	$\frac{45+934\alpha+90\beta}{1024}$	$\frac{113+30\alpha-30\beta}{128}$	$\frac{105+302\alpha+210\beta}{512}$	$\frac{-63+126\alpha+130\beta}{256}$	$\frac{105(1-2\alpha+2\beta)}{512}$	$\frac{15(-1+2\alpha-2\beta)}{128}$	$\frac{45(1-2\alpha+2\beta)}{1024}$	$\frac{5(-1+2\alpha-2\beta)}{512}$	$\frac{1-2\alpha+2\beta}{1024}$

Table 35: Coefficients of filtering schemes at node 4

	a_0	a_1	a_2	a_3	a_4	a_5	a_6	a_7	a_8	a_9	a_{10}
T10	$\frac{-1+2\alpha}{1024}$	$\frac{5(1-2\alpha)}{512}$	$\frac{45(-1+2\alpha)}{1024}$	$\frac{15+98\alpha}{128}$	$\frac{407+210\alpha}{512}$	$\frac{63+130\alpha}{256}$	$\frac{105(-1+2\alpha)}{512}$	$\frac{15(1-2\alpha)}{128}$	$\frac{45(-1+2\alpha)}{1024}$	$\frac{5(1-2\alpha)}{512}$	$\frac{-1+2\alpha}{1024}$
P10	$\frac{-1+2\alpha-2\beta}{1024}$	$\frac{5(1-2\alpha+2\beta)}{512}$	$\frac{-45+90\alpha+934\beta}{1024}$	$\frac{15+98\alpha+30\beta}{128}$	$\frac{407+210\alpha-210\beta}{512}$	$\frac{63+130\alpha+126\beta}{256}$	$\frac{-105+210\alpha+302\beta}{512}$	$\frac{15(1-2\alpha+2\beta)}{128}$	$\frac{45(-1+2\alpha-2\beta)}{1024}$	$\frac{5(1-2\alpha+2\beta)}{512}$	$\frac{-1+2\alpha-2\beta}{1024}$

Table 36: Coefficients of filtering schemes at node 5

References

[1] Saul S. Abarbanel and Alina E. Chertock, *Strict stability of high-order compact implicit finite-difference schemes: The role of boundary conditions for hyperbolic pdes, i*, Journal of Computational Physics **160** (1999), 42–66.

[2] Yves Adam, *Highly accurate compact implicit methods and boundary conditions*, Journal of Computational Physics **24** (1976), 10–22.

[3] Carlos E Cadenas and Vianey Villamizar, *Comparison of least squares fem, mixed galerkin fem and an implicit fdm applied to acoustic scattering*, Appl. Num. Anal. Comp. Math. **1** (2004), 128–139.

[4] Mark H. Carpenter, David Gottlieb, and Saul Abarbanel, *The stability of numerical boundary treatments for compact high-order finite-difference schemes*, Journal of Computational Physics **108** (2003), 272–295.

[5] Ward Cheney and David Kincaid, *Numerical mathematics and computing*, Thomson Brooks/Cole, Belmont, CA, 2004.

[6] L. Collatz, *The numerical treatment of differential equations*, Springer-Verlag, New York, 1966.

[7] A.K. De and V. Eswaran, *Analysis of a new high resolution upwind compact scheme*, Journal of Computational Physics **218** (2006), no. 2, 398–416.

[8] Joseph E. Flaherty, *Numerical solution of partial differential equations*, Troy, New York, 1999.

[9] Datta V. Gaitonde and Miguel R. Visbal, *High-order schemes for navier-stokes equations: Algorithm and implementation into fdl3di*, Tech. report, Air Vehicles Directorate, Air Force Research Laboratory, August 1998.

[10] S.K. Godunov and V.S. Ryabenkii, *Difference schemes: An introduction to the underlying theory*, Elsevier Science Publishers, New York, 1987.

[11] Richard S. Hirsh, *Higher order accurate difference solutions of fluid mechanics problems by a compact differencing technique*, Journal of Computational Physics **19** (1975), 90–109.

[12] Z. Kopal, *Numerical analysis*, Wiley, New York, 1961.

[13] H.-O. Kreiss and L. Wu, *On the stability definition of difference approximations for the initial boundary value problems*, Appl. Num. Math. **12** (1993), 213.

[14] Roland E. Larson, Robert P. Hostetler, and Bruce H. Edwards, *Calculus with analytic geometry*, Houghton Mifflin, New York, 1998.

[15] Sanjiva K. Lele, *Compact finite difference schemees with spectral-like resolution*, Journal of Computational Physics **103** (1992), 16–42.

[16] Randall J. LeVeque, *Finite difference methods for ordinary and partial differential equations*, SIAM, Seattle, 2007.

[17] Jichun Li and Miguel R. Visbal, *High-order compact schemes for nonlinear dispersive waves*, Journal of Scientific Computing **26** (2006), 1–23.

[18] T.K Sengupta, G. Ganeriwal, and S. De, *Analysis of central and upwind compact schemes*, Journal of Computational Physics **192** (2003), 677–694.

[19] Scott E. Sherer, *Scattering of sound from axisymetric sources by multiple circular cylinders*, Journal of the Acoustical Society of America **115** (2003), 488–496.

[20] Scott E. Sherer and Miguel R. Visbal, *High-order overset-grid simulations of acoustic scattering from multiple cylinders*, Tech. report, Air Vehicles Directorate, Air Force Research Laboratory.

[21] C. Strikwerda, John, *Initial boundary value problems for the method of lines*, Journal of Computational Physics **34** (1979), 94–107.

[22] Andrei I. Tolstykh, *High accuracy non-centered compact difference schemes for fluid dynamics applications*, World Scientific, New Jersey, 1994.

[23] R. Vichnevetsky, *Stability charts in the numerical approximation of partial differential equations: A review*, Mathematics and Computers in Simulation **21** (1979), 170–177.

[24] R. Vichnevetsky and J. B. Bowles, *Fourier analysis of numerical approximations of hyperbolic equations*, SIAM, Philadelphia, 1982.

[25] Vianey Villamizar and Matthew Weber, *Boundary-conforming coordinates with grid line control for acoustic scattering from complexly shaped obstacles*, Numerical Methods for Partial Differential Equations **23** (2007), 1445–1467.

[26] Miguel R. Visbal and Datta V. Gaitonde, *High-order accurate methods for complex unsteady subsonic flows*, AIAA Journal **37** (1999), 1231–1239.

[27] _____, *Very high-order spatially implicit schemes for computational acoustics on curvilinear meshes*, Journal of Computational Acoustics **9** (2000), no. 4, 1259–1286.

[28] _____, *On the use of higher-order finite-difference schemes on curvilinear and deforming meshes*, Journal of Computational Physics **181** (2002), 155–185.